

INTEGRATING GIS AND REMOTE SENSING TECHNOLOGY FOR MANAGING
TEF PRODUCTION IN ETHIOPIA


by

Balehager Ayalew
A Dissertation
Submitted to the
Graduate Faculty
of
George Mason University
in Partial Fulfillment of
The Requirements for the Degree
of
Doctor of Philosophy
Earth Systems & Geoinformation Science

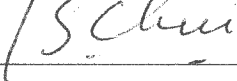
Committee:



Dr. John J. Qu, Dissertation Director



Dr. William E. Roper, Committee Member



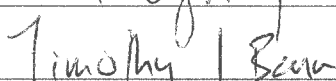
Dr. Long S. Chiu, Committee Member



Dr. Chaowei (Phil) Yang, Committee Member



Dr. Peggy Agouis, Department Chairperson



Dr. Timothy L. Born, Associate Dean for Student and Academic Affairs, College of Science



Dr. Vikas Chandhoke, Dean, College of Science

Date: 06/13/2013

Summer Semester 2013
George Mason University
Fairfax, VA

Integrating GIS and Remote Sensing Technology for Managing Tef Production in
Ethiopia

A Dissertation submitted in partial fulfillment of the requirements for the degree of Doctor
of Philosophy at George Mason University

By

Balehager Ayalew
Professional Engineering Degree
George Washington University, 2004
Master of Science
George Washington University, 2001
Bachelor of Science
University of the District of Columbia, 2000

Director: John J. Qu, PhD, Professor
Earth Systems & Geoinformation Science

Summer Semester 2013
George Mason University
Fairfax, VA

Copyright: Balehager Ayalew
All Rights Reserved

DEDICATION

To my late father Ayalew Tadela and my mother Aster Araya, who have been there for me from day one. Thank you for all of the love, support, encouragement and dedication. To my sister Abesha, who has been there for me for the last twenty years and who has the patience of a saint. Thank you for all of your love, support, help, encouragement and dedication. To my adorable children Dagmawe, Abyssinia and Zebasil, each share equally my pride and joy.

This is a tribute to all of you.

ACKNOWLEDGEMENTS

I would like to express the deepest appreciation to my dissertation director and committee chair Professor John J. Qu, who has the attitude and the substance of a genius. He continually and convincingly conveyed a spirit of adventure in regard to research and an excitement in regard to interest of study. Without his guidance and persistent help this dissertation would not have been possible.

I would like to thank my committee members, Professor Long S. Chiu and Professor Chaowei (Phil) Yang, whose work demonstrated to me that concern for global affairs supported by an “engagement” in comparative literature and modern technology, should always transcend academia and provide a quest for our times.

Over the past twelve years I have received support and encouragement from a great number of individuals. But my last committee member Professor William E. Roper has been a mentor, colleague, and friend. His guidance has made this a thoughtful and rewarding journey. I greatly appreciated for what you have done for me.

In addition, Professor Richaed Gomez provided data collection spent countless hours listening to me talk about my research and provided needed encouragement and insights. Asnake Negussie, a fellow class-mate and a friend at the University of the District of Columbia for giving me a push to get started, helped me through the school year as I tried to juggle working, supporting my family and completing my dissertation. I would also like to thank the teachers who took part in this study for generously sharing their time and ideas. I have learned much through our conversations.

Finally, I'd be remiss if I didn't acknowledge the innumerable sacrifices made by my family and friends, in shouldering far more than their fair share of the parenting and household burdens while I pursue this final degree.

TABLE OF CONTENTS

	Page
LIST OF TABLES.....	IX
TABLE	
PAGEIX	
LIST OF FIGURES.....	X
FIGURE	
PAGEX	
LIST OF ABBREVIATIONS.....	XI
ABSTRACT	XIII
1. INTRODUCTION.....	1
1.1. IMPORTANCE OF PRECISION AGRICULTURE	1
1.2. PROBLEM STATEMENT	3
1.3. OBJECTIVES AND SCOPE.....	4
1.4. ORGANIZATION OF THE REPORT	5
1.5. MAJOR DATA SOURCES	6
1.6. SUMMARY	6
2. LITERATURE REVIEW.....	8
2.1. PRECISION AGRICULTURE DEFINITION.....	8
2.2. CHARACTERIZATION OF TEF AND VEGETATION SPECIES IN ETHIOPIA	12
2.2.1. Afroalpine and Subafroalpine Ecosystem.....	12
2.2.2. Dry Evergreen Montane Forest and Grassland complex.....	13
2.2.3. Moist Evergreen Montane Forest Ecosystem	14
2.2.4. <i>Acacia-Comiphora</i> Woodland Ecosystem	14
2.2.5. Combretum-Terminalia Woodland Ecosystem	15
2.2.6. Lowland, Semi-evergreen Forest Ecosystem	16

2.2.7. Desert and Semi-desert Scrubland Ecosystem	16
2.2.8. Aquatic Ecosystem	17
2.2.9. Tef species in Ethiopia.....	18
2.3. DROUGHT AND TEF CROP STRESS	19
2.3.1. Crop and Soil Property within the Field	21
2.3.2. Crop Yield Management System	23
2.4. REMOTE SENSING FOR CROP MONITORING.....	26
2.4.1. Tef Reflectance Characterization Using Spectroradiometer	31
2.4.1.1. Ground Measurements	31
2.4.1.2. Tef Reflectance Spectra	36
2.4.1.3. Relationship Between Satellite Data and Ground Measurements	39
2.4.2. Multispectral Remote Sensing.....	40
2.4.3. Hyperspectral Remote Sensing	43
2.4.4. Comparison on Hyperspectral and Multispectral Data	44
2.4.5. Change Detection for Tef Crop Inventory	45
2.4.6. Vegetation Indices	47
2.4.7. Combining GIS and GPS with Remote Sensing	52
2.4.8. Tef Crop Yield profile estimation	54
2.4.8.1. Performance in Remote Sensing Technique	55
2.4.8.2. Remote Estimation of Tef production	57
2.4.8.3. Band Selection to Determine Optimal Number of Bands for Tef crop variables estimation	60
2.4.8.4. Accuracy Assessment of crop characteristics estimation	68
2.5. CHAPTER SUMMARY	71
3. TEF SUITABILITY ANALYSIS	75
3.1. CLIMATE	78
3.2. TOPOGRAPHY	79
3.3. LAND USE/LAND COVER	82
3.4. COUNTRY SCALE SOIL INFORMATION.....	84
3.5. LOCAL SCALE SOIL SURVEY AND MAPPING	85

3.5.1. Pre-Fieldwork	86
3.5.2. Field Survey.....	87
3.5.3. Soil Laboratory Analysis	88
3.5.4. Post field Work Activities	89
3.5.4.1. Data Compilation and Analysis	89
3.5.4.2. Soil Classification and Mapping	90
3.5.5. Description of the Major Soil Types of the Survey Area	92
3.5.5.1. Luvisols	93
3.5.5.2. Cambisols	94
3.5.5.3. Vertisols	96
3.5.6. DESCRIPTION OF THE SOIL MAPPING UNITS	98
3.5.6.1. Mapping Unit Representation	99
3.5.6.2. Soil Mapping Unit Description	100
3.6. TEF SUITABILITY.....	106
3.7. CHAPTER SUMMARY	108
4. TEF LOCAL SCALE MAPPING	109
4.1. STUDY AREA.....	110
4.2. SATELLITE DATA	111
4.3. GPS DATA.....	115
4.4. IMAGE CLASSIFICATION	116
4.4.1. Change Detection.....	122
4.4.2. Accuracy Evaluation.....	126
4.5. CHAPTER SUMMARY	130
5. CONCLUSIONS AND FUTURE DIRECTION	132
5.1. CONCLUSIONS.....	132
5.2. APPLICATIONS OF THIS RESEARCH.....	134
5.3. LIMITATIONS OF THIS WORK.....	135
5.4. FUTURE WORKS.....	135
REFERENCES.....	138

BIOGRAPHY	149
------------------------	------------

LIST OF TABLES

Table	Page
Table 1. Tef production and productivity along years 1990 to 1994.	24
Table 2. Area, production and yields of cereals in Ethiopia, 2003/04 and 2007/08	25
Table 3. Satellite remote sensing platforms (Source: MULLA, 2013).	42
Table 4. Multi-spectral broad-band for precision agriculture. Source: Mulla (2013).	49
Table 5. Hyperspectral narrow-band for precision agriculture. Source: Mulla (2013). ...	51
Table 6. Summary Characteristics of Control Morphological of the Ada'a Soils	92
Table 7. Categorized soil textural classes for the soil mapping unit	99
Table 8. Categorized slopes classes for the soil mapping unit	100
Table 9. Description of soil legend	101
Table 10. Indicative physical and chemical properties of the Ada'a mapping units	102
Table 11. Major soils of the study area and their distribution	103
Table 12. Raster calculation values used to generate tef suitability map.	106
Table 13. Most common high spatial resolution commercial satellites	110
Table 14. Parameter specification of the GIS instrument onboard Geoeye-1 satellite. ..	112
Table 15. Parameter specification of the REIS instrument onboard Rapideye satellite.	114
Table 16. Spectral, texture and spatial attributes of image objects.	118
Table 17. Change detection results in pixels	124
Table 18. Change detection percent (%) results.	125
Table 19. Change Detection square meters results	126
Table 20. Confusion matrix of accuracy verification of Geoeye-1 classification result	128
Table 21. Confusion matrix of accuracy verification of Rapideye classification result.	130

LIST OF FIGURES

Figure	Page
Figure 1. Electromagnetic spectrum. Source: http://www.redorbit.com	27
Figure 2. Spectral signatures of vegetation.	28
Figure 3. Radiation geometry of the field environment. Source: Milton, 1987.....	32
Figure 4. Direct irradiant flux and diffuse radiant flux. Source: McCoy, 2005	33
Figure 5. Instrument configuration for measurement. Source: Mac Arthur, 2011.	34
Figure 6. Wavelength (nm) & reflectance in Tef Source: (Hanna & Rethwisch, 2003) ..	38
Figure 7. Contour plot NDVI values Source: Thenkabail <i>et al.</i> (2000).....	66
Figure 8. Workflow of research activities developed within the project.	77
Figure 9. Average rainfall from July 11 to October 10 during 2006-2010.....	79
Figure 10. Elevation range map suitable for tef growing.	81
Figure 11. Cultivated land in Ethiopia.	83
Figure 12. Soil types in Ethiopia.....	84
Figure 13. Location of the local scale soil survey and mapping study area.	86
Figure 14. Tef field soil pit surveyed area	87
Figure 15. Adaa soil mapping unit.....	104
Figure 16. Ada'a Soil Map.....	105
Figure 17. Estimated suitability map for tef production.	107
Figure 18. Study area and image acquisition location maps.	111
Figure 19. Geoeye-1 image bands 3, 2 and 1 on R, G and B channels, repectively.	113
Figure 20. Rapideye image bands 3, 2 and 1 on R, G and B channels, repectively.	115
Figure 21. Field samples collected in October 2011 using a hand-held GPS.	116
Figure 22. Geoeye-1 resulting object-based image classssification.	120
Figure 23. Rapideye resulting object-based image classssification.	121
Figure 24. Change detection final map, exposed soil mask.....	123
Figure 25. Samples points for accuracy verification of Geoeye-1 image classification.	128
Figure 26. Samples points for accuracy verification of Rapideye image classification	129

LIST OF ABBREVIATIONS

AVHRR - Advanced Very High Resolution Radiometer
AVIRIS - Airborne Visible/Infrared Imaging Spectrometer
AWC - Available Water Content
CEC - Cation Exchangeable Capacity
DEM - Digital Elevation Model
DGVI - Derivative Greenness Vegetation Indices
DN - Digital Number
DZARC - Debre Zeit Agricultural Research Center
EIAR - Ethiopian Institute of Agricultural Research
EPIC - Erosion Productivity Impact Calculator
EVI2 - Vegetation Index
FAO – Food and Agriculture Organization
FEWS - Famine Early Warning System
fPAR - Fraction of the Photosynthetic Radiation
GHI - Global Hunger Index
GIS - Geographic Information Systems
GMT - Greenwich Mean Time
GNDVI - Green Normalized Difference Vegetation Index
GPS - Global Positioning Systems
GRVI - Green Red Vegetation Index
GYURI - General Yield Unified Reference Index
HI - Harvest Index
IFOV - Instantaneous Field of View

IUCN - International Union for Conservation of Nature
LAI - Leaf Area Index
LL R2M - Lambda–Lambda R² Models
LULC – Land Use/Land Cover
MCARI - Modified Chlorophyll Absorption in Reflectance Index
MoARD - Ministry of Agriculture & Rural Development
MSAVI - Modified Soil-Adjusted Vegetation Index
NDVI - Normalised Difference Vegetation Index
NE - Noise Equivalent
NG - Normalised Green
NIR - Nir Near-Infrared
NOAA - National Oceanic and Atmospheric Administration
NR - Normalised Red
OM - Organic Matter
OMBVI - Optimum Multiple-Band Vegetation Indices
OMNBR - Optimal Multiple Narrow Band Reflectance Indices
PAR - Photosynthetically Active Radiation
PATs - PA Technologies
PCA - Precision Conservation Agriculture
PCA - Principal Component Analysis
PCA1BV - Principal Component Band 1 Brightness Values
PCA2BV - Principal Component Band 2 Brightness Values
RMSE - Root Mean Square Error
RPC - Rational Polynomial Camera
RS - Remote Sensing
RVI - Ratio Vegetation Index
SDA - Stepwise Discriminant Analysis

SR - Simple Ratios

STD-PCT - Standard Principal Component Transformation

TBVI - Two-Band Vegetation Indices

TCARI - Transformed Chlorophyll Absorption in Reflectance Index

TM - Thematic Mapper

UN – United Nations

USGS - United States Geological Survey

VF - Versus Vegetation Fraction

VI - Vegetation Index

WC - Water Content

WDRVI - Wide Dynamic Range Vegetation Index

WGS-84 - World Geodetic System 1984

ABSTRACT

INTEGRATING GIS AND REMOTE SENSING TECHNOLOGY FOR MANAGING TEF PRODUCTION IN ETHIOPIA

Balehager Ayalew, Ph.D.

George Mason University, 2013

Director: Dr. John J. Qu

The Pressure on global food system will increase and food production must increase as well to meet global demand for food. More food must be produced sustainably through implementation of existing knowledge, technology and best practice, and by investment in new science and innovation. Precision agriculture provides a means to monitor the food production chain and manage both the quantity and quality of agricultural product. Resource misallocation has serious impacts on sustainability and food security. One of the answers to this problem is the adoption of precision agriculture. This study deals with development and adaptation of precision agriculture tools for sustainable food production in Ethiopia, specifically to facilitate the production of existing tef crops and encouraging establishment of new ones. Geographic Information Systems provide ideal environment for spatial analysis to be performed. Ethiopia's climate and environment conditions were aggregated and formed the basis of tef suitability mapping for respective data layers in the GIS system. Additional detailed local scale soil survey data were collected and entered into the GIS tool. These large data bases of information were collected from the Ethiopian Ministry of Water Resources and Ethiopian Institute of Agricultural

Research, Debre Zeit Agricultural Research Center (EIAR-DZARC). Soil sample and data were also collected and analyzed at approximately 50 sample sites in the study area. The analysis of all these data sets provided insights critical to farmers and politicians making decision on establishing new tef crops or choosing the most appropriate crop with respect to projected local conditions for maximum production of tef. Another part of this study used high spectral resolution imagery with Geoeye-1 and Rapideye remote sensing systems to identify tef crop conditions. Using object-based classification and change detection analysis of multi-temporal data, tef crops were mapped within the study area. This methodology showed the potential for regional scale mapping and analysis that are important for tef production estimation, planning and food security assurance. Recommendations were made for adapting this methodology to other areas of Ethiopia and implementing a tef crop monitoring system by integrating hyperspectral data analysis and field sampling to improve overall tef production within Ethiopia.

1. INTRODUCTION

1.1. IMPORTANCE OF PRECISION AGRICULTURE

A growing population reaching nine billion by 2050, intense land, water and energy competition and more evident effects of climate change will increase pressure on global food system over the next 40 years (Foresight, 2011). Crop yield has fallen in many areas and water scarcity has increased (Rosegrant & Cline, 2003). Global distribution of croplands during the twentieth century diminished greatly (from ~0.75 ha/person in 1900 to ~0.35 ha/person in 1990) (Ramankutty & Olejniczak, 2008). Another challenge is the large, growing food security gap in certain places around the world. As much as half of the food grown and harvested in underdeveloped and developing countries never gets consumed (Floros *et al.*, 2010). To meet global food demand 40 years from now, agricultural production must be 60 percent higher by weight compared to 2005 global food production (FAO, 2012).

Undernourished people surpassed 1 billion in 2009 with a slight decline in 2010 to 925 million (Global Hunger Index, International Food Policy research institute, 2010, FAO, 2010). In Sub-Saharan Africa around 239 million people suffer from hunger (Sasson, 2012). Ethiopia, historically one of the most affected countries, diminished its Global Hunger Index between 1990 and 2010 (Von Grebmer, *et al.*, 2010) and progressed from 71% malnourished people in 1990-92 to 44% (representing 35 million Ethiopians) in 2004-06. Nevertheless, the numbers are still considered unacceptable and hunger is a major challenge to be overcome (FAO, 2009; FAO, 2010).

According to the British Government Office for Science more food must be produced sustainably through the spread and implementation of existing knowledge, technology and best practice, and by investment in new science and innovation. This is a substantial change in the food system if food security is to be provided for nine billion people (Foresight, 2011). In this sense, precision agriculture provides a means to monitor the food production chain and manage both the quantity and quality of agricultural produce. Optimizing production by accounting for variability and uncertainties within agricultural systems and adapting production inputs that are site-specific within a field allows better use of resources to maintain the quality of the environment while improving the sustainability of the food supply (Gebbers *et al.*, 2010). Practices such as over-application of fertilizers, for example, results in input losses through leaching and runoff, generating adverse effects on resource quality (e.g. on soil and water). There are, in turn, consequential impacts for plants, ecosystems, the economy, and population. Resource misallocation, therefore, has serious implications for sustainability and food security. One answer to this problem is the adoption of precision agriculture (Tey & Brindal, 2012).

In southern Africa initiatives of precision conservation agriculture (PCA) includes the precision application of small doses of inputs such as fertilizers. In this approach, soil and water conservation management practices are implemented by taking into account spatial and temporal variability across natural and agricultural landscapes (Berry *et al.*, 2003). These technologies (amongst other practices) have demonstrated to be an important strategy for farmers in low potential zones, where a majority of the most resource-poor and vulnerable farm households exist. Over four years PCA practices have consistently increased cereal yields by 50 to 300% in more than 50,000 farm households. Adoption of these practices every year leads to build

up of soil fertility and organic matter resulting in a more sustainable system (Twomlow *et al.*, 2009).

1.2. PROBLEM STATEMENT

Ethiopia has a population of over 67 million, 84% of whom live in rural areas. Over half of the Ethiopian population lives on less than US\$1 a day and over 80% of the population relies on agriculture for their livelihood. Around 35 million people in Ethiopia were hungry circa 2006 (Von Grebmer, *et al.*, 2010). Main factors affecting food production in Ethiopia are related to poor climate (unreliable rainfall), lack of arable land, land degradation, and poor land management.

Growing concerns about the need to increase crop productivity without causing environmental injury have led to the deployment of site-specific strategies in soil nutrient management. With the advancements in image processing and increase in computational power, the use of remote sensing and merging of satellite data to extract spatial and temporal information for precision agriculture is growing (Anderson *et al.*, 2012).

The need to increase production per field area optimizes use of inputs, maximizing output and minimizing environmental losses is urgent. Precision agriculture and associated technologies can provide the necessary tools for better decision making, policy planning and crop monitoring and management. Not only expansion of crop planted area is needed but also increased production per field is crucial, considering lack of agricultural production per/capita.

Increasing production depends on many factors, including the knowledge of factors leading to low yield rates, inputs needed and appropriate application of crop management practices. The goal of this dissertation research is to develop an

integrated system that can provide such information leading to a solution for achieving sustainable production and food security.

1.3. OBJECTIVES AND SCOPE

Food safety and sustainable production of *Eragrostis tef* in Ethiopia are based on increasing yield rates and planted area. Planning new tef crops and management of crop production sustainably depends on crop and environment monitoring. The main goal of this dissertation research is stated as:

Integration of remote sensing and GIS based methodologies for monitoring, estimate early assessment and maximizing production of tef while minimizing their environmental impacts.

The first steps for applying remote sensing and GIS technologies for sustainable crop management depends largely on the construction of a database, integrating information from several aspects of tef cultivation related variables for precision agriculture management. The specific goals for this dissertation are:

- To develop a database that integrates climate, topography, land use/land cover and soil information;
- To demonstrate tef crop mapping based on multi-temporal, multi-spectral and high spatial resolution image processing of a culturally important and threatened plant species;
- To apply geographic information system incorporating soil, topography, climate and tef spatial information for suitable areas of tef production in Ethiopia;

1.4. ORGANIZATION OF THE REPORT

This dissertation research summarizes the results from efforts directed to gathering information on physical environment and tef crops in Ethiopia. Chapter 1 explains the importance of precision agriculture in sustainable crop management, presents the objectives and scope of this study summarizes discussion main results obtained from this research.

The concept of precision agriculture is explained in Chapter 2. The important aspects on precision agriculture, remote sensing for crop estimation and monitoring as well as agronomic characteristics of tef crops are discussed. Detailed aspects important for future achievements planned for the continuation of this research project are also discussed. The relationship between crop, ground and satellite spectral data are discussed as well as techniques for hyperspectral data processing for tef crop characteristics estimation.

Chapter 3 describes the development of geographic information system integrating climate data, topography, land use/land cover (LULC) and soil information is described. Methodology and results on local scale tef crop mapping using object-based image classification and change detection technique are discussed in Chapter 4.

Conclusions of this research report and future achievements for crop estimation and management under a sustainable and precision agriculture perspective are presented in Chapter 5.

1.5. MAJOR DATA SOURCES

Sources of data for geographic information system database and tef crop monitoring used in this report include:

- climate data from FEWS (Famine Early Warning System);
- topographic data from U.S. Geological Survey's EROS Data Center
- land use land cover data from Ethiopian Institute of Agricultural Research, Debre Zeit Agricultural Research Center (EIAR-DZARC).
- country scale soil data obtained from ETHIOGIS
- local scale soil data from Ministry of Water Resources
- Rapideye data (RapidEye Earth Imaging System)
- Geoeye data (GeoEye Imaging System)
- GPS field data acquired with navigation commercial equipment

1.6. SUMMARY

The fact that Agriculture in Ethiopia is diverse and widespread geographically, covering large tracts of land only understates the crucial need for use of geographic information systems (GIS) as a management tool that can be used to achieve food security. GIS is playing an increasing role in agriculture production throughout the world by helping farmers increase production, access information faster, reduce costs, and manage their land more efficiently. Administration and monitoring of farm subsidies management, inputs and farm operations can be facilitated by geographic information systems.

The geographic information system we recently organized can be used in modeling for integrated regional agricultural planning for championing the security of land tenure and consolidation efforts. Acquisition of information and its organization

in a geographic information system allows spatial analysis needed for planning new tef crops according to suitability of climatic, topographic and edaphic conditions. Public policy making, however, needs to consider not only environmental characteristics of the land but human interaction with it as well. Land use/land cover mapping provides information on the current status of land use as well as future trends and scenario analysis.

Achieving agricultural growth through optimum utilization of the land resources however is not enough to guarantee food security in Ethiopia. Although new crop implantation as well as optimal management of resources are important, increase yield and food shortages prevention are also key to sustainable farming. Remote sensing systems can provide necessary information for planning ahead and improving crop production. In this sense, results obtained with satellite image processing are considered a good first step to establish a monitoring system for tef production in Ethiopia. Identification of tef crops presented good results using change detection and object-based classification techniques. The use of multi-temporal images can be considered a good approach for tef mapping. Because tef is a fast growing crop, it can be easily identified before tef planting and at a time of maturing stage.

This dissertation research is expected to provide advances in planning the establishment of new tef crops aided by GIS and identification of tef crops through Remote Sensing imagery and analysis. These techniques are the first steps for estimation of tef crop agronomical variables. Geospatial tools such as remote sensing, GPS and GIS are necessary to ultimately realize sustainable food security and optimum productivity of tef as a culturally important and threatened species.

2. LITERATURE REVIEW

2.1. PRECISION AGRICULTURE DEFINITION

Precision Agriculture (PA) is a management strategy that uses information technologies to combine data from multiple sources and support decisions related to crop production (Sonka *et al.*, 1997). It is a system that involves crop management according to field variability and site-specific conditions (Seelan *et al.*, 2003). The major difference between conventional crop management and PA would be the application of modern information technologies to collect process and analyze data from multiple sources at different spatial and temporal resolution (Sonka *et al.*, 1997).

Precision agriculture comprises a set of technologies that combines sensors, information systems, enhanced machinery, and informed management to optimize production by accounting for responding to variability and uncertainties within agricultural systems (Gebbers & Adamchuk, 2010). Adapting production site-specific inputs within a field allows for better use of resources to maintain the quality of the environment improving the sustainability of the food supply. Precision agriculture provides a means to monitor the food production chain and manage both the quantity and quality of agricultural produce. (Gebbers & Adamchuk, 2010).

From these concepts and definitions, PA implementation can be initially translated into recognition of spatial variability and its interpretation followed by actions or procedures that are spatially varied. In other words, it allows for more

detailed identification of the differences within crops, understanding how these differences occur and the implication of this variability in the outcome. It also aids in planning actions taking into account the differences and seeking greater sustainability in all three dimensions - economic, environmental and consequently the social (Inamasu *et al.*, 2011).

PA has three main components: data acquisition on an appropriate scale and frequency, data analysis and interpretation, management and implementation of a response in an adequate spatial and temporal scale. It is likely that the most significant impact of PA on agriculture occurs in the way management decisions regarding the spatial and temporal variability of plant production system will be taken (Sonka *et al.*, 1997).

PA research started in the US, Canada, Australia, and Western Europe in mid-to late 1980s. Since then, its advantages are perceived and adopted around the world, not only in developed countries. Diverse types of PA technologies have been experimented throughout the world in developing countries as well, like China, Korea, Indonesia, Bangladesh, Sri Lanka, Turkey, Saudi Arabia, Australia, Brazil (Zhang *et al.*, 2002).

Rapid socio-economic changes in some developing countries are creating new scopes for the application of PA. The implications of dramatic shifts for economic development, poverty reduction and energy consumption, and urbanization in some developing countries are immense. Application of PA technologies based on the need of specific socio-economic condition of a country will make PA suitable not only for developed countries but also for developing countries and can work as a tool to reduce the gap between the developed world and the rest of the world (Mondal & Basu, 2009).

Factors in favor of associated adoption of PA technologies (PATs) can be grouped in the following categories: (1) socio-economic factors (farmers who are older and have higher education level), (2) agro-ecological factors (farmers whose farm has better soil quality, is self-owned, and is large), (3) institutional factors (farmers who face greater pressure for sustainability), (4) informational factors (farmers who have hired consultants and agreed on the usefulness of extension services), (5) farmer perception (farmers who perceived that PATs would bring profitability), and (6) technological factors (farmers who have used computers) (Tey & Brindal, 2012). The impact of PA technologies on agricultural production is expected in two areas: profitability for the producers and ecological and environmental benefits to the public (Zhang *et al.*, 2002).

In Australia the adoption rate of PATs increased significantly to 20% in 2008 compared to previous records of 2002 adaptation rates (Robertson *et al.*, 2012). Estimated annual benefits showed that the initial capital was recovered within 2-5 years of the outlay (Robertson *et al.*, 2009). Grain growers in Australia consider that PA systems are profitable, can recover the initial capital outlay within a few years providing intangible benefits from the use of the technology (Robertson *et al.*, 2007).

Not only in developed countries PATs are showing good socio-economic impacts. Sugarcane, corn and soy production chains in Brazil were analyzed and a simulated of its adoption showed a 10% increase in productivity (common when PATs are successfully adopted) leading to an increase of 5 to 6 billion dollars impact on Brazilian Gross Domestic Product and more than 450 thousand new jobs (Costa & Guilhoto, 2011). Authors consider that if negative impacts on pollution caused by the excessive use of fertilizers were evaluated, impacts would be even greater. Sugarcane production by companies that adopt PA practices is about twice its size that of companies that do not adopt them, in Brazil. Not only higher yields were

gained, benefits are also associated with managerial improvements, lower costs, minimization of environmental impacts and improvements in sugarcane quality. There is a growing interest on the use of PA practices amongst sugarcane companies, considering that 96% of them reported interest on increasing its use. (Silva *et al.*, 2011).

Satellite imagery has one of the highest adoption rates (76%) amongst PA technologies among sugarcane producers in Brazil (Silva *et al.*, 2011). Many farmers, especially in underdeveloped countries, are uncertain as to whether to adopt available PA technologies on their farms. Motivations for widespread uptake of PA technologies may come from strict environment legislation, public concern over excessive use of agro-chemicals, and economic gain from reduced agricultural inputs and improved farm management efficiency. Success of PA technologies will have to be measured by economic and environmental gains (Zhang *et al.*, 2002).

Remote sensing (RS) technology plays an important role in PA and its significance is increasing. Remote Sensing using space-borne sensors is a tool, par excellence, for obtaining repetitive (with a temporal resist from minutes to days) and synoptic scale (with local to regional coverage) observations on the spectral behavior of crops as well as their growing environment, i.e., soil and atmosphere (Seelan *et al.*, 2003).

Farmers throughout the world are constantly searching for ways to maximize their returns. Remote Sensing, Geographic Information Systems (GIS), and Global Positioning Systems (GPS) may provide technologies needed for farmers to maximize the economic and environmental benefits of precision farming (Seelan *et al.*, 2003).

2.2. CHARACTERIZATION OF TEF AND VEGETATION SPECIES IN ETHIOPIA

The new official classification of ecosystems in Ethiopia is as follows: Afroalpine and Sub-Afroalpine, Dry Evergreen Montane Forest and Grassland Complex, Moist Evergreen Montane Forest, *Acacia-Comiphora* Woodland, *Combretum-Terminalia* Woodland, Lowland Semi-Evergreen Forest, Desert and Semi-Desert Scrubland and Inland Waters (Institute of Biodiversity Conservation, 2005) discussed below.

2.2.1. Afroalpine and Subafroalpine Ecosystem

Ethiopia has the largest extent of afroalpine and subafroalpine habitats in Africa. These environments are peculiar in that there are no seasonal variations in temperature, but rather pronounced diurnal variations with “summer every day and winter every night” with strong insolation and outward radiation, frequent frost heaving on bare soil all year round (Hedberg, 1995 *apud* Institute of Biodiversity Conservation, 2005). Until as recently as 10,000 years ago (Messerli *et al.*, 1977 *apud* Institute of Biodiversity Conservation, 2005), the highlands of Ethiopia were widely covered with Afroalpine moorlands and grasslands. But, man has altered large regions of the highlands for centuries, mostly through conversion to agriculture. The rate of change is very alarming. The conversion results in the reduction of the original species richness. Thus the original afroalpine and subafroalpine natural communities are now restricted almost entirely to scattered and not easily accessible areas, which are surrounded and isolated by agricultural areas. More attention is needed to stop further the threats and rate of destruction (Institute of Biodiversity Conservation, 2005).

The ecosystem includes areas, which on the average are higher than 3200 m. The subafroalpine areas occur between 3200 and 3500 m, while the afroalpine areas occur between 3500 m and 4620 m. The ecosystem is characterized by the most conspicuous giant Lobelia, *Lobelia rhynchopetalum*, and evergreen shrubs including the heather, *Erica arborea* and perennial herbs such as *Helichrysum* species (Institute of Biodiversity Conservation, 2005).

2.2.2. Dry Evergreen Montane Forest and Grassland complex

This ecosystem represents a complex system of successions involving extensive grasslands rich in legumes, shrubs and small to large-sized trees to closed forest with a canopy of several strata occurring between (1600-) 1900-3300 m. This ecosystem covers much of highland areas and mountainous chains of Ethiopia in Oromia region (Shewa, Arsi, northern Bale and western Hararge), Amhara Region (Gojam, Welo, Gonder), Tigray Region (Tigray) and SNNP region (Shewa, Sidamo and Gamo Gofa). The areas with Dry Evergreen Afromontane forest have canopies usually dominated by Tid/Gatira (*Juniperus procera*) as a dominant species, followed by Weira/Ejersa (*Olea europaea* subsp. *cuspidata*), etc. Zigba/Birbirs (*Podocarpus falcatus*) is also found in sheltered valleys. The areas with Afromontane woodland, wooded grassland and grassland include the natural woodlands and wooded grasslands of the plateau with *Acacia abyssinica* and *A. negrii*. The grasslands occur in the areas where human activity has been largest and most intense, and found at altitudes between 1500 and 3000 m. The montane grassland in most places is derived from forest and other woody vegetation types. There exists also some edaphic grassland. The evergreen scrub vegetation occurs in the highlands of Ethiopia either as an intact scrub in association with the dry evergreen montane

forest or usually as secondary growth after deforestation of the dry evergreen montane forest (Institute of Biodiversity Conservation, 2005).

2.2.3. Moist Evergreen Montane Forest Ecosystem

This ecosystem is in most cases characterized by one or more closed strata of evergreen trees, which may reach a height of 30 to 40 m. The vegetation type in this ecosystem can be further divided into two (Friis, 1992; Sebsebe Demissew *et al.* 2004). One type includes what is traditionally referred as the Afro-montane rainforest. These forests occur in the southwestern part of the Ethiopian Highlands at between 1500 and 2600-m elevation and the Hareenna Forest on the southern slopes of the Bale Mountains. The forests characteristically contain a mixture of Zigba (*Podocarpus falcatus*) and broadleaved species as emergent trees in the canopy including Kerero (*Pouteria (Aningeria) adolfi-friederici*). Kerkha (the mountain bamboo- *Arundinaria alpina*) is also one of the characteristic species, although not uncommon is found locally. There are also a number of medium-sized trees, and large shrubs. The second type includes the Transitional Rainforest, which includes forests known from the western escarpment of the Ethiopian Highlands, in Wellega, Illubabor and Kefa. The forest type occurs between 500 and 1500 m elevation. The characteristic species in the canopy includes *Pouteria (Aningeria) altissima*, *Anthocleista schweinfurthii*, *Ficus mucoso* and species of *Garcinia*, *Manilkara* and *Trilepisium* (Institute of Biodiversity Conservation, 2005).

2.2.4. *Acacia-Comiphora* Woodland Ecosystem

This ecosystem is characterized by drought resistant trees and shrubs, either deciduous or with small, evergreen leaves occurring between 900 and 1900 m. This

vegetation type occurs in the northern, eastern, central and southern part of the country mainly in Oromia, Afar, Harare, Somali, and Southern Nations, Nationalities and Peoples Regional States. The trees and shrubs form an almost complete stratum and include species of Grar/Lafo (*Acacia senegal*, *A. seyal*, *A. tortilis*), Bedeno (*Balanites aegyptiaca*), and Kerbe (*Commiphora africana*, *C. boranensis*, *C. ciliata*, *C. monoica* and *C. serrulata*). The ground cover is rich in sub-shrubs, including species of *Acalypha*, *Barleria*, *Aerva*, and succulents with a number of Ret/Argessa (*Aloe*) species. The characteristic mammals include African Wild Ass, Grevy's Zebra and Black Rhinoceros. The characteristic birds include Hunter's Sunbird, Shining Sunbird, Somali Golden-breasted Bunting, Salvadori's Seedeater, Yellow-throated Serin, Ruppell's Weaver, White-headed Buffalo Weaver Golden-breasted Starling and Abyssinian Bush Crow (Institute of Biodiversity Conservation, 2005).

2.2.5. Combretum-Terminalia Woodland Ecosystem

This ecosystem is characterized by small to moderate-sized trees with fairly large deciduous leaves. These include Yetan Zaf (*Boswellia papyrifera*), *Anogeissus leiocarpa* and *Stereospermum kunthianum* and species of Weyba (*Terminalia*), *Combretum* and *Lannea*. The solid-stemmed lowland bamboo, Shimel (*Oxytenanthera abyssinica*) is prominent in river valleys [and locally on the escarpment] of western Ethiopia. 14 The vegetation type occurs along the western escarpment of the Ethiopian Plateau, from the border region between Ethiopia and Eritrea to western Kefa and the Omo Zone (in the SNNP Region); it is the dominant vegetation in Benshangul-Gumuz and Gambella Regions, and the Dedessa Valley in Wellega in Oromia Region, where it occurs between 500 and 1900 m. The vegetation in this ecosystem has developed under the influence of fire. The soil erosion rate is

very high especially at the onset of rains (Institute of Biodiversity Conservation, 2005).

2.2.6. Lowland, Semi-evergreen Forest Ecosystem

This ecosystem includes forests that are restricted to the Lowlands of eastern Gambella Region in Abobo and Gog Weredas. They occur between 450 and 650 m on sandy soils. They are semi-deciduous, with a 15-20 m tall, more or less continuous canopy in which *Baphia abyssinica* is dominant, mixed with less common species including *Celtis toka*, *Diospyros abyssinica*, *Malacantha alnifolia*, and *Zanha golungensis* and species of *Lecaniodiscus*, *Trichilia* and *Zanthoxylum* (Institute of Biodiversity Conservation, 2005).

2.2.7. Desert and Semi-desert Scrubland Ecosystem

This ecosystem is characterised by highly drought tolerant species of Grar/Lafto (*Acacia brichettiana*, *A. stuhlmanii* and *A. walawensis*), Etan (*Boswellia ogadenensis*) Kerbe (*Commiphora longipedicillata* and *C. staphyleifolia*), as well as succulents, including species of *Euphorbia* and *Aloe*. The doum palm (*Hyphaene thebaica*), grasses such as *Dactyloctenium aegyptium* and *Panicum turgidum* are also characteristic species. The characteristic birds include Kori Bustard, Arabian Bustard, Blackhead Plover, Temminck's Courser, Two-banded Courser, Tawny Pipit, Chestnut-bellied Sandgrouse, Lichtenstein's Sandgrouse, Singing Bush Lark and Masked Lark. This ecosystem type occurs in the Afar Depression, the Ogaden, around Lake Chew Bahir and the Omo Delta below an altitude of 500 m. The semi-desert parts are found in the northern western and Northeastern parts of the country (Amhara, Tigray and Afar), Southern (Oromia and Southern Nations and Nationalities

and Peoples Region) and the Southeastern and eastern (Somali) parts. The northern parts of Afar and northeastern Tigray are predominantly deserted. Fragmentation and overgrazing of the rangeland has also affected wild animals. In this ecosystem, Wild Ass is critically endangered and has appeared in the 1996 IUCN list of threatened animals (Institute of Biodiversity Conservation, 2005).

2.2.8. Aquatic Ecosystem

This ecosystem consists of both running (lotic) and standing (lentic) inland water bodies, including rivers, lakes, reservoirs, swamps, wetlands and aquatic bodies with transient water contents during some time of the year. The strict IUCN definition of wetlands has been slightly modified to include all types of lakes in this document. Although the floristic composition of the riverine vegetation varies depending on altitude and geographical location, in general it is mainly characterised by species of *Celtis africana*, *Mimusops kummel*, *Tamarindus indica*, etc. The swamps, reservoirs and shores of lakes are dominated by species of sedges and grasses. Aquatic resources in this ecosystem include over 180 fish species of which some 30 to 50 are endemic. In addition several invertebrates groups with variable endemicity are present (Golubstov and Mina, 2003 *apud* Institute of Biodiversity Conservation, 2005). In the rivers and lakes, numerous species of planktonic and benthic fauna have been reported. Moreover, the aquatic ecosystem harbours over 200 species of phytoplankton, including many important Bluegreen algal species such as *Spirulina (Arthrospira)*. Studies of the planktonic life forms started only recently. These diverse aquatic habitats serve as breeding, feeding and roosting sites for a large number of resident and migrant birds including the endemics such as Spot-breasted Plover, Blue-winged Goose and Rouget's Rail and about 10 species that are globally threatened. Aquatic mammals that frequently use this ecosystem

include Hippopotamus, Nile Lechwe, Common Waterbuck and Bush Elephant. The habitat is also used by considerable species of reptiles such as the Nile crocodile. Some of the lakes harbour endemic fish species; for example Lake Tana is unique for its *Barbus* flock. This is the only remaining stock after the demise of similar population in Lake Lanao (Philippines). Thus this lake has international significance and serves as a natural laboratory for evolutionary investigation. Baro and Akobo are also 'hotspot' of aquatic biodiversity (Institute of Biodiversity Conservation, 2005).

2.2.9. Tef species in Ethiopia

Ethiopia has a very high genetic diversity in four of the world's widely grown food crops (wheat, barley, sorghum, peas), in three of the world's most important industrial crops (linseed, castor, and cotton), in the world's most important cash crop (coffee), in a number of food crops of regional or local importance (tef, finger millet, cowpeas, lentil, enset, etc) and in a number of groups of forage plants of world importance (clovers, lucerns, oats, etc.). Ethiopia is one of the twelve Vavilov Centers of crop diversity. In this regard the contribution of Ethiopian farmers in generating and maintaining the diversity of many crop plants has been indispensable. Ethiopia is considered as the primary gene center for field crops such as Noun (*Guizotia abyssinica*), Tef (*Eragrostis tef*), and Ethiopian mustard (*Brassica carinata*). Introduced field crops have developed wide ranges of genetic diversity under local ecological conditions and agricultural practices (Institute of Biodiversity Conservation, 2005).

The species classification of the genus *Eragrostis* exhibit its taxonomic complexity; spike morphology, including size of palea and lemma, has been found to be the most useful feature for classifying the genus into broad groups of species (Phillips, 1995 *apud* Demissie, 2000). Nevertheless, it is estimated that the genus

contains about 350 species, which are widely spread throughout the tropical and subtropical regions of the world. Forty-three percent of the species are known to occur in Africa alone. South America, Asia, Australia, Central America, North America and Europe contribute 18%, 12%, 10%, 9%, 6%, and 2% in that order (Costanza, 1974 *apud* Demissie, 2000). The reports in the number of *Eragrostis* species that were recorded in Ethiopia are not consistent except that both annual and perennial species exist as a culturally important and threatened species. According to Cufodontis (1974 *apud* Demissie, 2000) 54 species are found in Ethiopia, out of which 14 are said to be endemic. Recent estimates indicated that only 44 species are found in Ethiopia (Phillips, 1995 *apud* Demissie, 2000). Both figures indicate that there exists a considerable proportion of endemism in the country, and thus a large gene pool that may be useful for tef improvement (Demissie, 2000).

2.3. DROUGHT AND TEF CROP STRESS

Rainfed farming is dominant in Ethiopia and has low productivity because of erratic and insufficient rainfall during the growing season (Gommes & Petrassi, 1994). In Ethiopia, the 1984 drought caused the deaths of about 1 million people, 1.5 million head of livestock perished, and 8.7 million were affected in all. In 1987, more than 5.2 million people in Ethiopia were severely affected. Rainfall records indicate that, in some parts of the sub-Saharan Africa, the drought in 2000 was worse than that experienced in 1984 (Drought Monitoring Center, 2000 *apud* Rojas et al., 2011).

Rainfed farming is dominant in Ethiopia and has low productivity because of erratic and insufficient rainfall during the growing season (Meze-Hausken, 2004). Arid and semiarid regions of the world, such as Ethiopia, suffer much from this crop production constraint because of the inadequacy, irregularity or intensity of their natural rainfall patterns. Frequently recurrent droughts supplemented with lack of

efficient use of existing water resources have amplified the impact of drought on the livelihood of Ethiopian farmers (Mengistu, 2009). Widespread drought can lead to crop failures, with associated deterioration in food security (Senay & Verdin, 2003).

The maximum yield of plants, determined by their genetic potential, is seldom achieved because factors such as insufficient water or nutrients, adverse climatic conditions, plant diseases, and insect damage will limit growth at some stage. Plants subjected to these biotic and abiotic constraints are said to be stressed. The term "stress" can be defined as any disturbance that adversely influences growth (Jackson, 1986).

The lowlands of Ethiopia and the main productive areas of Kenya have been affected by the 1984 drought (Gommes & Petrassi, 1994). In Ethiopia, the 1984 drought caused the deaths of about 1 million people, 1.5 million head of livestock perished, and 8.7 million were affected in all. In 1987, more than 5.2 million people in Ethiopia were severely affected. Rainfall records indicate that, in some parts of the sub-Saharan Africa, the drought in 2000 was worse than that experienced in 1984 (Drought Monitoring Center, 2000 *apud* Rojas *et al.*, 2011).

Whether or not they are detectable by sight or touch, changes that take place as a result of stress affect the amount and direction of radiation reflected and emitted from plants. Reflectance of light from a plant canopy depends not only on the reflectance properties of individual leaves and stems but also on the ways in which they are oriented and distributed. Under stress it is likely that both of these factors will change. Changes that take place as a result of stress affect the amount and direction of radiation reflected and emitted from plants. Remote-sensing techniques are capable of measuring radiation and therefore offer the possibility of quantitatively assessing plant stress caused by biotic and abiotic factors (Jackson, 1986).

2.3.1. Crop and Soil Property within the Field

Tef belongs to the grass family, Poaceae, sub-family Chloridoideae (Eragrostoidae), tribe Eragrostidae, sub-tribe Eragrostae, and genus Eragrostis. The genus Eragrostis comprises about 350 species (Watson and Dallwitz 1992). Although the crop species have had several synonyms previously used by several authors, its presently most accepted binomial nomenclature is *E. tef* (Zucc.) Trotter. In cultivation as a cereal, tef is the only species in the genus Eragrostis and together with finger millet (*Eleusine crochana* L.) they constitute the sole two species in the sub-family Chloridoideae cultivated for human consumption of the grains. (Assefa *et al.*, 2011)

According to the survey recently conducted by Mamush (2011, personal communication) tef is a staple food for at least 40% of the Ethiopians (34 million). However many agree that majority of the Ethiopians consume tef at least 3 times a week. In Ethiopia, tef grain is mainly used for food after baking the ground flour into pancake-like soft and sour bread, “injera”, which forms the major component of the favorite national dish of most Ethiopians. It is also consumed in the form of porridge, and slightly fermented or un-fermented non-raised breads (“kita” and “anebabero”) (Davison *et al.*, 2004). Although recent economic feasibilities might have limited such uses, the grain is also used for brewing native beer, “talla”, and more alcoholic cottage liquor, “katikalla” or “arakie”. Tef is produced mainly for food but its straw is also used as animal feed and as construction material for houses. (Assefa *et al.*, 2011).

Tef has higher market prices than the other cereals, for both its grain and straw. Tef grain is not attacked by weevils, which means that it has a reduced postharvest loss in storage and requires no pest-controlling storage chemicals. Tef is

also gaining popularity as healthy food (Spaenij- Dekking *et al.*, 2005) in the western world menus. Tef is high in iron content and contains no gluten (Roseberg *et al.*, 2006).

The long-sustained extensive cultivation of tef in Ethiopia can be attributed to its relative merits over other cereals both in husbandry and utilization (Ketema 1993). Of these, its merits in cultivation, include: (1) versatile adaptation 0– 3000 m above sea level; (2) resilience to both drought and water-logging stresses; (3) fitness for various cropping systems; (4) use as a catch and low-risk reliable crop especially in replacement cultures for failures of early sown long-season crops (e.g. maize and sorghum) due to environmental calamities or pests; and (5) little or no serious threats of disease and pest epidemics, at least, in its major production belts. (Assefa et al, 2011).

On the other hand, its beneficial features with respect to utilization involve: (1) best quality and most consumer-preferred injera of the grains; (2) high returns in flour (Ebba 1969) and in injera; (3) minimal post-harvest losses due to storage pests and diseases coupled with high storage longevity (storability); (4) importance of the straw mainly as fodder for cattle and as a binder of mud used for plastering walls of local houses; and (5) cash crop value owing to the high market prices of both the grains and the straw (Assefa et al, 2011).

Tef performs well from 1800 up to 3000 Masl. An average rainfall of 300-700 mm with enough distribution especially at early stage is good for tef. However in areas where 800-1200mm rainfall tef gives a good harvest. Tef performs well on various soil types (Mamo *et al.*, 2000). Through implementation of appropriate or recommended technologies tef can be grown in different soil types. Loomy black soils (Vertisols) are the best for tef growing. Most tef growing areas of Ethiopia has

black soils. tef growth in those areas is preferred because of its improved development. However, water has to be drained out well in black soils.

Production of Tef in Ethiopia is not mechanized yet. Plough is done by oxen. Oxen called “Maresha” are the only means of plough in almost all tef growing areas and this practice has been done since thousands of years ago. Tef fields have to be well ploughed 3 to 4 times before planting. Tef seeds are tiny, weight about 19-42 mg (Yifru, 1998). The conventional tillage by maresha includes a primary tillage, followed by repeated secondary shallow tillage, aiming at controlling weeds, conserving moisture and aerating the soil (Melesse *et al.*, 2008).

Planting of Tef is done by broadcasting the feeds by hand. Seed rate in most tef farmers of the country is 25-50 kg/ha. (MoARD, 2010). A new technology for transplanting seedlings is to be introduced in 90 farmers training centers. In this case seed rate is increased up to 400 gr/ha.

Main weed species causing damages to tef plants are *Cyperus* spp, *Sefaria* spp. *Guizofia* spp, *Convolvulus* spp and *Argemone* spp. Mainly hand weed removal as weed control is applied but some areas are treated with chemicals.

Tef is less attacked by diseases compared to cereals and grains however rust and damping off can attack the crop. No fungicides or chemicals are sprayed to tef crops. Tef is harvested by driving animals over the grass and the remaining threshing activities are carried by human labor.

2.3.2. Crop Yield Management System

Much of the increase in crop production in the past decade has been due to increases in area cultivated, although better yields also contributed to the augmented production in Ethiopia during 2004/05–2007/08 period (Table 1. Tef production and

productivity along years 1990 to 1994.) (MoARD, 2011). With little suitable land available for expansion of crop cultivation, especially in the highlands, future tef production growth will need to come from yield improvements. Current cereal yields are low, by international standards, indicating growth potential. Current use of inputs is at a low level, suggesting substantial scope for raising productivity through irrigation, improved seeds, and application of fertilizers (Taffesse *et al.*, 2011). Poverty-reduction strategy adopted by Ethiopia seeks to achieve growth through the commercialization of smallholder agriculture (Gebreselassie & Sharp, 2008).

Table 1. Tef production and productivity along years 1990 to 1994.

Description		1990	1991	1992	1993	1994	Average
Area (M.ha)		2.59	2.48	2.56	2.4	2.25	2.46
Produce (M.Qts)		21.76	24.38	29.93	30.28	31.79	27.63
Productivity (t ha)		9.69	10.14	11.67	12.2	12.28	11.2
Proportion to cereals and grains in %	Area	27.84	28.33	29.32	28.28	28.37	28.37
	Production	18.71	18.93	21.82	20.89	20.46	20.16

Source: MoARD, 2011

According to the Central Statistics Authority of Ethiopia (CSA, 2010) and the Ministry of Agriculture of the Federal Democratic Republic of Ethiopia (MOARO 2010, unpublished paper), Tef is cultivated on about 2.59 million hectares of land (Table 2. Area, production and yields of cereals in Ethiopia, 2003/04 and 2007/08).

Covering around 30% of the total average of cereal and grain, its area showed 35% increase since the last ten years. Tef is grown at large in four regional states of Ethiopia, Tigray, Amhara, Oromia and South, with an average yield of 10.86, 12.85, 12.15, 11.88 Quintals per hectare in that order. It fetches the highest market price of any food grain in Ethiopia (Gebreselassie and Sharp, 2008).

Table 2. Area, production and yields of cereals in Ethiopia, 2003/04 and 2007/08

Cereal crop	2003/04				2007/08				Growth rate (%)			
	Area 000 ha	Production 000 tons	Yield Tons/ha	Area share %	Area 000 ha	Production 000 tons	Yield Tons/ha	Area share %	Area	Production	Yield	Area share %
Barley	911	1,071	1,2	13,4	985	1,355	1,4	11,4	8,1	26,5	17, 0	-14,9
Maize	1,300	2,455	1,9	19,1	1,767	3,750	2,1	20,4	35,9	52,7	12, 3	6,8
Millet	303	304	1,0	4,5	399	538	1,3	4,6	31,7	77,0	34, 4	2,2
Sorghum	1,242	1,695	1,4	18,2	1,534	2,659	1,7	17,7	23,5	56,9	27, 0	-2,7
Tef	1,985	1,672	0,8	29,1	2,565	2,993	1,2	29,6	29,2	79,0	38, 6	1,7
Wheat	1,075	1,589	1,5	15,8	1,425	2,314	1,6	16,4	32,6	45,6	10, 0	3,8
Other	35	44	1,3	0,5	55	108	2,0	0,6	57,1	145,5	56, 1	20,0
Total Cereal	6,816	8,786	1,3	100	8,675	13,609	1,6	100	27,3	54,9	21, 7	

Source: Yu *et al.*, 2010

Yihun *et al.*, (2013) observed that a maximum grain yield of 3.3 t/ha was obtained under irrigation when tef was not subject to any water stress. This is three fold the yield farmers currently harvest from rainfed agriculture. The yield and water productivity differences are insignificant between a full irrigation and a 25% deficit irrigation distributed throughout the growth period at seeding rates of 25 kg/ha and 10 kg/ha. The authors recommend, when water is scarce and irrigable land is relatively abundant as is the case in Ethiopia, adopting the 25% water deficit irrigation with 10 kg/ha seeding rate may be optional. A maximum water deficit of 50% during the late season stage has an insignificant impact on Tef yield and water productivity.

Tef sensitivity to drought depends on the stage during which the stress occurs. The grain filling stage of tef was the most sensitive to water stress and

severe water stress caused significant reduction in physiological performance of tef (Mengistu, 2009; Mengistu & Mekonnen, 2012). This is probably the best time to provide sufficient water for tef optimum development and production from the existing level of water stress. Tsegay *et al.*, 2012 also noticed that water stress particularly at the later development stage of crops affected tef productivity as the result of earlier cessation of the rainfall. The authors observed an increase of 27% in reference harvest index of tef in response to mild water stress during the yield formation of up to 33%.

Increased yield was also observed by Assefa *et al.*, (2011) while studying the optimum tillage frequency, time and weeding frequency for tef production. Grain yield increased linearly as tillage frequency increased. Twice weeding increased yield by 39% over un-weeded. The highest grain yield was obtained when seven times plow was combined with weeding twice which resulted in an increase of yield by 96% over the lowest yield treatment (one plow + roundup + un-weeded). However, three times plowing combined with hand weeding at tillering was found to be an economical practice with the highest marginal rate of return and net benefit. It is, therefore, recommended to small-scale farmers around as a way of promoting sustainable crop production with fewer unfavorable effects on the environment

2.4. REMOTE SENSING FOR CROP MONITORING

Remote sensing is the science and art of obtaining information about an object, area, or phenomenon, through the analysis of data acquired by a device that is not in contact with the object, area, or phenomenon under investigation (Lillesand & Kiefer, 1994).

The Sun is the main energy source for the entire solar system and generates a large amount of energy that is radiated to the entire space. The solar radiation reaches the Earth where it is partly reflected back to space and partly absorbed by terrestrial objects transformed into heat or other forms of energy. Radiant energy can also be generated on Earth by heated objects or by other physical phenomena (Stefen & Moraes, 1993).

If we organize all our knowledge on different types of electromagnetic radiation, we have a graph like Figure 1, called electromagnetic spectrum, which was built based on the wavelengths (or frequencies) known radiation. The spectrum is divided into regions or bands whose names are related to the way in which radiation can be produced or detected (Stefen & Moraes, 1993).

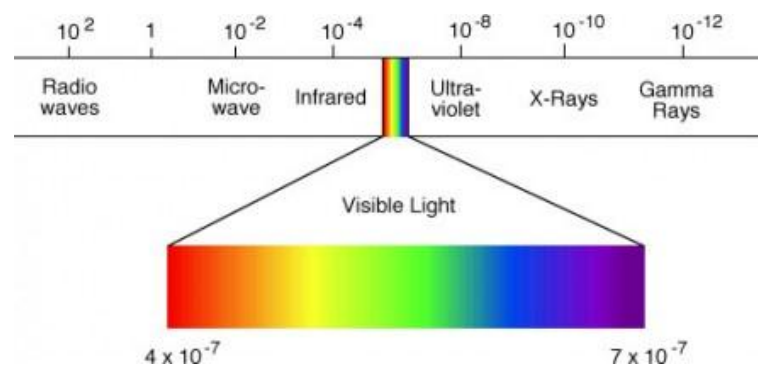


Figure 1. Electromagnetic spectrum. Source: <http://www.redorbit.com>

When radiation interacts with an object, it can be reflected, absorbed or transmitted. In general the portion absorbed is transformed into heat or some other type of energy and the reflected spreads through space. The factor that measures the ability of an object to reflect the radiant energy indicates its reflectance, whereas the ability to absorb radiant energy is indicated by its absorbance and, likewise, the ability to transmit radiant energy is indicated by its transmittance (Jensen, 1986).

We can measure the reflectance of an object for each type of radiation that composes the electromagnetic spectrum and then realize, through this experience, that the reflectance of the same object can be different for each type of radiation that reaches it. The curve in Figure 2 shows how a green leaf has different values of reflectance for each wavelength, from the blue band to the near-infrared band. This type of curve, which displays the reflectance of an object for each wavelength, is called a spectral signature and depends on the properties of the object (Lillesand & Kiefer, 1994).

Source: <http://www.inpe.br/unidades/cep/atividadescep/educasere/apostila.htm>

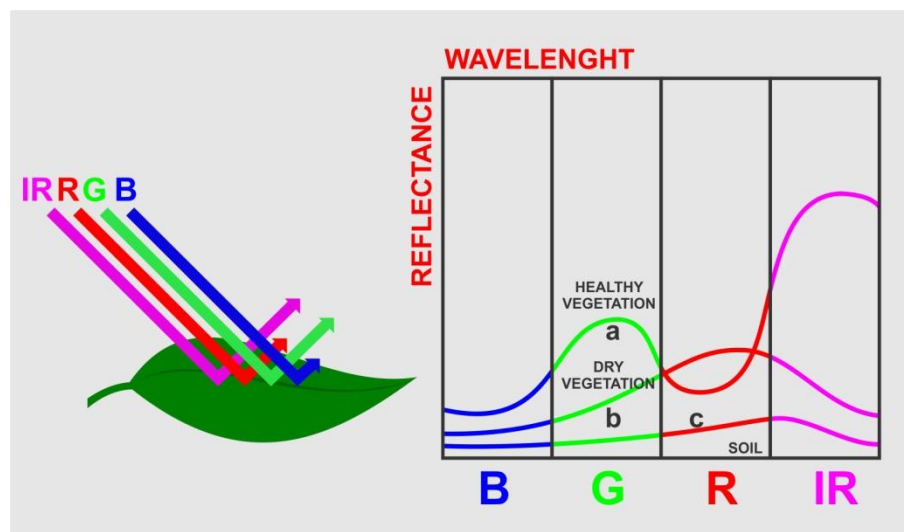


Figure 2. Spectral signatures of vegetation.

The term resolution in remote sensing unfolds in truth in three different (and independent) parameters: spatial resolution, spectral resolution and resolution radiometric (Crosta, 1993).

Spatial resolution refers to the ability of the sensor system to distinguish and measure the targets. This ability is based on geometric projection of the detector onto

earth surface, defining the field of view area of the instrument at a certain altitude and at a specific time. The angle defined by this projection is called instantaneous field of view (IFOV). The IFOV defines the area of the land targeted to a given altitude by instrument sensor (Florenzano, 2002). It is related to the size of the smallest object that can be located in fields or detected in an image. The basic unit in an image is called a pixel. One-meter spatial resolution means each pixel image represents an area of one square meter. The smaller an area represented by one pixel, the higher the resolution of the image.

Spectral resolution is a measure of the spectral bands width and sensor system sensitivity to distinguish between levels of intensity of signal return (Novo, 1989). For a better understanding of this concept, Jensen and Jackson (2001) emphasize two important points: the wavelength detected by the sensor and the number of spectral bands. More bands and smaller band width means improved target discrimination and better spectral resolution (Melo, 2002).

Radiometric resolution refers to the ability of the sensor system to detect variations in spectral radiance received. The radiance of each pixel goes through a digital encoding, obtaining a numerical value, expressed in bits, called Digital Number (DN). This value is easily translated into an intensity or a visual gray level located in a finite interval $(0, K-1)$, where K is the number of possible values, called quantization levels (Schowengerdt, 1983). Spectral resolution refers to the number of bands and the wavelength width of each band. A band is a narrow portion of the electromagnetic spectrum. Shorter wavelength widths can be distinguished in higher spectral resolution images. Multispectral imagery can measure several wavelength bands, such as visible green or NIR. Landsat, Quickbird, and Spot satellites use multispectral sensors. Hyperspectral imagery measures energy in narrower and more numerous bands than multispectral imagery. The narrow bands of hyperspectral

imagery and more sensitive to variations in energy wavelengths and, therefore, have a greater potential to detect crop stress than multispectral imagery. Multispectral and hyperspectral imagery are used together to provide a more complete picture of crop conditions.

The number of gray levels is expressed in bits, or in other words, expressed as a function of binary digits number needed to store, in digital form, the maximum gray level value. This value is always a power of 2, for example 8 bits mean 28, equals to 256 gray levels. The differences are larger in levels 2 and 4 than in levels 256 and 2048, due to the fact that the human eye does not have sensitivity to changes in intensity above 30 gray levels (Crosta, 1993).

Temporal resolution refers to the frequency at which the sensor passes the same place, in a specific period of time. This cycle is related to the orbital platform characteristics (height, speed, inclination), and the sensor total aperture angle. The temporal resolution is of great interest especially in studies related to changes in the Earth's surface and its monitoring (Lillesand & Kiefer, 1994).

Rapid advances in remote sensing for precision agriculture have occurred over the last twenty five years. Satellite imagery has improved in spatial resolution, return visit frequency and spectral resolution. Aerial hyperspectral imagery has revolutionized the ability to distinguish multiple crop characteristics, including nutrients, water, pests, diseases, weeds, biomass and canopy structure. Ground-based sensors have been developed for on-the-go monitoring of crop and soil characteristics such as N stress, water stress, soil organic matter and moisture content (Mulla, 2013).

2.4.1. Tef Reflectance Characterization Using Spectroradiometer

2.4.1.1. Ground Measurements

Field spectroscopy involves the study of the interrelationships between the spectral characteristics of objects and their biophysical attributes in the field environment (Milton, 1987). Spectroscopy can be considered a multichannel radiometry (Harris, 2005). Radiometry is the measurement of optical radiant energy. It also refers more generally to the principles and laws behind the generation, propagation, and detection of optical radiation (Wolfe, 1998). Although it is the science of measuring light in any portion of the electromagnetic spectrum, in practice, the term is usually limited to measurement of infrared, visible, and ultraviolet light using optical instruments (Ashdown, 2002).

The most widely used methodology in field spectroscopy concerns measurement of the reflectance of composite surfaces in situ. Increasingly, spectral data are being incorporated into process-based models of the Earth's surface and atmosphere, and it is therefore necessary to acquire data from terrain surfaces, both to provide the data to parameterize models and to assist in scaling-up data from the leaf scale to that of the pixel (Milton *et al.*, 2009).

The radiation geometry of the field environment is shown in the Figure 3. Positions of the primary source of irradiation (the Sun) and the sensor are each defined by two angles, the angle from the vertical (the zenith angle, θ) and the angle measured in the horizontal plane from a reference direction (the azimuth angle, ϕ). (Milton, 1987)

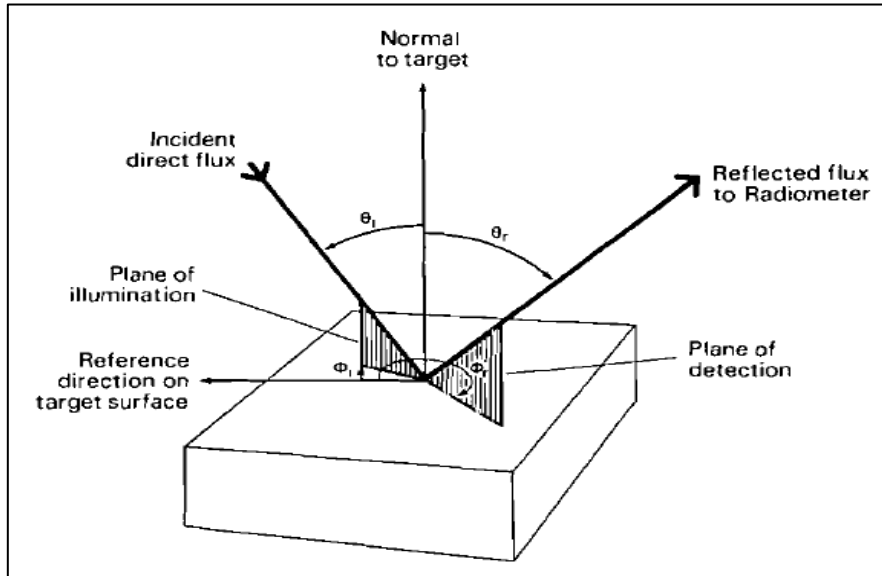


Figure 3. Radiation geometry of the field environment. Source: Milton, 1987.

Ignoring skylight, the energy from the Sun and the energy reflected to the sensor can be thought of as being confined to two slender elongated cones, each subtending a small angle at the target surface, termed solid angles and measured in steradians (sr) (McCoy, 2005).

Consider the incident solar energy (irradiance) and the reflected energy (radiance) as two elongated cones, each forming small solid angles at a point on the target surface (Figure 4). The reflectance of that particular point on the target can be expressed as a ratio of the radiance to the irradiance. The practical alternative to measuring the indicatrix is to measure samples of radiance from the target along with the radiance of a standard white reflectance panel to represent irradiance. In order to fully express the hemispherical reflection characteristics of an entire target, rather than only a point, it would be necessary to measure the irradiance and radiance at all possible sensor positions and all possible source positions. This hemisphere of reflected radiation within a specified spectral range is referred to as the target's

spectral indicatrix (Goel, 1988; Curran, Foody, Kondratyev, Kozoderov, & Fedchenko, 1990) (McCoy, 2005).

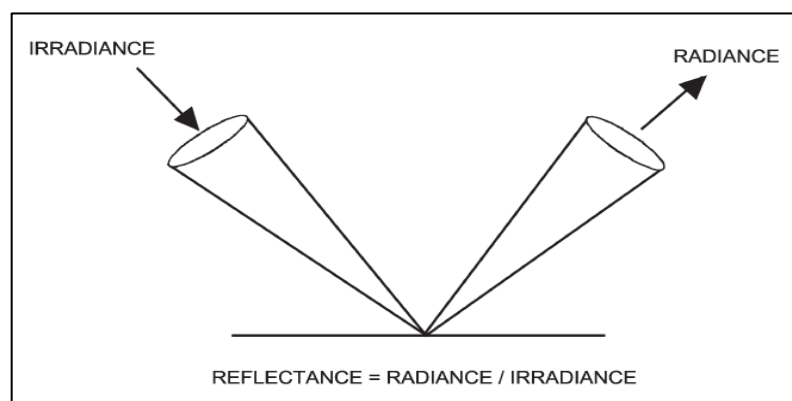


Figure 4. Direct irradiant flux and diffuse radiant flux. Source: McCoy, 2005

The practical alternative to measuring the indicatrix is to measure samples of radiance from the target along with the radiance of a standard white reflectance panel to represent irradiance (Figure 5). Reflectance (R), then, is a ratio of target radiance to panel radiance. Reflectance (R), then, is a ratio of target radiance to panel radiance.

$$R = \left(\frac{\text{radiance of target}}{\text{radiance of panel}} \right) * k \quad (1)$$

The constant, k , a panel correction factor, is a ratio of solar irradiance to panel radiance and ideally should be near 1. We assume that the reference panel is a Lambertian reflector; hence, it would have the same correction constant regardless of variations in zenith or azimuth angles of the incident radiation (Nicodemus, 1977; Robinson & Biehl, 1979; Jackson, Clarke, & Moran, 1992) (McCoy, 2005).

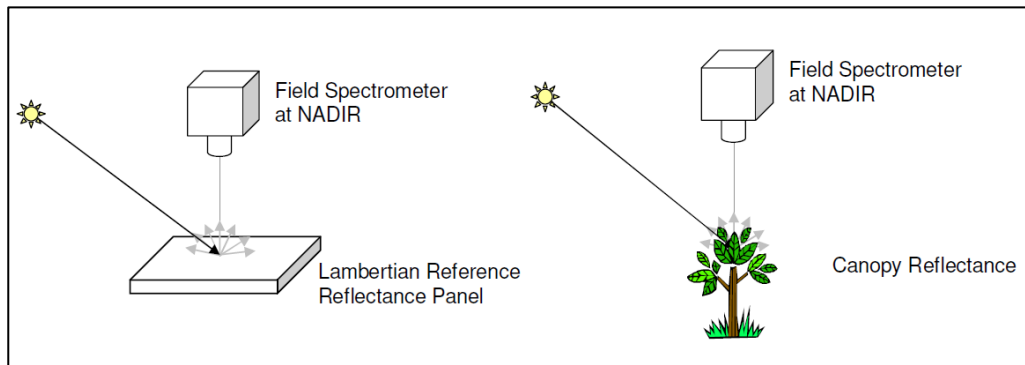


Figure 5. Instrument configuration for measurement. Source: Mac Arthur, 2011.

A variety of passive remote sensors are used to obtain data of Earth surface materials, such as (Nasa, 2013):

- Radiometer: an instrument that quantitatively measures the intensity of electromagnetic radiation in some band of wavelengths in the spectrum. Usually a radiometer is further identified by the portion of the spectrum it covers; for example, visible, infrared, or microwave.
- Spectrometer: a device designed to detect, measure, and analyze the spectral content of the incident electromagnetic radiation is called a spectrometer. Conventional, imaging spectrometers use gratings or prisms to disperse the radiation for spectral discrimination.
- Spectroradiometer: a radiometer that can measure the intensity of radiation in multiple wavelength bands (i.e., multispectral). Oftentimes the bands are of a high spectral resolution - designed for the remote sensing of specific parameters such as sea surface temperature, cloud characteristics, ocean color, vegetation, trace chemical species in the atmosphere, etc

Field measurements are usually made using a mast or tripod to ensure a fixed geometry between the sensor, the standard panel and the target. Hand-held

measurements are less precise because of the variable geometry of the operator to the target and of the target to the instrument (Milton, 1987).

According to McCoy (2005), the following field procedures are suggested for improving accuracy of field data collected:

1. Maintain a consistent viewing geometry relative to the solar azimuth angle. This procedure assures that spectral samples are taken from the same portion of the target radiance hemisphere with each measurement. The operator must change the viewing azimuth through the course of the day as the solar azimuth angle changes. This is easy to do by standing with one's back to the sun at every measurement site while measuring both the reference panel and the target. Of course, this position must be assumed in a way that does not cast the operator's shadow on the reference panel or the target. Consistency in distance of the sensor from the target must also be maintained as a part of the viewing geometry.

2. Determine that the reference panel and the target each overfill the FOV of the sensor while taking a measurement. This is a condition that must be considered in order to establish an appropriate distance from the sensor to either the panel or the target.

3. Vehicles and persons other than the operator should be kept several meters away from the target. The operator should wear dark clothing and, as mentioned above, stand facing away from the sun. Tripods or truck-mounted booms should be painted flat black. These precautions will reduce the variability of measurements.

4. Multiple measurements should be taken when measuring vegetation foliage in order to compensate for movement of the target by wind.

5. Measurements should be made at a time when direct solar flux is the dominant incident radiation. Ideally, there should be a perfectly clear sky with no haze, but in the real world this is an elusive condition.

6. Field work should be limited to periods of high sun. Great variation in incident radiation occurs as sunlight passes through longer stretches of atmosphere with increasing path lengths through haze and dust. It is best to restrict measurements to a period about 2 hours before and after solar noon.

2.4.1.2. Tef Reflectance Spectra

The absorption and reflection of solar radiation is the result of many interactions with different plant materials, which varies considerably by wavelength. Water, pigments, nutrients, and carbon are each expressed in the reflected optical spectrum from 400 nm to 2500 nm, with often overlapping, but spectrally distinct, reflectance behaviors. Leaves vary widely in both shape and chemical composition (McCoy, 2005).

Vegetation reflectance is known to be primarily a function of tissue (leaf, woody stem and standing litter) optical properties, canopy biophysical attributes (for example, leaf and stem area, leaf and stem orientation, and foliage clumping), soil reflectance, illumination conditions, and viewing geometry. Foliage interacts with radiation and processes of absorbance, reflection and transmittance occurs. Leaf optical properties are a function of leaf structure, water content and the concentration of biochemical (Asner, 1998).

Relative concentrations of plant pigments such as chlorophyll, carotenoids, and anthocyanins vary significantly and influence vegetation reflectance at the same extent. Chlorophyll concentrations in leaves are broadly correlated with photosynthetic rates. Leaf pigments only affect the visible portion of the shortwave

spectrum (400 nm to 700 nm). Water features centered around 970 nm and 1190 nm are pronounced and can be readily measured from hyperspectral sensors. Plants of different species inherently contain different amounts of water based on their leaf geometry, canopy architecture, and water requirements. Leaf water affects plant reflectance in the near-infrared and shortwave infrared regions of the spectrum. Plants contain carbon in many forms, including sugars, starch, cellulose, and lignin. Cellulose and lignin display spectral features in the shortwave infrared range of the shortwave optical spectrum. Nitrogen concentrations in foliage are linked to maximum photosynthetic rate and net primary production. Some proteins that contain nitrogen affect the spectral properties of leaves in the 1500 nm to 1720 nm range (Asner, 1998).

The amount of foliage and the architecture of the canopy are also meaningful in determining the scattering and absorption properties of vegetation canopies. Vegetation with mostly vertical foliage, such as grass, reflects light differently than foliage with more horizontally-oriented foliage, seen frequently in trees and tropical forest plants (Asner, 1998).

Tef reflectance spectra of plants under water stress and unstressed plants grown in Blythe (California, U.S.) were measured using a field spectroradiometer (Hanna & Rethwisch, 2003). Although environmental conditions and plant response in U.S. are very different than those in arid climate Ethiopia, analysis of spectral behaviour of tef plant leaves and canopy is very important to understand tef reflectance in satellite imagery and as a comparison with future studies.

Hanna & Rethwisch, (2003) considered that characteristics of tef plants such as the presence of culms, spikelets, lateral veins, pedicels, panicle, flowering scales and flower scale colors can affect the spectral signature of the crop collected at ground- and satellite-level. Additionally, appearance of the plant as a bunch of grass

with large crowns and many tillers could affect the spectral signature of the plant. The spectra of tef grass exposed to different types of water stress was evaluated and showed lower peaks in the reflectance in the stressed vegetation than the unstressed (Figure 6). For the authors, the reason may be the shape of leaves affected by stress and reduction in the greenish part rather than in the unstressed. Possibly photosynthesis chemical pigmentation and activity could be affected by plants suffering from water stress. The more greenish part could be seen in the range of 700-1100-1350-1550nm in the spectra. The peaks of 750-900nm showed less reflectance (i.e. 0.45 % reflectance) in the stressed plants and the opposite in the less stressed plants (i.e. 0.55-0.80 %reflectance).

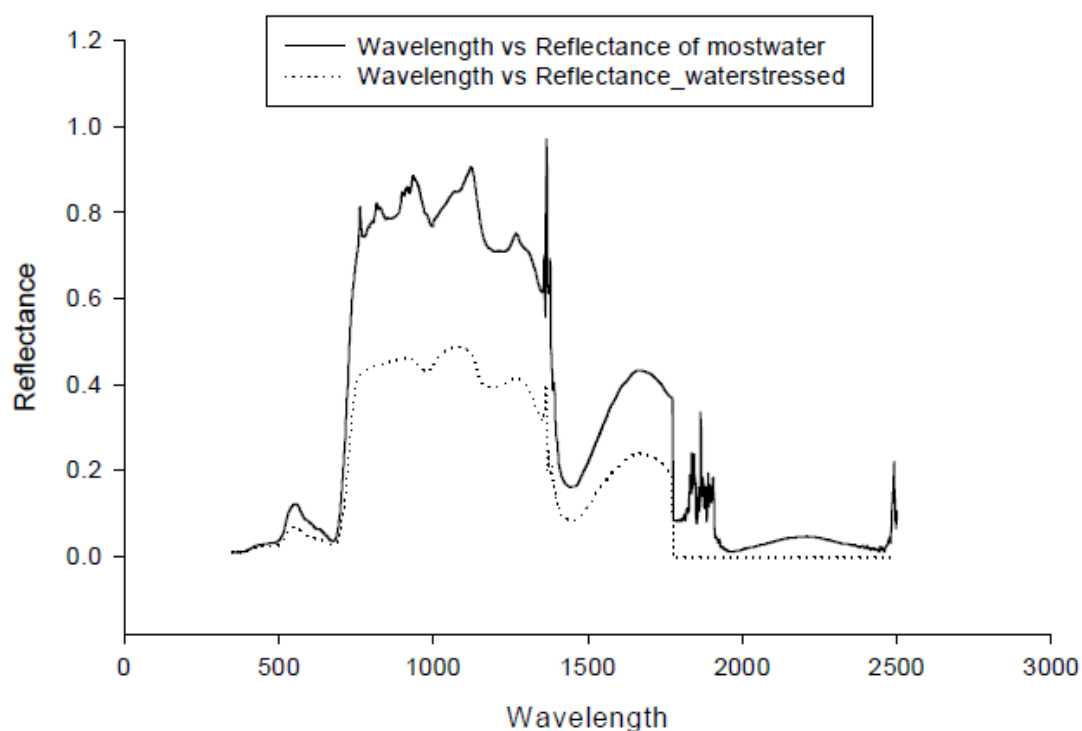


Figure 6. Wavelength (nm) & reflectance in Tef Source: (Hanna & Rethwisch, 2003)

When t-test was used, in classifying the difference in radiometer reflectance, it showed that the two treatments were different in wavelength of 1150-1350 and 1350-1550, which is in the range of water absorption. This is due to the impact of the water-stress treatment ($t=14.25$ and $P\leq 0.044$).

Reflectance curves of these two treatments have the same pattern of characteristics. However, the less stressed Tef grass showed higher spectral reflectance in wavelength of 750-1200 and 1300-1500 than the stressed plants as shown in Figure 6. This is due to the differences in type of treatment impacted on leaf shapes. The less stressed plants were having more greenish surface area parts than the stressed plants. The more greenish surface in leaves will indicate less reflectance in the water absorption area in the spectra in the 900-1300 nm. In this respect, the reflectance response of both treatments on the Tef grass crop that were studied can be explained by the spectral absorptive of chlorophyll at the wavelength near 700-750 nm and of leaves and chloroplast suspensions. The feature of water absorption has the characteristics to identify the different treatments applied to the same crop, which may affect the characteristic features of the leaves of the plants. This is shown in reflectance curves of Figure 6 (Hanna & Rethwisch, 2003).

2.4.1.3. Relationship Between Satellite Data and Ground Measurements

Several studies have shown good agreement between field spectral data and satellite data, in narrow bands hyperspectral sensors. Zhou *et al.* (2013), for example, compared field spectra with simulated Hyperion and real HJ-1A satellite data to estimate chlorophyll-a concentration. The same indices defined using field measured plant spectra were selected as the best predictors for pigment content showing a good correlation with actual leaf chlorophyll-a content ($R^2 = 0.8241$).

Nidamanuri & Zbell, (2011) used field reflectance data to classify HyMap airborne hyperspectral images and found that field spectral signatures are similar to those acquired with airborne sensor for some crops but not for every crop studied.

AVIRIS images from Blythe area, California, acquired in 1997 were compared with the ground-truth data collected on July 19 2000. Similarities for the spectra of tef grass crop extracted from both methods were found. This similarity allowed validating the spectra from images and field reflectance data. The peaks of spectral reflectance from AVIRIS and the spectroradiometer data are very similar and the most important region in the spectra is the region of 650-900, 900-1200, 1400- 1600 and 1600-2000 nm.

Field reflectance data collected for tef grass showed perfect match between the ground-truth spectral library and data extracted from AVIRIS especially for the two treatments (i.e. Tef exposed to less water stress and vice versa). This study showed that there is an excellent agreement between the predicted and the actual crop type and treatments (i.e. The correlation is between 85-90% match). The similarities are supported by the regression and correlation relationship between the reflectance obtained from AVIRIS images and the field reflectance data ($R^2=0.56-0.98$ and $P<0.01$) (Hanna & Rethwisch, 2003).

2.4.2. Multispectral Remote Sensing

With increasing population pressure throughout the world and the need for increased agricultural production, there is a definite need for improved management of the world's agricultural resources. To make this happen, it is first necessary to obtain reliable data on the types of resources and the quality, quantity and location of these resources. Satellite- or aerial-based remote sensing technologies will become

important tools in improving the present systems of acquiring and generating agricultural and natural resource data (Liaghat & Balasundram, 2010).

Remote sensing technology is a key component of PA and is being used by an increasing number of scientists, engineers and large-scale crop growers. At present higher-resolution satellite imagery overcomes previous constraints and permits the use of such data as a quick and easy tool for territorial management, including agricultural analysis, statistics and subsidy control (Liaghat & Balasundram 2010).

Bhatti, Mulla, and Frazier (1991) were the first to demonstrate that Landsat remote sensing had significant capabilities for estimating spatial patterns in soil organic matter, soil phosphorus and crop yield potential for use in precision agriculture applications (*apud* Mulla, 2013). Satellite remote sensing has been widely applied and is recognized as a powerful and effective tool for estimating crop characteristics (ADAM *et al.*, 2007; ZENEBE, 2012).

Satellites have been used for remote sensing imagery in agriculture (Table 1) since the early 1970's when Landsat 1 was launched in 1972. Multispectral Scanner System (MSS) sensors on Landsat 1 collected imagery in the green, red and two infrared bands at a spatial resolution of 80 m and a return frequency of 18 days (Mulla, 2013).

These applications of remote sensing in conventional agriculture soon led to applications in precision agriculture. The first application of remote sensing in precision agriculture occurred when Bhatti *et al.*, (1991) used Landsat imagery of bare soil to estimate spatial patterns in soil organic matter content, which were then used as auxiliary data along with ground based measurements to estimate spatial patterns in soil phosphorus and wheat grain yield (Mulla, 1997).

According to Mulla (2013), several trends are apparent in satellite based remote sensing (Table 3). Firstly, the spatial resolution of imaging systems has improved from 80 m with Landsat to sub-metre resolution with GeoEye and Worldview. Secondly, the return visit frequency has improved from 18 days with Landsat to 1 day with Worldview. Thirdly, the number of spectral bands available for analysis has improved from four bands (bandwidths greater than 60 nm) with Landsat to eight or more bands (bandwidths greater than 40 nm) with Worldview.

Satellite (year)	Spectral bands (spatial resolution)	Return frequency (d)	Suitability for PA
Landsat 1 (1972)	G, R, two IR (56 × 79 m)	18	L
AVHRR (1978)	R, NIR, two TIR (1090 m)	1	L
Landsat 5 TM (1984)	B, G, R, two NIR, MIR, TIR (30 m)	16	M
SPOT 1 (1986)	G, R, NIR (20 m)	2–6	M
IRS 1A (1988)	B, G, R, NIR (72 m)	22	M
ERS-1 (1991)	Ku band altimeter, IR (20 m)	35	L
JERS-1 (1992)	L band radar (18 m)	44	L
LiDAR (1995)	VIS (vertical RMSE 10 cm)	N/A	H
RadarSAT (1995)	C-band radar (30 m)	1–6	M
IKONOS (1999)	Panchromatic, B, G, R, NIR (1–4 m)	3	H
SRTM (2000)	X-band radar (30 m)	N/A	M
Terra EOS ASTER (2000)	G, R, NIR and 6 MIR, 5 TIR bands (15–90 m)	16	M
EO-1 Hyperion (2000)	400–2500 nm, 10 nm bandwidth (30 m)	16	H
QuickBird (2001)	Panchromatic, B, G, R, NIR (0.61–2.4 m)	1–4	H
EOS MODIS (2002)	36 bands in VIS-IR (250–1000 m)	1–2	L
RapidEye (2008)	B, G, R, red edge, NIR (6.5 m)	5.5	H
GeoEye-1 (2008)	Panchromatic, B, G, R, NIR1, NIR2 (1.6 m)	2–8	H
WorldView-2 (2009)	P, B, G, Y, R, red edge, NIR (0.5 m)	1.1	H

Table 3. Satellite remote sensing platforms.

Multispectral sensors are those that obtain image information in more than one band, up to several, say 20 or fewer, bands. Hyperspectral sensors are those that obtain image information in many, say 50 to several hundred, bands. The term, ultraspectral, has recently been coined to describe those sensors that obtain information in a very high number of bands, say several hundred or more (Thomasson, 2010).

Multispectral remote sensing systems use parallel sensor arrays that detect radiation in a small number of broad wavelength bands. Most multispectral satellite systems measure between three and six spectral bands within the visible to middle

infrared region of the electromagnetic spectrum. There are, however, some systems that use one or more thermal infrared bands. (Smith, 2001a). Multispectral remote sensing allows for the discrimination of different types of vegetation, rocks and soils, clear and turbid water, and selected man-made materials (Smith, 2001a). To obtain data of a higher spectral resolution compared to multispectral data, hyperspectral sensors on board satellites or airborne hyperspectral imagers are used (Smith, 2001b).

2.4.3. Hyperspectral Remote Sensing

Hyperspectral remote sensing collects reflectance data over a wide spectral range at small spectral increments (typically 10 nm). It provides the ability to investigate spectral response of soils and vegetated surfaces in narrow spectral bands (10 nm wide) across a wide spectral range. This is not possible with multispectral imaging that traditionally collects reflectance data in broadband (greater than 40 nm wide) centered in the B, G, R and NIR regions of the spectrum. When collected across large spatial extents at fine spatial resolution, hyperspectral imaging provides powerful insight into the spatial and spectral variability in reflectance for a bare or vegetated surface.

Hyperspectral sensors are used to estimate spatial crop patterns biomass (Yang *et al.*, 2000) and yield (Doraiswamy *et al.*, 2003) using the Normalised Difference Vegetation Index (NDVI). Wu *et al.*, 2010 used red edge reflectance based vegetation indices to estimate chlorophyll canopy content and leaf area index for several agricultural crops.

Hyperspectral imaging differs from multispectral imaging in the continuity, range and spectral resolution of bands. In theory, it offers the capability of sensing a wide variety of soil and crop characteristics simultaneously, including moisture status,

organic matter, nutrients, chlorophyll, carotenoids, cellulose, leaf area index and crop biomass (Goel *et al.*, 2003; Haboudane *et al.*, 2002; Zarco-Tejada *et al.*, 2005).

Nidamanuri & Zbell, 2011 attempted to classify HyMap airborne hyperspectral images based on field reflectance spectra as the training data for crop mapping. Researchers found that there exists some crops whose spectral signatures are similar to characteristic spectral signatures with possibility of using them in image classification, but this is not true for every crop tested.

Kumar *et al.*, 2013 used hyperspectral data to identify plant type, age, growth stage, pruning, light conditions, and disease incidence in tea plantations. Using stepwise discriminant analysis (SDA) and principal component analysis (PCA) of hyperspectral data, authors found that the Green and near-infrared (NIR) were the best regions for discrimination of different types of tea plants as well as tea growing in sunlit and shade conditions. For discriminating age of plantation, growth stage, and diseased and healthy bush, Blue region was most appropriate. The Red and NIR regions were found suitable to discriminate pruned and unpruned tea.

Adam *et al.*, (2007) used multispectral imagery and hyperspectral ground-based measurements for detection of spatial variation in nitrogen (N) status of the crop to allow more targeted N applications. Researchers also used thermal remote to identify spatial variations in crop water status. They concluded that this information could be used for irrigation scheduling whereas farmers in non-irrigated regions could use these data to avoid costly N applications on water-limited crops.

2.4.4. Comparison on Hyperspectral and Multispectral Data

Thenkabail *et al.* (2000) compared broad band Landsat TM band indices and hyperspectral narrow band indices for cotton, potato, soybeans, corn and sunflower

crop variables estimation. Observed crop characteristics included wet biomass, leaf area index, plant height and yield. It was found that narrow band OMNBR models were able to explain additional 3% to 40% when compared to broad band NDVI-type models and two-band narrow models explained additional 3% to 6% variability. They concluded that narrow band models perform significantly better than broad bands.

Thenkabail *et al.*, (2004) compared field reflectance acquired with a spectroradiometer to Hyperion data of shrubs, grasses, weeds, and agricultural crop species from the four ecoregions of African savannas. The results showed that the band centers of 13 of the 22 wavebands were within $\pm 0.017 \mu\text{m}$ of the band centers of Hyperion best bands. Authors consider that a significant number of wavebands have similar or near-similar waveband centers across vegetation types.

2.4.5. Change Detection for Tef Crop Inventory

Landscape spatial pattern is dependent driven by interacting physiographic and physiological processes, and are characterized by the temporal and spatial scales at which the resulting patterns are assessed (Hall & Hay, 2003).

Timely and accurate change detection of Earth's surface features is extremely important for understanding relationships and interactions between human and natural phenomena in order to promote better decision making. Remote sensing data are primary sources extensively used for change detection in recent decades. In general, change detection involves the application of multi-temporal datasets to quantitatively analyse the temporal effects of the phenomenon. (Lu *et al.*, 2004).

Many change detection techniques have been developed. Image differencing, principal component analysis and post-classification comparison are the most common methods used for change detection. More recently, spectral mixture

analysis, artificial neural networks and integration of geographical information system and remote sensing data have become important tools for change detection applications (Lu *et al.*, 2004).

The current study adopted a change detection technique involving an object-oriented approach for post-classification comparison. The underlying premise for using remote sensing data is that a change in the status of an object must result in a change in radiance values. However, variables such as atmospheric condition, solar angles, misregistration, and phenology reduce the 'signal-to-noise ratio'. Moving from pixel level to object level image processing allows change detection at their characteristic scales of expression (Hall & Hay, 2003).

Modern classification techniques can be applied to more efficiently extract information from traditional remote-sensing sources. Pixel based and object-based classification techniques were successfully combined to increase change detection accuracy from 0.81 to 0.88 (Aguirre-Gutiérrez *et al.*, 2012).

While assessing, evaluating and monitoring the nature and extent of land cover changes in an urban environment in Egypt, Afify (2011) examined the effectiveness change detection techniques. Change detection techniques namely; post-classification, image differencing, image rationing and principal component analysis were applied. The results indicated that the post classification change detection technique provided the highest accuracy while the principal component analysis technique gave the least accuracy. For both the generated change/unchange and classified change images the post-classification change detection technique has provided the highest overall accuracy (73.90%, 66.70%) and kappa coefficient of agreement (0.48, 0.45).

Results such as those obtained in above mentioned studies encouraged adoption of object-based post-classification change detection approach for tef

detection and monitoring. Some advantages of this method, as proposed by Hussain *et al.* (2013) include: 1) all the available objects could be used for object-based change detection; 2) allows thematic, geometric and topological change measure; 3) changes are based on classification comparison; 4) complete “from-to” change matrix. Limitations of the technique are related to: 1) difference in sizes and correspondence of image objects from multi-temporal images because of segmentation; 2) when searching for objects extracted from one image in a second image, locational error can cause incorrect change results; 3) dependent on the accuracy of the segmentation; 4) classification accuracy influences the change detection accuracy. To overcome these limitations, classification accuracy must be carefully controlled.

2.4.6. Vegetation Indices

The basic understanding of leaf reflectance has led to the development of various vegetation indices to quantify various agronomic parameters, e.g. leaf area, crop cover, biomass, crop type, nutrient status, and yield. These tools are still being developed as we learn more about how to use the information contained in reflectance's from a range of different sensors. Early assessment of yield reductions could avert a disastrous situation and help in strategic planning to meet the demands. (Gitelson, 2013).

The usefulness of optical indices from hyperspectral remote sensing in the assessment of vegetation biophysical variables both in forestry and agriculture have been demonstrated (Haboudane *et al.*, 2002). For example in semi-arid regions, Groten (1993) observed that the seasonal accumulated NDVI values are correlated well with the reported crop yields.

Spectral indices are often used to assess various attributes of plant canopies, such as leaf area index (LAI), biomass, chlorophyll content or N content. Those indices are, however, the combined response to variations of several vegetation and environmental properties, such as Leaf Area Index (LAI), leaf chlorophyll content, canopy shadows, and background soil reflectance. Of particular significance to precision agriculture is chlorophyll content, an indicator of photosynthesis activity, which is related to the nitrogen concentration in green vegetation and serves as a measure of the crop response to nitrogen application (Mulla, 2013).

Many broadband spectral indices (Table 5) other than NDVI are available for use in precision agriculture, as reviewed by Mulla (2013). These indices reflect two historical trends in remote sensing for crop characteristics; namely, the prediction of ratios of reflectance in the red (R) and NIR bands versus ratios in the green (G) and NIR bands. The normalized red (NR) index focuses on the portion of the spectrum where chlorophyll strongly absorbs radiation. In contrast, the normalized green (NG) index focuses on the portion of the spectrum where pigments other than chlorophyll (carotenoids, anthocyanins, xanthophylls) absorb radiation. Similarly, there are two forms of the ratio vegetation index (RVI), one that consists of the ratio of NIR to R reflectance, the other green red vegetation index (GRVI) that consists of the ratio of NIR to G reflectance. Two forms of the NDVI exist, one that involves NIR and R reflectance, the other green normalized difference vegetation index (GNDVI) involves NIR and G reflectance (Mulla, 2013).

Index	Definition	Reference
NG	$G/(NIR + R + G)$	Sripada et al., 2006
NR	$R/(NIR + R + G)$	Sripada et al., 2006
RV	NIR/R	Jordan, 1969
GRVI	NIR/G	Sripada et al., 2006
DVI	$NIR - R$	Tucker, 1979
GDVI	$NIR - G$	Tucker, 1979
NDVI	$(NIR - R)/(NIR + R)$	Rouse et al., 1973
GNDVI	$(NIR - G)/(NIR + G)$	Gitelson et al., 1996
SAVI	$1.5 * [(NIR - R)/(NIR + R + 0.5)]$	Huete, 1988
GSAVI	$1.5 * [(NIR - G)/(NIR + G + 0.5)]$	Sripada et al., 2006
OSAVI	$(NIR - R)/(NIR + R + 0.16)$	Rondeaux, Steven, & Baret, 1996
GOSAVI	$(NIR - G)/(NIR + G + 0.16)$	Sripada et al., 2006
MSAVI2	$0.5 * [2 * (NIR + 1) - \sqrt{(2 * NIR + 1)^2 - 8 * (NIR - R)}]$	Qi, Chehbouni, Huete, Keer, & Sorooshian, 1994

Table 4. Multi-spectral broad-band for precision agriculture. Source: Mulla (2013).

Brogea & Leblanc (2001) used broadband and hyperspectral vegetation indices for estimation of green leaf area index and canopy chlorophyll density. Hansen & Schjoerring (2003) used hyperspectral reflectance data to estimate canopy biomass and nitrogen status in wheat crops using normalized difference vegetation indices and partial least squares regression. Wu *et al.* (2008) successfully estimated chlorophyll content from hyperspectral vegetation indices.

Hyperspectral vegetation indexes are increasingly being applied to crop variables estimation, accompanying the growing availability of ground- and satellite based hyperspectral sensors (Haboudane *et al.*, 2004; Thenkabail *et al.*, 2004). Tian *et al.*, 2011 applied newly developed vegetation indices for estimating rice leaf nitrogen content concentration and pointed three narrow band indices with excellent performance for the task ahead.

Thenkabail *et al.*, (2000) considers that hyperspectral data can be used to construct three general categories of predictive spectral indices, including 1) optimal multiple narrow band reflectance indices (OMNBR), 2) narrow band NDVI, and 3) SAVI. Only two to four narrow bands were needed to describe plant characteristics

with OMNBR. This method of selecting optimal narrow bands to estimate crop variables will be further discussed in Chapter 5.

Tian *et al.*, (2011) derived new spectral narrow band indices that he found useful for estimating leaf nitrogen concentration in rice. Regions of the electromagnetic spectrum with special interest for this purpose are between 401-496nm; 550–600nm and 705-717nm.

A variety of narrow band hyperspectral indices (Table 5) are available for use in precision agriculture as reviewed by Mulla (2013). Many of these have the same form as broadband spectral indices, but differ in that the reflectance bands for hyperspectral indices are narrow (10 and 20 nm wide) bands centered around a single specific wavelength. These indices variously respond to canopy or leaf scale effects of leaf area index, chlorophyll, specific pigments, or nitrogen stress. Simple ratios (SR) 1 through 7 and normalized difference indices (NDI) 1 through 3 typically respond to leaf level changes in chlorophyll. In contrast, NDVI responds to canopy scale changes in leaf area index and chlorophyll. GNDVI, modified chlorophyll absorption in reflectance index (MCARI), transformed chlorophyll absorption in reflectance index (TCARI), MCARI2, Optimized Soil-Adjusted Vegetation Index (OSAVI), and MSAVI respond to canopy scale changes in chlorophyll, with the latter two indices being designed to compensate for soil reflectance effects. (Mulla, 2013).

Index	Definition	Reference
Greenness index (G)	R_{550}/R_{677}	Smith, Adams, Stephens, & Hick, 1995
SR1	$NIR/red = R_{800}/R_{670}$	Daughtry, Walthall, Kim, de Colstoun, & McMurtry, 2000
SR2	$NIR/green = R_{800}/R_{550}$	Buschman & Nagel, 1993
SR3	R_{700}/R_{670}	McMurtry, Chappelle, Kim, Meisinger, & Corp, 1994
SR4	R_{740}/R_{720}	Vogelmann, Rock, & Moss, 1993
SR5	$R_{675}/(R_{700} * R_{650})$	Chappelle et al., 1992
SR6	$R_{672}/(R_{550} * R_{708})$	Datt, 1998
SR7	$R_{650}/(R_{550} * R_{708})$	Datt, 1998
DI1	$R_{800} - R_{550}$	Buschman & Nagel, 1993
NDVI	$(R_{800} - R_{680})/(R_{800} + R_{680})$	Lichtenthaler, Lang, Sowinska, Heisel, & Mieh, 1996
Green NDVI (GNDVI)	$(R_{800} - R_{550})/(R_{800} + R_{550})$	Daughtry et al., 2000
PSSRa	R_{800}/R_{680}	Blackburn, 1998
PSSRb	R_{800}/R_{635}	Blackburn, 1998
ND11	$(R_{780} - R_{710})/(R_{780} - R_{680})$	Datt, 1999
ND12	$(R_{850} - R_{710})/(R_{850} - R_{680})$	Datt, 1999
ND13	$(R_{734} - R_{747})/(R_{715} + R_{726})$	Vogelmann et al., 1993
MCARI	$[(R_{700} - R_{670}) - 0.2(R_{700} - R_{550})](R_{700}/R_{670})$	Daughtry et al., 2000
TCARI	$3 * [(R_{700} - R_{670}) - 0.2 * (R_{700} - R_{550})(R_{700}/R_{670})]$	Haboudane et al., 2002
OSAVI	$(1 + 0.16)(R_{800} - R_{670})/(R_{800} + R_{670} + 0.16)$	Rondeaux et al., 1996
TCARI/OSAVI		Haboudane et al., 2002
TVI	$0.5 * [120 * (R_{750} - R_{550}) - 200 * (R_{670} - R_{550})]$	Broge & Leblanc, 2000
MCARI/OSAVI		Zarco-Tejada, Miller, Morales, Berjón, & Agüera, 2004
RDVI	$(R_{800} - R_{670})/\sqrt{R_{800} + R_{670}}$	Rougean & Breon, 1995
MSR	$(R_{800}/R_{670} - 1)/\sqrt{R_{800}/R_{670} + 1}$	Chen, 1996
MSAVI	$0.5[2R_{800} + 1 - \sqrt{4R_{800}^2 + 1}] - 8(R_{800} - R_{670})]$	Qi et al., 1994
MTVI	$1.2 * [1.2 * (R_{800} - R_{550}) - 2.5 * (R_{670} - R_{550})]$	Haboudane et al., 2004
MCARI2	$\frac{1.5[2.5(R_{800} - R_{670}) - 1.3(R_{800} - R_{550})]}{\sqrt{(2R_{800} + 1)^2 - (6R_{800} - 5\sqrt{R_{670}}) - 0.5}}$	Haboudane et al., 2004

Table 5. Hyperspectral narrow-band for precision agriculture. Source: Mulla (2013).

Structural indices are derived from the reflectance of near infrared (NIR) and red wavelengths. The reflectance in NIR region is primarily controlled by the internal leaf structure. Multiple reflections in the internal mesophyll structure, caused by the differences in the refractive index of the cell walls and the inter-cellular air cavity, result in high reflectance in NIR region. Hence, these indices, which use NIR and red reflectance, are called structural indices. The spectral region of the red-NIR transition (700–750 nm) is known as the red edge, and it has been shown to have large information content for vegetation spectra. This region is influenced by the combined effects of strong chlorophyll absorption in the red wavelengths and large reflectance in the NIR wavelengths. The slope of this region is a strong indicator of crop health (Jian *et al.*, 2007).

2.4.7. Combining GIS and GPS with Remote Sensing

Ma *et al.* (2006) consider that remote sensing knowledge and techniques integration with GIS and GPS technologies provides quick data acquisition needed for PA helping farmers manage their crops. This is in fact the main contribution for increasingly usage of PA.

Precision agriculture has generated a very high profile in the agricultural industry over the last decade of the second millennium, but the fact of within-field spatial variability, has been known for centuries. With the advent of the satellite-based Global Positioning System, farmers gained the potential to take account of spatial variability (Sttaford, 2000). The global positioning system (GPS) makes possible to record the in-field variability as geographically encoded data. It is possible to determine and record the correct position continuously. This technology considers the agricultural areas, fields more detailed than previously; therefore, a larger database is available for the user (Neményi *et al.*, 2003).

According to Zhang *et al.* (2002), monitoring the crops variability can be achieved by two approaches: the map-based approach and the sensor-based approach. With available technologies of GPS, remote sensing, yield monitoring, and soil sampling, the map-based approach is generally easier to implement. This approach requires the following procedure: grid sampling a field, performing laboratory analyzes of soil samples, generating a site-specific map, and, finally, using this map to control a variable-rate applicator. A positioning system, such as a GPS, is usually required for this approach. The sensor-based approach, on the other hand, measures the desired properties, such as soil and plant properties, using real-time sensors in an 'on-the-go' fashion and controls variable-rate applicator based on the

measurements. For the sensor-based approach, a positioning device is not always needed.

Most experimental precision-agriculture systems are map-based systems, because most on-the-go sensors for monitoring the field, soil, and field variability are too expensive, not sufficiently accurate, or not available. Spatial databases have been generated using various GIS systems by integrating maps derived from remote sensing, soil sampling, yield monitoring, and various sensors. Advanced geo-statistical methods are used to analyze the spatial and temporal variability (Pena-Yewtukhiw *et al.*, 2000). Crop-modeling techniques have been incorporated to develop yield potential maps as a base for fertilizer prescription (Werner *et al.*, 2000). These maps can be used to predict variability in crop growth and crop disease based on projected climatic conditions. Thus, PA provides an ideal tool for agricultural risk assessment and rational farm-work scheduling.

When using management zones for site-specific applications, remote sensing is used to delineate the homogeneous zones and GPS is involved to control the application or to guide the implement (Zhang *et al.*, 2002).

While remote sensing provides data for accessing crop variables (Gitelson, 2013; Haboudane *et al.*, 2002; Broge & Leblanc, 2001; Wu *et al.* 2008), GIS allows spatial analysis and planning even at field-level (Runquist *et al.*, 2001; Ess *et al.*, 1997) while GPS equipment close the circle (Sttaford, 2000), providing geographical positioning for variable-rate applications .

2.4.8. Tef Crop Yield profile estimation

The techniques to estimate crop yield and production include statistical sampling methods, agro-climate models, crop growth models, remote sensing, and integrated methods (Chen *et al.*, 2008).

Because of the seasonal rhythm of vegetation, the micro-structure of plant cells and the macro-structure of vegetation canopies changes accordingly and the spectral response of individual vegetation types or of a population also changes periodically (Chen *et al.*, 2008).

Crop yield and production data are key indicators for national food security and sustainable development of society (Chen *et al.*, 2008). Monitoring agricultural crop conditions during the growing season and estimating the potential crop yields are both important for the assessment of seasonal production. Accurate and timely assessment of particularly decreased production caused by a natural disaster, such as drought or pest infestation, can be critical for countries where the economy is dependent on the crop harvest (Doraiswamy *et al.*, 2003).

In Ethiopia, characterised by climatic uncertainties, forecasting tef crop yield well before harvest is crucial. Given that drought is a common occurrence in the country, timely and quantitative information on expected tef crop yield will improve food production and country's food security. A timely assessment of emergency situation will also allow government to intervene with specific measures that support local farmers (Zenebe, 2012).

The use of remote sensing to estimate variations in crop yield is very common in agricultural research (Thomasson, 2003). Ferencz *et al.*, (2004) used models for estimating the yield of different crops in Hungary from satellite remote sensing and field data. The correlation between the remote sensing estimated and classical yield

data for eight crops was found to be more than 99%. Wheat, corn, sugar beet, barley, alfalfa, rye and maize for silage and pea yield could accurately be estimated for operational use for county-, region- and country-level. The authors stated that not only the methods proved to be an effective tool in regional yield estimation, but also can be applicable in developing countries, because use only relatively simple technology and are not expensive.

The only work found relating remote sensing data and tef crop variables is the one developed by Hanna & Rethwisch in 2003. Data from a farm in California, U.S. for soil water content (WC), pH, organic matter (OM) and nitrogen (N%) were collected. Yield was also evaluated using statistical data from several years. Spectroradiometer and AVIRIS (Airborne Visible/Infrared Imaging Spectrometer) sensors were used, showing that there is an excellent agreement between the predicted and the actual crop variable (i.e. the correlation is between 85 – 90% match).

Remote sensing images are capable of identifying crop health as well as predicting its yield. In this study, Normalised Difference Vegetation Index (NDVI) calculated from remote sensing images will be used to monitor crop growth and relate to crop yield. The satellite data will be validated using ground truth in farmer's field (Zenebe, 2012).

2.4.8.1. Performance in Remote Sensing Technique

Moriondo *et al.* (2007) used NDVI data and CROPSYST model to estimate above-ground biomass and ultimately, wheat yield. The results obtained showed the high accuracy of the method in estimating wheat yield at the provincial level. Correlation coefficients equal to 0.77–0.73 were obtained between measured and

simulated crop yield, with corresponding root mean square errors (RSME) of 0.47 and 0.44 Mg/ha for Grosseto and Foggia, respectively.

Doraiswamy *et al.* (2003) used the crop model EPIC (Erosion Productivity Impact Calculator) to estimate crop parameters including yield. Remote sensing data was used to assess crop condition parameters and use these parameters as an input to the model. Authors found that results of the simulations with and without the use of remote sensing data suggest that remotely sensed data improves the consistency of the predictions, and that significantly better yields can be determined prior to crop harvest using remote sensing data.

Two methods for estimating the yield of different crops in Hungary from satellite remote sensing data were adopted by Ferencz *et al.* (2004). In the first method developed for field level estimation, reference crop fields were selected by using Landsat Thematic Mapper (TM) data for classification. A new vegetation index (General Yield Unified Reference Index (GYURI)) was deduced using a fitted double-Gaussian curve to the National Oceanic and Atmospheric Administration (NOAA) Advanced Very High Resolution Radiometer (AVHRR) data during the vegetation period. The correlation between GYURI and the field level yield data for corn for three years was $R^2=0.75$. The county-average yield data showed higher correlation ($R^2=0.93$). The second method presented uses only NOAA AVHRR and officially reported county-level yield data. The county-level yield data and the deduced vegetation index, GYURI, were investigated for eight different crops for eight years. The obtained correlation was high ($R^2=84.6-87.2$). The developed robust method proved to be stable and accurate for operational use for county-, region- and country-level yield estimation. The method is simple and inexpensive for application in developing countries, too.

As for tef yield remote sensing based yield estimation, no results are available so far. However, Zenebe (2012) presented a method that will be performed involving NDVI derived from remote sensing images to monitor crop growth and relate to crop yield in Tigray, Ethiopia.

This dissertation intends to collect field data, use RS data as ground truth and relate results to remote sensing image providing methods for remote yield estimation. The main idea is to use imagery with lower spatial resolution and higher spectral resolution than the ones used so far, such as Hyperion sensor. Unavailability of Hyperion data for the study area prevented conclusion of this step. Use of the Moderate Resolution Imaging Spectroradiometer (MODIS) data was considered not feasible given its best spatial resolution of 250m. As discussed elsewhere, agricultural fields in Ethiopia are characteristically small areas, incompatible with MODIS spatial.

2.4.8.2. Remote Estimation of Tef production

According to Chen *et al.* (2008) generally, there are three categories of models based on remote sensing: empirical models, physiological models and crop growth models. Empirical models are based on the hypothesis that biophysical crop parameters or ecological environmental parameters of the land surface such as biomass, LAI, temperature are correlated to final crop yield or production and remote sensing data are correlated to these above parameters of critical growth stages. Empirical relationships of yield estimation are simple to use, few ground-measurements are sufficient for model validation and accuracy is higher especially in homogeneous areas. Since a link between crop biomass and remote sensing is necessary, lacks flexibility and stability. Results at different stages may vary drastically.

A physiology-based model is based on crop physiological functions and assumes that crop production results from photosynthesis through which a fraction of incident solar radiation is converted into biomass. The simple model for crop yield estimation can be written as follows (Chen *et al.*, 2008):

$$DM = \int_{t_1}^{t_2} \varepsilon * fPAR * PAR . dt \quad (1)$$

$$Yield = DM * HI \quad (2)$$

where DM is dry matter production in a time period $t_2 - t_1$, ε is light use efficiency, PAR (MJ m^{-2}) is the incoming photosynthetically active radiation for the wave bands between 0.4 and $0.7\mu\text{m}$. PAR is part of the short wave solar radiation ($0.3\text{--}3\mu\text{m}$) and is absorbed by chlorophyll for photosynthesis in the crop. fPAR is the fraction of the photosynthetical radiation absorbed by the canopy. HI is the harvest index which means the ratio of grain mass to aboveground biomass. It is a universal model, suitable for more crop types and it only needs a relatively simple data set such as solar radiation and fPAR. Light use efficiently, in other hand, depends on the phenological state and environment conditions such as temperature and rainfall.

Crop growth model describes the primary physiological mechanisms of crop growth such as phenological development, photosynthesis and dry matter partitioning, and their interactions with the underlying environmental factors using mechanistic and sometimes empirical equations. Using crop growth models to estimate crop yield requires a lot of inputs that are specific to the crop, soil characteristics, management practices and local climate conditions. So it has limitations to use this kind of models in large regions because fewer inputs are generally available at this scale (Chen *et al.*, 2008).

Empirical relationships for crop yield monitoring and prediction are widely used for its simplicity. But its shortcoming is also obvious, the unstableness and sometimes site-specific relationship between yield and remote sensing data. Physiology-based models are mainly based on crop physiological functions, which is its strong point. But some parameters are not consistent over a large region and/or for different crops and sometimes not easily acquired by remote sensing or an in situ survey. Crop growth models have a long history and extensive use for crop growth monitoring, yield prediction and farm management around the world. Huge work of data collection and preparation hampered its good performance at a regional scale. During recent years, crop growth models with remote sensing data assimilation have been improved greatly at regional scales for better estimation of crop parameters (Chen *et al.*, 2008).

Ji-hua & Bing-fang (2008) and Bing-fang & Ji-hua (2010) reported that limitations on applying remote sensing in crop field level and environment information monitoring to support precision farming are related to: temporal and spatial resolution combined in one sensor, accuracy and information releasing channel. Especially due to complexity of agricultural landscapes in China, this is probably the same situation in developing and under-developed countries.

Crop yield was computed by estimating crop biomass and crop Harvest Index (HI) respectively. In crop biomass estimation, a process oriented model CASA (Field, 1995) was used. CASA model estimates biomass based on the vegetation characteristics and the environmental variables such as temperature, precipitation, are also considered. In harvest index (HI) estimation, the ratio between NDVI cumulated post-anthesis and that cumulated from emergence to maturity (fNDVI) was assumed to be indirectly related to HI. A model was developed based on this

assumption. The final crop yield could be gotten by multiplying crop biomass and HI (Bing-fang & Ji-hua, 2010)

2.4.8.3. Band Selection to Determine Optimal Number of Bands for Tef crop variables estimation

Hyperspectral data are extremely large and of high dimensionality. Many hyperspectral features are redundant due to the strong correlation between wavebands that are adjacent. Hence, the analysis of hyperspectral data is complex and needs to be simplified by selecting the most relevant spectral features (Abdel-Rahman *et al.*, 2013).

Several studies presented algorithms, models and indices for hyperspectral band selection such as regression algorithms, principal component analysis, correlation analysis, narrow band optimal combination indices, derivative greenness vegetation indices (Broge e Leblanc, 2001; Thenkabail *et al.*, 2002; Thenkabail *et al.*, 2004a; Chauhan *et al.*, 2012; Abdel-Rahman *et al.*, 2013; Mahlein *et al.*, 2013), amongst others.

Thenkabail and collaborators (2000, 2002 & 2004a) described in their articles approaches involving selection of narrow band optimal vegetation indices and their correlation with crop variables to determine and recommend number of hyperspectral bands, their centers and width in the visible and NIR regions of the spectrum. Their rigorous and exhaustive approach will be adopted as band optimization method in this study and will be reviewed in this section.

Three distinct types of narrow band indices were computed by Thenkabail *et al.*, 2000: 1) all possible two-band combination indices involving 490 narrow bands measured with field spectroradiometer; 2) stepwise linear regression indices

involving one, two, three and four or combinations all bands (optimum multiple narrow band reflectance (OMNBR) approach); 3) soil-adjusted narrow band indices.

The first type of indices, two-band NDVI combinations, was evaluated against crop biophysical variables using regression coefficients R^2 . Contour plots of the R^2 values were used to identify seven most correlated indices to LAI (leaf area index), WBM (wet biomass), grain yield and plant height. This procedure also allowed determination of band centers and band widths best correlated to cotton, potato, soybeans, corn and the pooled data for all crops. Two-band NDVI models explained between 64% to 88% variability in different crop variables.

The second type, OMNBR vegetation indices, was used as dependent variables of stepwise linear regression analysis while crop variables were used as independent ones. Highest R^2 value for one, two, three and four band OMNBR models were determined. Thenkabail et al (2000) found that optimal information on crops is not necessarily concentrated in the red and NIR wavelengths. Longer wavelength portion of red (651nm to 700nm), moisture-sensitive NIR (951nm to 1000nm), shorter wavelength portion of green (501nm to 550 nm) and longer wavelength portion of NIR (900 to 940nm) were identified as best predictors. Four-variable OMNBR models explained between 64% to 92% variability in different crop variables.

The band centers and widths determined by linear relationships were used to establish non-linear exponential models. The seven best hyperspectral models explained 65% to 92% variability for WBM and LAI of crops. Authors found that except in a few cases, nonlinear models performed better than linear model.

The third type, soil-adjusted vegetation indices analysis, reviewed that TSAVI performed better than other soil-adjusted indices. However, the increase in R^2 value

in soil-adjusted models over the other narrow band NDVI models was insignificant in most cases (5% increases being the exception) (Thenkabail *et al.*, 2000).

Thenkabail *et al.* (2002) studied and optimal hyperspectral indices selection for barley, wheat, lentil, cumin, chickpea and vetch and their correlation to leaf area index, wet biomass, dry biomass, plant height, plant nitrogen and canopy cover. They found that simple narrow-band two-band vegetation indices (TBVI) and the optimum multiple-band vegetation indices (OMBVI) (a similar approach to OMNBR indices) provided best results. Compared to Landsat TM broadband indices, TBVI explained up to 24 % greater variability and OMBVI explained up to 27 % greater variability in estimating different crop variables. Linear and non-linear models were fitted to obtain TBVI R^2 relation to crop variables. OMBVI were computed using the following model equation:

$$OMBVI_i = \sum_{j=1}^N a_{ij} R_j \quad (1)$$

Where $OMBVI_i$ is the crop variable i , R_j is the reflectance in bands j ($j=1$ to N with N = number of bands), and a_{ij} is the coefficient for reflectance in band j for the crop variable i . Piecewise linear regression model based on stepwise MAXR procedure was used for them to calculate R^2 coefficient of determination values.

Thenkabail *et al.* (2004a) adopted a similar approach to determine optimal wavebands that best describe vegetation characteristics based on a comprehensive analysis using principal component analysis (PCA), lambda–lambda R^2 models (LL R^2 M), stepwise discriminant analysis (SDA) and derivative greenness vegetation indices (DGI). These techniques will further described in the following.

The wavebands that provided best results using PCA, LL R^2 M and SDA were pooled together to determine their frequency of occurrence in the 0,395-2.500 μ m

range used by the authors. For Thenkabail *et al.* (2004), the four methods provide complimentary and supplementary information. PCA explains variability in data and reduces data redundancy. LL R²M eliminates all redundant bands and provides wavebands that best model vegetation characteristics. SDA tests the strength of data in separating or discriminating species types. DVGI integrates the near-continuous data over a region of wavelength highlighting how spectral slopes are sensitive to changes in biophysical and biochemical properties of vegetation and crops (Thenkabail *et al.*, 2004a).

The four methods (PCA, LL R²M, SDA, and DGVI; Sections 3.1, 3.2, 3.3, and 3.4) provide complimentary and supplementary information. The PCA explains variability in data and reduces data redundancy; LL R²M eliminates all redundant bands and provides wavebands that best model vegetation characteristics; and the SDA tests the strength of data in separating or discriminating species types. DGVI integrates the near-continuous data over a region of wavelength highlighting how spectral slopes are sensitive to changes in biophysical and biochemical properties of vegetation and crops. In the process, each one of the methods highlights wavebands that are most sensitive. By pooling the wavebands from these methods, we determine the frequency of occurrence of wavebands leading to a recommendation of 22 optimal wavebands.

2.4.8.3.1. Principle Component Analysis (PCA)

While there are a multitude of dimension reduction techniques for hyperspectral imaging data that have appeared in the literature, the principal component (PC) transform [also called principal component analysis (PCA)] is arguably the most popular (Li & Yeh, 1998). In hyperspectral imaging exploitation, PCA offers a straightforward approach for computation and is optimal in a statistical

sense of preserving a maximal amount of the variability (i.e., energy) present in the original data. PCA does not take into account any information about noise or the target signal of interest in the case of detection applications (Farrell Jr., 2005).

PCA is a feature extraction process that first transforms the original image into a principal component (PC) image through principal component transformation (PCT), and then extracts informative features from the principal component bands. For each pixel, every band of the PC image is a linear combination of the original bands from that same pixel. The transformation uses the global covariance or correlation matrix from the original image, whose image bands normally correlate with each other. After the transformation, every dimension is orthogonal to each other with no correlation among the PC bands. The total variance of the PC image equals the total variance in the original image, thus preserving the original data information after transformation. However, the first several bands in the PC image contain the majority of the variance in the original image. Most of the total variance from the original image is mapped to the first component with decreasing variance in the following bands. Image analysis can be implemented using features extracted from the variance ranked PC bands rather than from all image bands. A standard principal component transformation (STD-PCT) uses all spectral bands for transformation (Haibo & Tian, 2003).

The first principal component stores the maximum contents of the variance of the original data set. The second principal component describes the largest amount of the variance in the data that is not already described by the first principal component, and so forth (Taylor 1977). Although a number of principal components may be acquired in the analysis, only the first few principal components account for a high proportion of the variance in the data. In some situations, almost 100 per cent of the variance can be captured by these few components. Fung and LeDrew's study

(1987) indicates that the first four components can contain more than 95 per cent of the total variance and the other remaining components have little useful information for land use change (Li & Yeh, 1998).

Thenkabail et. al, 2004 performed principal component analysis (PCA) using the PROC PRINCOMP algorithm in SAS and observed that the first five principal components (PCs) explained 93–95% of the variability in the various weed species and agricultural crop species studied. The author could reduce data dimensionality from 168 to 5 bands only. The order in which bands were listed indicates the magnitude or ranking for that band based on its factor loadings.

The procedure for principal component vegetation indices established by Thenkabail *et al.* (2002) will be adopted in the future steps of this study. The authors used weightings of the first principal component to calculate new principal component band 1 brightness values (PCA1BV). Similarly, using the weightings of the second principal component, new principal component band 2 brightness values (PCA2BV) were calculated. Using the new principal component bands 1 and 2, a principal component vegetation index was computed using the following equation:

$$PCVI = \frac{(PCA1BV - PCA2BV)}{(PCA1BV + PCA2BV)} \quad (2)$$

2.4.8.3.2. Lambda-Lambda R^2 models (LL R^2 M) Model

Thenkabail *et al.*, (2000) used normalized difference vegetation index (NDVI) in all possible combinations of hyperspectral narrow bands in an investigation of agricultural crop biophysical variables estimation. Using lambda (λ_i) vs. lambda (λ_j) R^2 models (LL R^2 M) and plots of R^2 values they were able to select wavelengths best suited for predicting biophysical quantities. Crop characteristics included wet biomass, leaf area index, plant height, and yield. Ground-level hyperspectral

reflectance measurements of cotton, potato, soybeans, corn, and sunflower. Regression coefficients R^2 between all possible two-band narrow band vegetation indices and crop biophysical variables were determined. An example of these contour plots of the R^2 values is shown in Figure 6. Based on the results shown in the Figure 6, band centers and band widths that combine to form the best indices were determined.

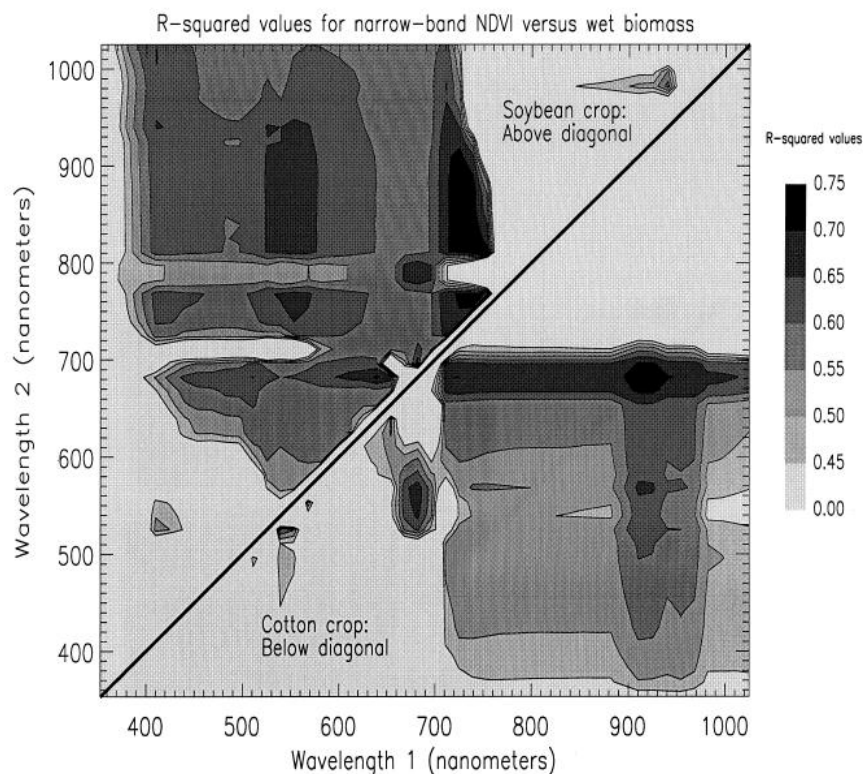


Figure 7. Contour plot NDVI values Source: Thenkabail *et al.* (2000).

Thenkabail *et al.*, 2004a also used the lambda (λ_i) vs. lambda (λ_j) R^2 models (LL R^2 M) to provide a rigorous search criterion or data-mining technique to highlight redundant wavebands from wavebands with unique information content (where $i, j = 168$ wavebands used in their study). A 168 (ki)168 (kj) band correlation (r) matrix was developed. The correlation (r) values were converted to R^2 and reported. The correlation coefficients (R^2) involving all possible combination of wavebands

calculated resulted in lambda-vs.-lambda plots, as described by Thenkabail *et al.* (2000). The areas of lowest correlation between wavebands indicate that the two bands contained unique information about the species (Thenkabail *et al.*, 2004a). Center and widths of wavebands with the least redundancy were identified.

2.4.8.3.3. Stepwise Discriminate Analysts (SDA)

Discriminant function analysis is a statistical analysis to predict a categorical dependent variable (called a grouping variable) by one or more continuous or binary independent variables (called predictor variables). Thenkabail (2002) and Thenkabail *et al.* (2002) used SDA to discriminate or separate vegetation and crop species using Wilk's lambda, Pillai trace, and average squared canonical correlation. At each step, if a band in the model failed to meet the criterion (f-test), the worst variable is removed. Otherwise, the band that contributed most to the discriminatory power of the model is entered. When all variables in the model met the criteria and the remaining variables are excluded, the stepwise selection process is stopped. The resulting output has a Wilk's lambda, Pillai trace, and average squared canonical correlation. The values of Wilk's lambda were indicative of separability or discriminatory power of spectral bands (i.e., the less the value of Wilk's lambda, the greater spectral differentiation between the species types) (Thenkabail *et al.*, 2004a).

2.4.8.3.4. Derivative Greenness Vegetation indices

A first-order DGI is computed by taking near-continuous spectra along regions where there is significant or rapid change in slope of spectra per unit change in wavelength. Based on the observation of the spectra and literature Thenkabail *et al.*, (2004) decided to use selected regions were located in 0.515–0.535 μm (DGI1), 0.540–0.560 μm (DGI2), 0.560–0.580 μm (DGI3), 0.650–0.670 μm (DGI4),

0.700–0.740 μm (DGVl5), 0.626–0.795 μm (DGVl6), 1.500–1.650 μm (DGVl7), and 2.080–2.350 μm (DGVl8). The chlorophyll red-edge portion is considered to have maximum sensitivity to changes in green vegetation per unit change in wavelength in the electromagnetic spectrum. The first-order DGVl (Elvidge & Chen, 1995) was computed using the equation:

$$DGVl = \sum_{\lambda_1}^{\lambda_n} \frac{[\rho'(\lambda_i) - \rho'(\lambda_j)]}{\Delta\lambda_i} \quad (1)$$

where λ_i and λ_j are the wavelengths at the midpoints of bands i and j , ρ' is the first derivative of the reflectance, λ_1 is the start of a DGVHl waveband, and λ_n is the end of a DGHVl waveband. Where i and j are band numbers, λ = center of wavelength, and ρ' = first derivative reflectance (Thenkabail et. al, 2004).

2.4.8.4. Accuracy Assessment of crop characteristics estimation

The performance of seven vegetation indices in estimating the vegetation fraction in maize and soybean crops was studied. For assessing the accuracy of vegetation fraction estimation, noise equivalent metric was applied. Noise equivalent takes into account not only the RMSE of the vegetation fraction estimation but also accounts for the sensitivity of the vegetation index to vegetation fraction, thus providing a metric accounting for both scattering of the points from the best-fit function and the slope of the best-fit function. Although all indices examined showed a close relationship with vegetation fraction, some are more accurate than others. These are the enhanced vegetation index (EVI2), wide dynamic range vegetation index (WDRVI), green- and red-edge normalized difference vegetation index (NDVI). (Gitelson, 2013).

To assess the performance of different vegetation indices in estimating vegetation fraction, the determination coefficient (R^2) or root mean square error (RMSE) was used. The R^2 values, as well as RMSE, represent the dispersion of the points from the best-fit lines. They constitute measures of how good the best-fit line is in capturing the relationship between vegetation index and vegetation fraction. However, when the best-fit function is nonlinear, the R^2 and the RMSE values may be misleading because sensitivity of the vegetation index to vegetation fraction does not remain constant. Thus, for nonlinear relationships, vegetation index (VI) versus vegetation fraction (VF), sensitivity of vegetation index to VF should be taken into account. To determine the accuracy of vegetation fraction estimation, we employed the noise equivalent (NE) of vegetation fraction (Viña and Gitelson 2005 *apud* Gitelson, 2013).

The accuracy of a method to estimate the variability of cropland is affected by lots of factors, such as the data used, scale, crop type, etc. There are lots of researches on it in the past years. Agricultural land use has as specific characteristic that the surface reflectance changes regularly in time with the growth of a crop. This may cause it difficult to calculate accurately the total sown area of a specific crop in case of different types of cropping systems (Chen *et al.*, 2008).

The crop parameters for monitoring the key crop and environment informally include crop biophysical parameters (leaf area index, vegetation coverage), crop biochemical parameters (nitrogen/chlorophyll content, etc.) and crop growing environment parameters (such as soil moisture, surface temperature). In addition to the spatial and temporal resolution problem, the accuracy of remote sensing derivation of field parameters is also a major problem. The accuracy was affected by spatial resolution, noise, atmospheric conditions, as well as other factors such as the accuracy of model inversion. Generally the inversion accuracy of crop biophysical

parameters, biochemical parameters and environment parameters can only achieve an accuracy of 85%, 80% and 90%, which cannot meet the need of operation and monitoring (Bing-fan & Ju-hua, 2010).

Thenkabail *et al.* (2004) used error matrices generated from the discriminant analysis model (SAS algorithm PROC DISCRIM) to assess classification accuracy. The classification criterion was based on either the individual within-group covariance matrices or the pooled covariance matrix; it also accounted for the prior probabilities of the groups. Each observation, from an independent dataset, was placed in the class from which it has the smallest generalized squared distance. DISCRIM was also used to compute the posterior probability of an observation belonging to each class. The generalized squared distance (D) function for crop types is:

$$D_j^2(X) = (X - \bar{X}_j)' COV^{-1}(X - \bar{X}_j) \quad (2)$$

where X is the vector of observations for a given pixel, \bar{X}_j is the mean of all observations for crop type j , and COV is the covariance matrix:

$$\bar{P}_{jr}(j|X) = \frac{\exp(-.5D_j^2(X))}{\sum_k \exp(-.5D_k^2(X))} \quad (3)$$

Error matrices were generated for different hyperspectral wavebands. This enabled us to see how the overall accuracies and Khat (Thenkabail *et al.*, 2002; Thenkabail *et al.*, 2004a) values increase with increases in input wavebands.

Overall accuracies were computed based on correctly classified pixels along the diagonal of an error matrix. Errors of commission and errors of omission were computed. The Khat was then computed so as to normalize the accuracy assessments between datasets and data types as follows:

$$K_{hat} = \left(N \sum_{i=1}^r X_{ii} - \sum_{i=1}^r X_{+1} X_{i+} \right) / \left(N^2 - \sum_{i=1}^r X_{i+} X_{+i} \right) \quad (4)$$

where r is the number of rows in the matrix; X_{ii} is the number of observations in row i and column i ; X_{i+} and X_{+i} are the marginal totals of i and column i , respectively; and N is the total number of observations. Overall accuracies and Khat were calculated for the best 1 band, best 2 bands, and so on, to all bands. The best bands were decided based on their frequency of occurrence.

Same method of accuracy assessment evaluation was compared with accuracy assessments of independent datasets. The accuracy assessment approach adopted by Thenkabail *et al.*, (2002; 2004a) will be adopted in next steps of this study.

2.5. CHAPTER SUMMARY

In this literature review, it has been showed that precision agriculture and its supporting technologies, such as remote sensing, GIS and GPS are becoming available, with better spectral and spatial resolution, at more frequent revisits and lower prices. Techniques and algorithms for data processing and analysis also improved, to be used for improvement of crop management, allowing for yields forecast and higher quality crops, while reducing inputs costs and environmental impacts. Precision agriculture applications, techniques, adoption rates, benefits and future achievements were referred to under the perspective of crop production.

The most important factors of *Eragrostis tef* crop production in Ethiopia as a culturally important and threatened species were highlighted and related to crop

management improvement using precision agriculture tools. Stresses such as drought and nutrient shortages were demonstrated to be remotely detectable through satellite imagery, allowing for better decision making process aided by geographic information systems. Applications of precision agriculture methods involving GPS for site-specific and variable-rate crop management were also discussed, completing the scenery of precision farming of cereal crops.

The feasibility of remote estimation of plant production was demonstrated. Performance of yield remote estimates was shown from literature examples. Techniques and methods were exemplified and models used by other authors to estimate crop conditions were reviewed. This chapter provided an overview on current remote sensing techniques for remote yield estimation and crop condition monitoring, with potential to be applied in sustainable agricultural development in Ethiopia.

As stated by Zenebe (2012), the importance of forecasting tef crop yield well before harvest is crucial in Ethiopia, characterized by climatic uncertainties. Besides improving food production and country's food security, providing timely and quantitative information on expected tef crop yield, that's improving Ethiopia's food scarcity problem could also benefit from the biological diversity of the flora, as pointed out by Asfaw & Tadesse (2001). According to the authors, several species endangered and threatened with extinction would be further threatened if they are left on their own without measures for conservation, cultivation and promotion.

Techniques for crop yield estimation based on hyperspectral and multispectral have shown reasonable results, especially with the newly developed vegetation indices for narrow band data. In addition to yield several crop characteristics such as estimated leaf area index (LAI), biomass, chlorophyll content or N content are under investigation for its remote estimation.

Approaches for tef yield estimation in Ethiopia were selected for analyzing the adapting of PA. The idea is to adopt waveband optimization for bands selection used for Thenkabail *et al.*, (2000, 2002; 2004a) to estimate tef yield using Hyperion and ground truth data for crops grown in the study area. It include a comprehensive analysis on participation of hyperspectral bands in crop spectral behavior at satellite-level composition.

Although crops analyzed were located in California (U.S.), the work published by Hanna & Rethwisch (2003) revealed that tef crop variables can also be estimated using hyperspectral data. Their research not only opens the way for tef crop variables and spectra evaluation on its origin, Ethiopia, but also propose to build a spectral library to be used in future works.

Improved tef crop management practices directed to higher yield production and reduction of plant stress are currently under development in Ethiopia. According to Dejene & Lemlem (2012), integrating sowing date, selection of tolerant varieties, spate irrigation and maintaining soil fertility will undoubtedly ensures sustainable production of tef even under terminal drought and reduces the vulnerability due to community's settlement in terminal drought prone areas of Ethiopia.

Following these recommendations and other practices presented in literature review, constraints, recommendations and advantages of tef production can be summarized as follows.

Main constraints for tef production are:

- inadequate seed bed preparation,
- planting harvesting and threshing operations are not mechanized yet,
- low productivity;

Principal recommendations for optimal tef crop production are:

- prepare detailed mechanization package for tef,
- support breeding programs for productivity,
- use of biotechnology for improvement of tef cultivars,
- preparation of appropriate fertilizer package.

The main economic reason of tef production to Ethiopia are:

- prices for its grain and straw are higher compared to other cereals,
- opportunity to be an export crop to Europe and Americas, mainly due to the absence of gluten in tef,
- performs better than other cereals (maize, sorghum, wheat, barley) under low moisture stress conditions,
- often it's shown as a rescue crop as it survives and produces grain even when other cereals have failed due to moisture shortage,
- tef has a high recovery potential when subjected to water logged conditions,
- gains of tef can be stored in any kind of locally available material without being attacked by weevils,
- no epidemic disease has threatened its performance so far,
- the straw is a nutritious and highly preferred feed for cattle compared to other cereals,
- the straw is also used as a sticking material for construction of farmer's houses and livestock shelters.

Being an endangered species, *Eragrostis tef* growth and sustainable cultivation should be encouraged and its use promoted among people. Tef crop yield estimation and use of precision agriculture for increasing production could serve as an incentive for convincing farmers of new crop establishment.

3. TEF SUITABILITY ANALYSIS

For this analysis, data for precipitation, topography, soil, and land use land cover will be combined to provide a preliminary suitability model that can be improved upon with higher resolution data.

The first step for tef suitability analysis is the calculation of rainfall data from May to September per dekad. After this, each averaged dekad during May to September is added to attain total average Kiremt rainfall using raster calculator. Values are then regrouped dividing values of the totals as 300, 600, 800, 1600. Sources of data for geographic information system database and tef crop monitoring used in this report include:

- climate data from FEWS (Famine Early Warning System);
- topographic data from U.S. Geological Survey's EROS Data Center
- land use land cover data from Ethiopian Institute of Agricultural Research, Debre Zeit Agricultural Research Center (EIAR-DZARC).
- country scale soil data obtained from ETHIOGIS
- local scale soil data from Ministry of Water Resources
- Rapideye data
- Geoeye data
- GPS field data acquired with navigation commercial equipment

The workflow graphically describes activities developed within the scope of this research project in order to acquire process and analyze information related to tef crops monitoring, production optimization and new crops establishment planning. Information on climate, topography, Land Use/Land Cover (LULC) and soil (country and local scale detail levels) were gathered and organized into a Geographic Information System (GIS), composing a database for spatial analysis as showing in Figure 8. Workflow of research activities developed within the project.. Tef suitability maps were produced based on the environmental and LULC information, resulting in indication of optimal, sub-optimal and excluded areas of tef production. Remote Sensing data acquired before tef crops planting and during crop maturity periods were processed. Object-based image classification and change detection techniques were used in order to produce tef maps, identifying locations of crops cultivated in the main growing season for 2011. Maps produced were included in GIS for further improvement of tef suitability maps as well as further spatial analysis.

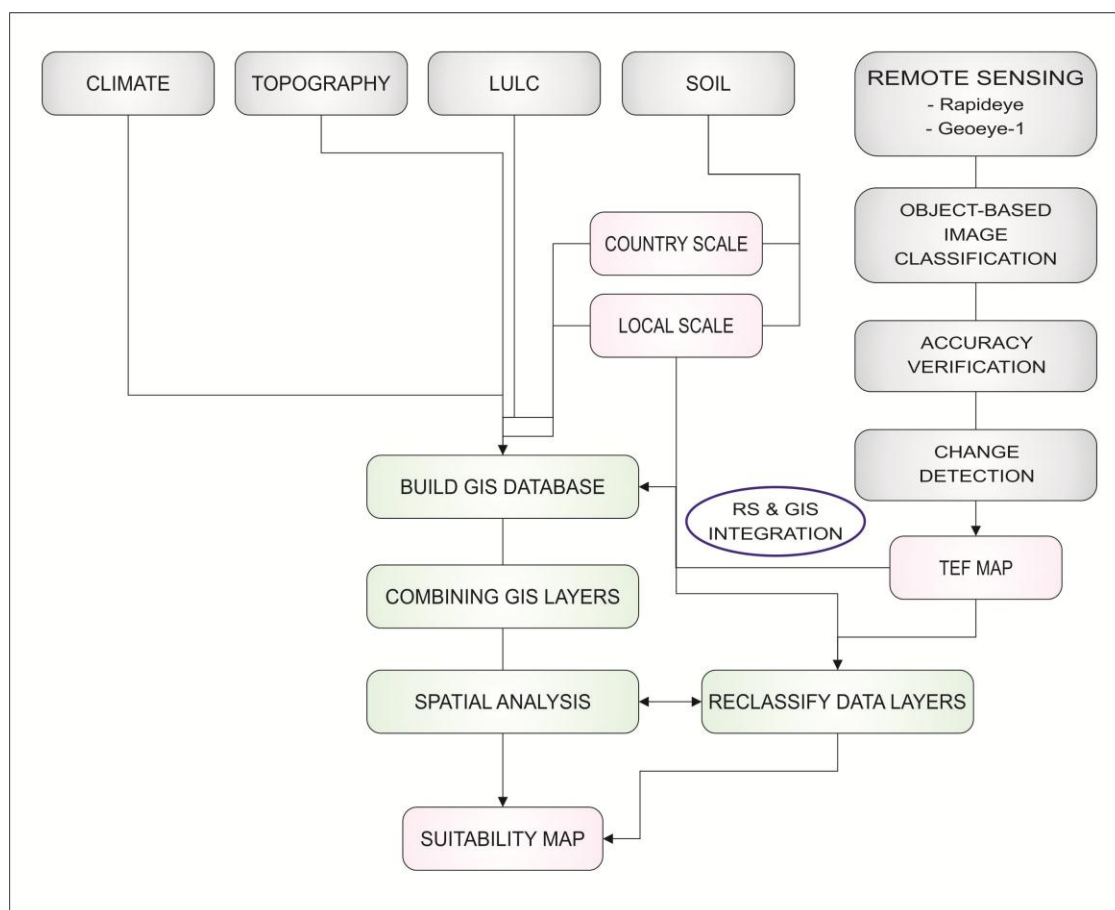


Figure 8. Workflow of research activities developed within the project.

Combination of data layers is done by reclassifying data layers and assigning optimal, possible, excluded classification ranges as prime numbers 2, 3 or 5 and then 1 and 0 respectively for each of the categories of data. For example, in the elevation classes equals to 1800-2200masl could be assigned value 2 as the optimal range, 0-1800masl and 2200-2600 masl is assigned value 1 as the possible range, and above 2600masl would be assigned 0 as a range excluded for tef production. In this way scenarios can be distinguished to see which factor is limiting. Using raster calculator, raster layers were multiplied and classes obtained with optimal combinations of possible ranges.

3.1. CLIMATE

Precipitation and temperature data were downloaded from FEWS (Famine Early Warning System) for 5 years (2006-2010). Precipitation data was downloaded in dekads. A dekad is a unit of time defined as follows: there are three dekads in a calendar month. The first ten days of a month constitute the first dekad of the month. The second ten days constitute the second dekad of the month, and the remaining days (8 to 11 days, depending upon the month) constitute the third dekad. Rainfall data was averaged from May to September per dekad.

For temperature, growing degree days and sunlight hours were downloaded. Rainfall data used to create the estimated average rainfall for the period of July 11 to October 10 is presented in Figure 9.

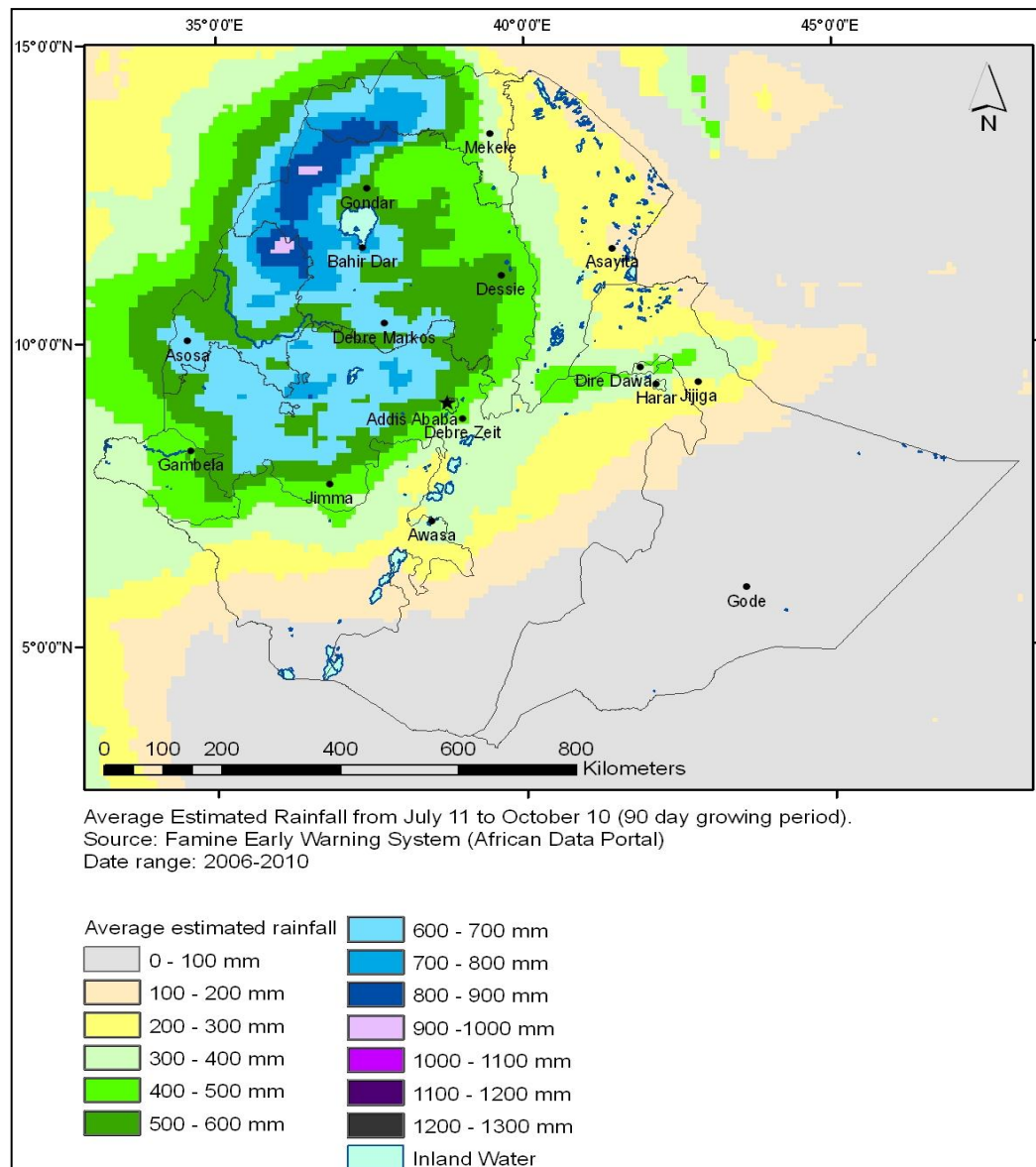


Figure 9. Average rainfall from July 11 to October 10 during 2006-2010.

3.2. TOPOGRAPHY

Topographic data was downloaded from U.S. Geological Survey's EROS Data Center, which provides global digital elevation model (DEM). USGS product is called GTOPO30, which is a global data set covering the full extent of latitude from 90 degrees south to 90 degrees north, and the full extent of longitude from 180

degrees west to 180 degrees east. The horizontal grid spacing is 30-arc seconds, resulting in a DEM having dimensions of 21,600 rows and 43,200 columns. The horizontal coordinate system is decimal degrees of latitude and longitude referenced to WGS84. The vertical units represent elevation in meters above mean sea level. The elevation values range from -407 to 8,752 meters. Minimal and maximum elevations from downloaded DEM were reclassified into 0-1800, 1800-2200, 2200-2600, 2600- 6000, No data and -9999 elevation classes. Optimal elevation used for tef in this study was between 1800-2200masl. The highest elevation used was 2600masl.

Topography data from FEWS (Famine Early Warning System) was used to create an elevation range map, presented in Figure 10.

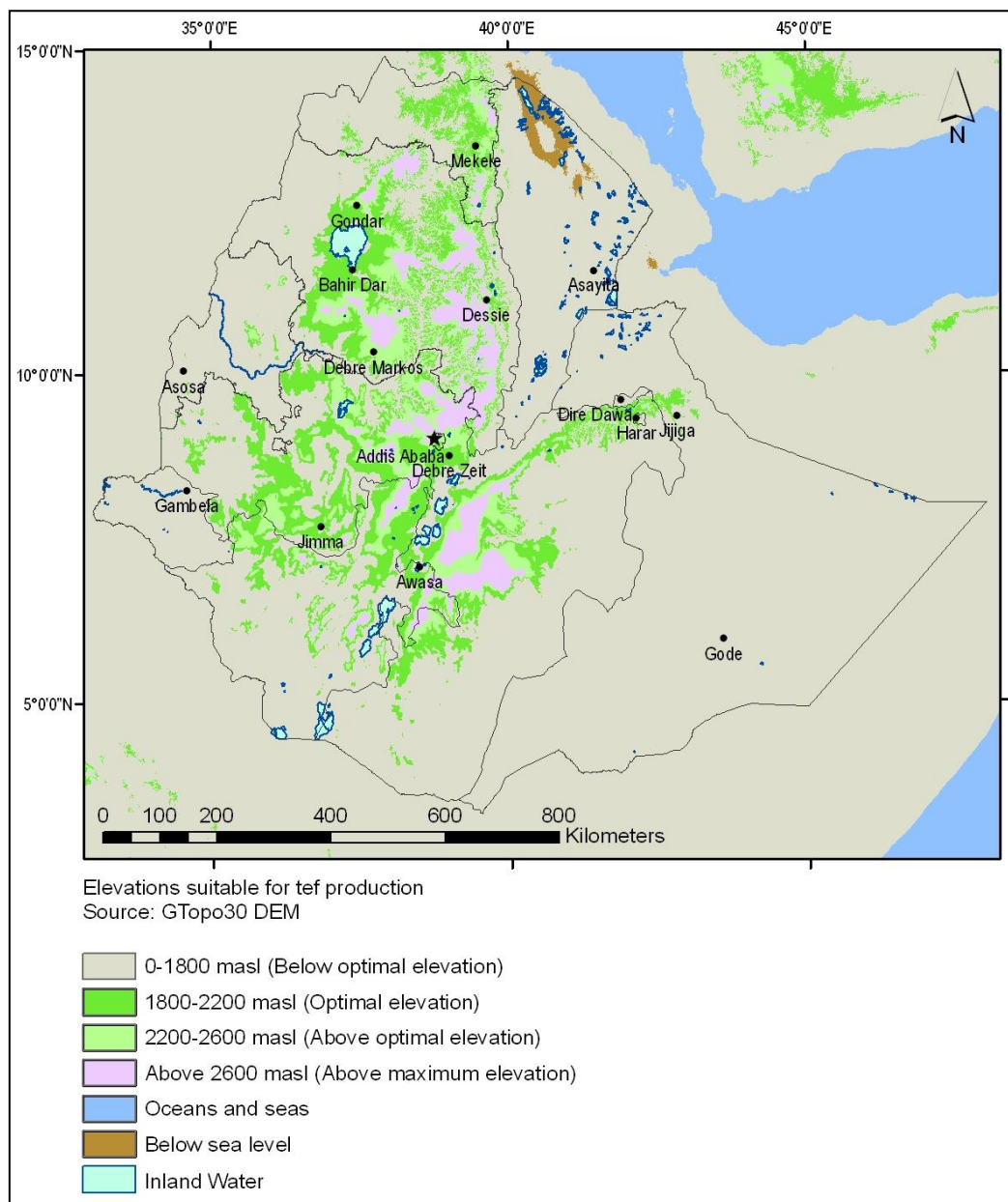


Figure 10. Elevation range map suitable for tef growing.

3.3. LAND USE/LAND COVER

Land use land cover data was obtained from Ethiopian Institute of Agricultural Research, Debre Zeit Agricultural Research Center (EIAR-DZARC). Land should only include that which is available for cultivation or other deemed available areas. We are using the dominant available area of land use land cover pixels and ignoring not relevant ones. This would exclude areas that are afro-alpine (Erica, grassland), bare land (exposed sand, exposed rock), forest (riparian, mountain mix, mountain broadleaf, bamboo, semi-evergreen), grassland, shrub land, urban, open water, wetland (seasonal swamp, perennial swamp), and woodland (dense, open).

The vector format maps were converted to raster format using grid size equals to 1000m. Land use/land cover classes were grouped in similar classes, such as forests, grasses, woodlands. Afro-alpine, bare land, forest, grassland, shrub land, urban, open water, wetland, and woodland classes were excluded.

Land Use/Land Cover generated using Ethiopian Institute of Agricultural Research; Debre Zeit Agricultural Research Center (EIAR-DZARC) data is presented in Figure 11.

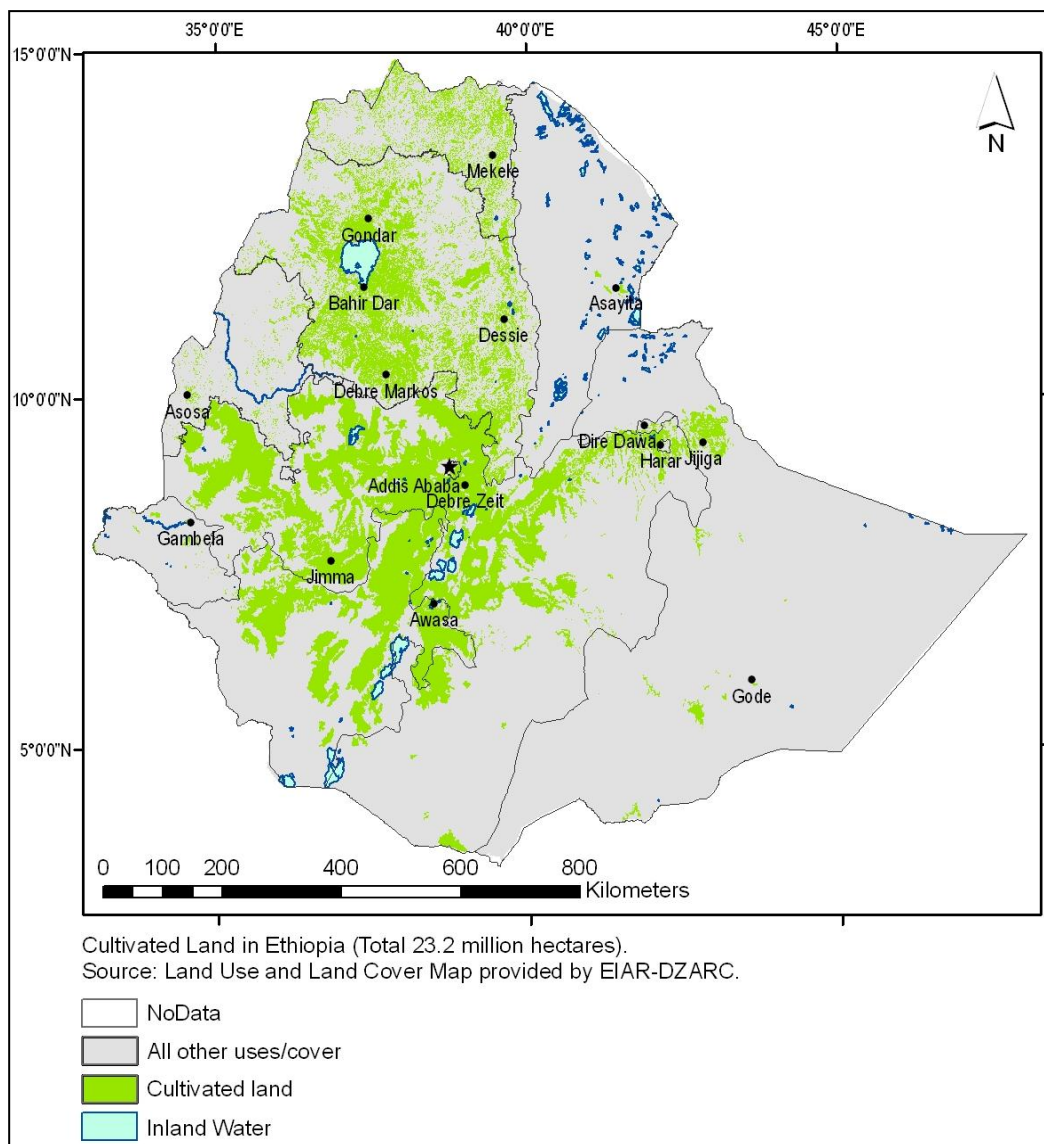


Figure 11. Cultivated land in Ethiopia.

3.4. COUNTRY SCALE SOIL INFORMATION

Country scale soil data were also obtained from ETHIOGIS. All classes corresponding to soil types like yermisols, xerosols, arenosols, and acrisols were excluded for suitability analysis. Soil type information collected from Ethiopian Institute of Agricultural Research, Debre Zeit Agricultural Research Center (EIAR-DZARC) was used to create the soil map presented in Figure 12.

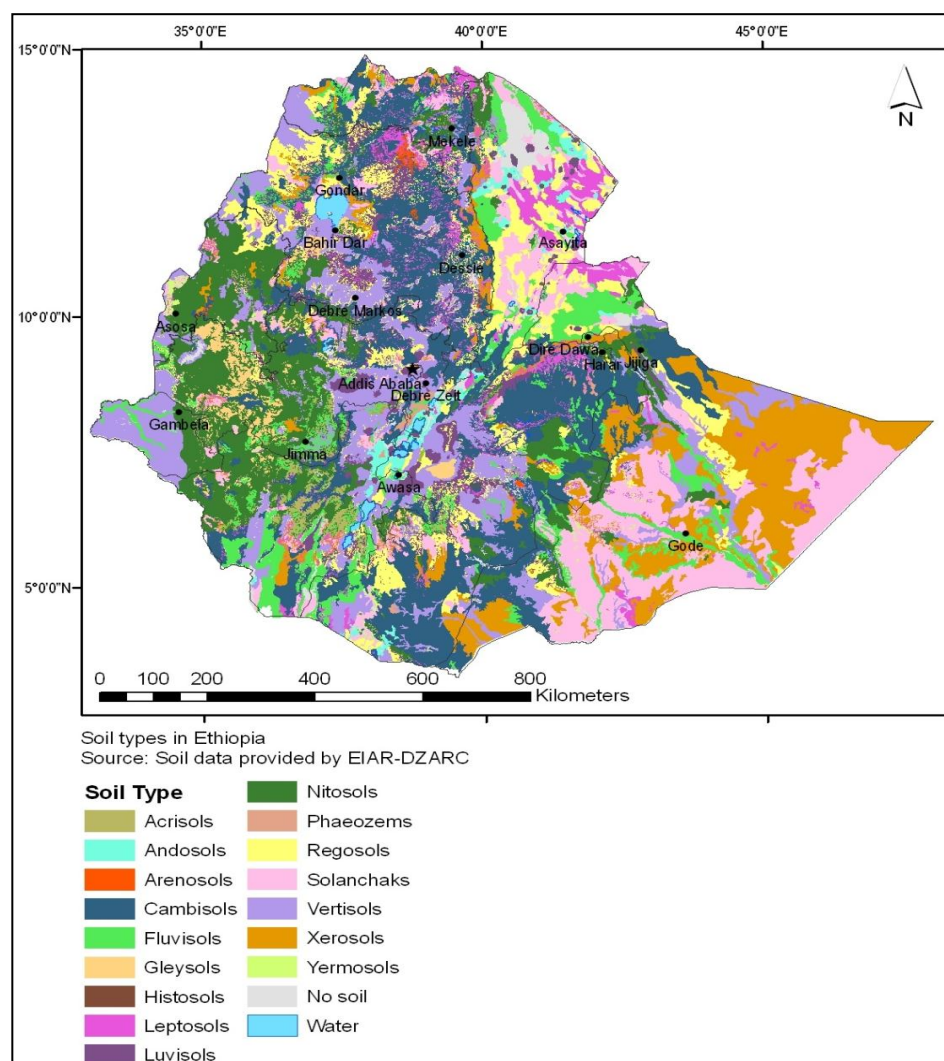


Figure 12. Soil types in Ethiopia.

3.5. LOCAL SCALE SOIL SURVEY AND MAPPING

Local scale soil sampling and survey along with laboratory analysis were performed by technicians and consultants under supervision of the Ministry of Water Resources, Federal Democratic Republic of Ethiopia. Field and analysis results were organized in a GIS allowing database integration and generation of soil mapping under the scope of this research project. These data will be used in the future to improve tef suitability maps.

The approach followed for the Ada'a soil survey has been based on feasibility level soil survey that intended to map the soils at 1:10,000 scales and identify potential areas for development under different land use types.

The Ada'a-debrezeit area is located in central highland of Ethiopia (in Oromia Regional State) between Debrezeit and Mojo towns at an elevation of about 1800 to 2160 m.a.s.l (within the co-ordinates of 8°30'N to 8°53'N and 38°50'E to 39°15'E). The area is traversed by the main Addis Ababa to Djibouti highway. Location of the study area is shown on Figure 13.

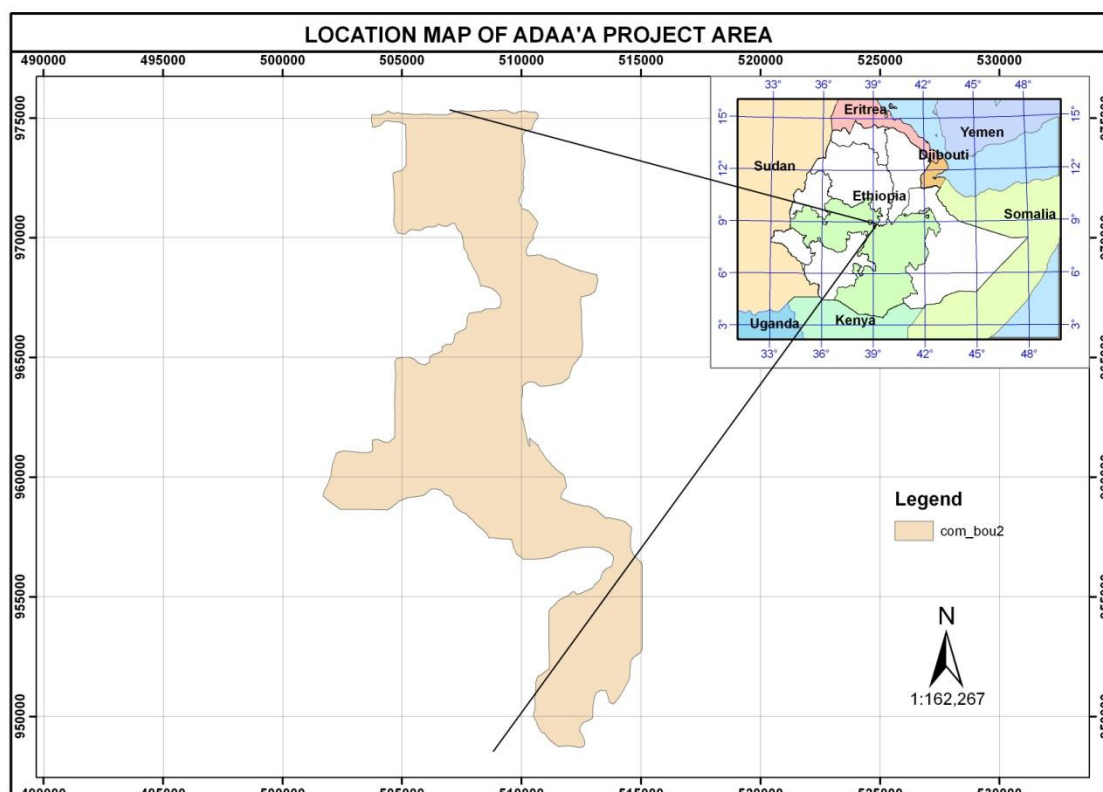


Figure 13. Location of the local scale soil survey and mapping study area.

3.5.1. Pre-Fieldwork

Activities were commenced with a review of available reports and maps of the study area. Review of previous studies were concentrated on the evaluation of their objectives and methodology and output in terms of data, maps and findings.

Field visit was made (together with the WWDSE soil survey technicians) before the start of actual soil survey to design and properly organize the activities and to evaluate the nature of the land escape. At this stage the soil survey technicians and the consultant have made thorough discussion on the approach to be followed for common understanding and uniformity. Before embarking the field work, required soil survey field equipment were properly checked; field description sheets for auger

boring, profile pits, hydraulic conductivity and infiltration rate tests formats were prepared and produced in a sufficient quantities.

3.5.2. Field Survey

Field survey conducted by a team of five groups under close supervision of the consultant Auger observations was done up to 1.2m or impenetrable material and pit descriptions to at least 2.0m (extending by augering 3.0 to 5.0m). Location of all pits and auger sites were recorded using GPS showing in Figure 14. Tef field soil pit surveyed area below.



Figure 14. Tef field soil pit surveyed area

Survey followed a basic 300m x 500m grid along transect (i.e., one auger site per 15 ha). Accessible areas were surveyed using 4WD vehicles and the inaccessible muddy areas (due to heavy rain) surveyed on foot. Progress along poorly maintained tracks was slow. A total of 667 auger hole observations were done for the actual grid survey.

Where impenetrable material occurred at shallow depth, mostly < 50 cm, three auger borings were made to exclude localized stone, rock or root. At each observation and description point, important site characteristics such as : site coordinates and number, location, landform and micro-topography, slope, position, parent material, surface stones and rockout crops, drainage, degree and type of erosion, land use, vegetation, and human influence were recorded. Soil profile characteristics such as depth, colour, texture, mottling, consistency, roots, presence of clay cutans, carbonates, mineral nodules and coarse fragments were also recorded.

Standard soil survey procedures were followed. Soils were described and classified according to the FAO “guidelines for soil description” (1990) and “world Reference base for Soil Resources” (1998). A total of 114 soil samples were collected and sent to the WWDSE for chemical and physical parameters analyses.

Infiltration (double-ring infiltrometer) and hydraulic conductivity (inverse auger hole method) measurements were conducted at representative soil pits (at least one per major soil type) thrice replicated. For infiltration, some tests were carried out on disturbed soil to more approximate irrigation on prepared land. .

For the available water content (AWC) undisturbed core samples were collected from the sampled profile pits and sent to the National Soil Research Center Laboratory (through WWDSE laboratory unit) in Addis Ababa for the moisture content analyses.

3.5.3. Soil Laboratory Analysis

The soil samples were collected from 21 representative profile pits and analysed in WWDSE Laboratory after the results for all soil samples were recieved,

compiled, encoded and analysed. Samples analysed in the laboratory were carried out on air dried fine earth fraction (<2mm). Each parameter analyzed was based on standard methods and procedures. The following parameters were carried:

- soil particle size distribution (texture) following hydrometer procedure,
- bulk density (gm/cm^3), on dry weight basis from pF ring samples.
- soil pH in H_2O and 1M KCl at a soil to solution ratio of 1:2.5,
- EC (ms/cm) at a soil to water ratio of 1:2.5 using EC meter.
- exchangeable Na, K, Ca, Mg ($\text{meq}/100\text{gm}$ of soil) following ammonium acetate leachate using Atomic Absorption Spectrophotometer (AAS),
- cation exchangeable capacity (CEC) ($\text{meq}/100\text{gm}$ of soil) following ammonium acetate method at pH 7,
- organic carbon (%) (walkley and Black method),
- total nitrogen, N (kjeldahl method) ,
- available phosphorous, p (Olson) $\text{mg p}_2\text{O}_5$ kg/soil ,
- free CaCO_3 (by acid neutralization method),
- field capacity and permanent wilting points (at 1/3 and 15 atm using pressure plate extraction).

Results of the analyses are used in the classification and description of the major soils and soil mapping unit.

3.5.4. Post field Work Activities

3.5.4.1. Data Compilation and Analysis

All the physical data (collected in the field) and results from laboratory analysis were compiled, encoded and transformed to generate statistical and cartographic information. Databases were established for:

- Auger hole and profile location points;
- Soil profile and site description;
- Soil auger and site observation;
- Soil laboratory analytical results;
- Soil physics (i.e. hydraulic conductivity and infiltration tests) data; and
- Identified soil types and soil mapping unit.

3.5.4.2. Soil Classification and Mapping

Based on field soil survey information, laboratory analyses and other relevant features soil types and mapping units were delineated, classified, characterized and mapped. Soil profile descriptions and auger observations in the field enabled to identify and delineate primary soil types. Laboratory results were used to confirm preliminary results of field observations.

soils of the survey area were classified on the basis of the revised FAO/UNESCO-ISRIC legend of the soil map of the world (1990) and world reference base for soil resources (1998).

Soil texture, topography, effective depth, colour, mottling, presence of clay cutans, mineral nodules, drainage characteristics and profile development were the major physical properties of the soil used as a basis of classification; and

CEC, base saturation, organic matter, exchangeable sodium percentage, free carbonates, pH, electrical conductivity, etc., were the important chemical characteristics of the soil used for classification of the major groups and soil units.

3.5.4.2.1. Soil Genesis

Soil forming factors, such as parent material, climate, topography, organisms (fauna and flora) and time were considered to be independent from each other but

can have simultaneous interactions. The stated soil forming factor would result in soil development of the area. Therefore, the genesis of the soils identified in the survey area was the result of interactions between the soil forming factors. Climate influences soil development by affecting the degree of weathering.

Climate and time effects are most pronounced on stable surfaces. On such surfaces past climate instead of the present climates may account for the soil conditions. In some crest areas weathering and decomposition are pronounced giving rise to deep and slightly well developed soils (such as Luvisols). Topography plays an important role in soil genesis, primarily through modification due to the impact of climate. Thus, on steeper slopes (close to mountains and hills) water runs rapidly retarding soil development. Where topography is steeper, soils are shallower, because erosion has not give them time to develop. Soils developed on recent alluvial and colluvial deposits are at the moderate stage of development, which were evidenced by their moderate to weak structure. In most of the flat, nearly flat and gradually undulating topography in the lower landscale positions, imperfectly to poorly drained soils are formed.

Parent material is important in soil development because different rocks are composed of different minerals which breaks under weathering to various soil minerals. Basalt and other basic rocks are rich in ferromagnesian minerals which breakdown to clay minerals, resulting to clay textured soils.

3.5.4.2.2. Soil Morphology

Soil morphology is described using soil characteristics such as soil depth, colour, texture, consistence, structure, drainage, etc. Summary of the dominant morphological characteristics for major soils identified in the Ada'a plains are given in Table 6.

Table 6. Summary Characteristics of Control Morphological of the Ada'a Soils

Soil group	Depth	Colour	Texture	Structure	Consistency	Drainage
Vertic Cambisols (CMvr) (sometimes found in association with Luvisols and associated vertic integrate)	Deep to very deep With vertic horizon starting between 20/25 and 90/100cm below the surface	Dark gray to dark grayish brown; yellowish brown	Clayloam, sandy/silty loam, clay (most soil texture is loamy to clayey); clay illuviation in the cambic horizon)	Moderate fine and medium angular and subangular blocky, prismatic, structure	Friable, sticky and plastic	imperfect and Imperfect to poor
Chromic Luvisols (LVcr) (mostly found on the crest slope)	Deep to very deep	Brown to dark brown surface horizon over a (greyish) brown to strong brown or red argic sub surface horizon	Clay, clay loam, silty clay loam, loam, silty loam	Weak friable to strong fine and medium granular, angular and, sub-angular blocky	Very friable to friable, slightly to moderately sticky and plastic	Moderate to well
Pellic and chromic Vertisols (VRpe and VRvr) found in depressions and level to gradually undulating areas	Deep to very deep (form wide and deep cracks up on drying)	Grayish brown, dark brown to very dark gray, black, dark grayish brown, etc (colour differences between vertisols are often indicative of differences in drainage status)	Clay, heavy clay, clay loam, silty clay, silty clay loam	Fine to coarse moderate to strong sub-angular and angular blocky structure. In some cases massive and/or prismatic structure is developed in the sub-soil	Dry vertisols have a very hard and firm consistent; wet vertisols are (very) plastic and sticky and friable only over a narrow moisture range.	Imperfect, poor and very poorly

3.5.5. Description of the Major Soil Types of the Survey Area

Soils of the survey area were categorized with the individual soil type specific criteria. The texture ranges from sandy loam, through silty loam, and silty clay loam, clay to heavy clay. In most cases there were good correlation between land form and soil texture. The clayey texture soils have moderately wider cracks. Mostly vertisols contain calcium carbonate concretion and gravels in depth. In where it was observed

that there exist compact and hard layers with in the soil profiles. Some major features and description of the identified soils characteristics are highlighted as follows:

3.5.5.1. Luvisols

This soil has an increase clay content within a profile depth. There exist clay skins at least 3 to 5 percent of both horizontal and vertical ped faces.

Luvisols are soils having an argillic horizon, which has a base saturation of 50% or more at least in the lower parts of the B-horizons. These soils are derived from colluvial and alluvial parent material. It is observed that sub-surface horizon has distinct higher clay content than the overlying horizon.

Concentration of clay in the B horizon, removal of carbonates from the initial material of that horizon (i.e., soil shows marked textural differentiation within its profile, due to top layer clay depletion and accumulation of clay in sub-surface horizons). Gradual textural change noted within the profile and unconsolidated material of alluvial and colluvial deposits are parent material.

Luvisols are potentially suitable for a wide range of agriculture due to their favorable physical properties. A typical pedon belonging to the luvisols has the following profile characteristics.

0 – 15 :Dark reddish brown (7.5YR 3/2, moist sandy loam, no mottle, weak friable granular structure. Slightly hard when dry, friable when moist, none to slightly sticky and slightly plastic when wet; common fine and medium random tubular pores, common fine and medium, few coarse roots, rare to few termite galleries; non-calcareous, smooth gradual boundary:

15 – 80 :reddish brown (7.5YR 3/3) moist, clay loam; no Mottles; moderately strong medium angular blocky structure, hard when dry, friable when

moist, common fine and medium random tubular pores, few fine, medium and coarse pores; rare termite galleries, non-calcareous, smooth gradual boundaries.

80 – 150 :red (5YR 4/6), moist, light clay, no mottles, moderately fine angular blocky structure, hard when dry, friable when moist common very fine random tubular pores, few fine, very few medium and coarse roots, few soft black manganese nodules, non-calcareous, wavy abrupt boundary .

150 – 180: yellowish red (5YR 5/6), slightly moist, very fine clay loam, no mottle; weak medium angular block structure, hard when dry, friable when moist, slightly sticky and slightly plastic when wet, many fine random tubular pores; very few fine and medium roots, rare termite galleries, rare calcareous; abrupt wavy boundary with.

180 – 200: red (2.5 YR 4/8), slightly moist, grit, no mottles, weak Sub-angular blocky, rare pores, very rare fine roots, slightly calcareous.

3.5.5.2. Cambisols

Soils with fine earth clay fraction (between 25-30 and 100cm) texture of sandy loam or finer. It has stronger chroma, redder hue and higher clay content than the underlying horizon. The soil has less carbonate than the underlying horizon.

The soils are structured as grayish brown to black in colour, the texture is loamy to clayey, the beginning of clay illuviation was detected in the horizon and more clay content is normally detected in the upper horizon. Some of its profiles have slightly to moderately calcareous as the profile depth increases. It is a soil with beginning horizon differentiation evident from changes in colour, structure, etc.

Parent material of the soil was noted as medium to fine structured material derived from colluvial and alluvial deposits. Sign of beginning clay illuvation was detected in the cambic horizon but the clay content was higher in the upper horizon. By and large, cambisols make a good agricultural land and are intensively used, when properly managed.

Pedon belonging to cambisols has the following profile characteristics:

0 – 20: light brownish gray (10YR 6/2), moist; silty clay loam; no mottle; weak fine sub angular blocky structure, friable when moist; slightly sticky and plastic, few fine random tubular pores; many fine and medium, few coarse roots; non calcareous, distinct straight boundary with:

20 – 35: gray (10YR 6/1), moist; sandy clay; no mottle, weak sub angular blocky structure; hard when dry, firm when moist, few to rare fine random tubular pores, many fine and medium rare coarse roots, slightly calcareous; gradual boundary with:

35 – 90: very dark gray (10YR 3/1), moist; clay, few rare yellowish red mottle; weak coarse prismatic breaking to coarse angular blocky structure; very hard when dry; very firm when moist, rare fine random tubular pores; few fine and medium roots, clear/gradual boundary.

90 - 150 : Dark brown (10YR 3/3), clay loam, calcareous very fine clay loam, yellowish red mottle; weak medium angular block structure, hard when dry, friable when moist, slightly sticky and slightly plastic when wet, many fine random tubular pores; very few fine and medium roots, rare termite galleries, rare calcareous; diffuse wavy boundary with.

150 – 200: dark gray (10YR 4/6), moist, clay loam, massive, very hard when dry, very firm when moist, very few fine pores, very slightly calcareous; sharp boundary with rocks of basement complex.

3.5.5.3. Vertisols

Vertisols have high clay content in all horizons, which develop cracks from the soil surface downward and have one or more of the following: gilgai, micro-relief, intersecting slickensides or wedge shaped structure at some depth between 25/30 to 90/100cm from the surface. Vertisols are deep to very deep, imperfectly to poorly drained, formed on flat to almost flat topography in the lower landscape positions.

Vertisols are very hard to extremely hard when dry, and very sticky and plastic when wet, which reflects poor workability. Vertisols are productive soils if properly managed.

Colour differences noted between Vertisols (i.e., pellic and chromic), which are often indicative of differences in drainage status. The more reddish hue or stronger chroma of relatively better drained vertisols reflect higher contents of free iron oxides. Poorly drained vertisols are low in Kaolinite and have less free ferric iron; their hue are less red and chromas are weaker. A pedon belong to the vertisols has the following profile characteristics:

0 – 25: Very dark grayish brown (10YR 3/2), moist, silty clay, no mottles, moderately strong subangular blocky structure; hard when dry, firm when moist, sticky and plastic when wet, many fine random tubular pores; common fine and medium roots, non calcareous, gradually wavy boundary. Black (10YR2/1) moist, very firm, very sticky, very sticky and very plastic; moderate, medium, angular/sub angular

blocky structure; common, fine and medium, pores, common fine and medium roots, diffused, smooth horizon boundary.

25 – 65: very dark gray (10YR 2/2), Slightly moist, clay, few to common reddish brown mottles, strong very coarse prismatic structure breaking to medium and coarse angular blocky, hard when dry firm when moist, sticky and plastic when wet, common fine random tubular pores, common fine and medium roots, gradually wavy boundary with:

65 – 120: very dark gray (10YR 2/1), Slightly moist, clay, common reddish brown and yellowish red mottle, strong coarse angular blocky to prismatic, extremely hard when dry, extremely firm when moist, sticky and plastic when wet, few very fine random tubular pores; common fine and few medium roots, slightly , calcaous, clear irregular boundary with:

120 – 160 : very dark gray (2.5Y 3/0), slightly moist, silty clay, common yellowish brown mottle, very weak medium angular blocky/prismatic, extremely hard when dry, extremely firm when moist, sticky and plastic when wet, few very fine medium tubular pores, very rare fine roots, strongly calcarous, clear irregular boundary. Dark grayish brown (10YR4/2) moist, firm, very sticky and very plastic moderate, coarse, wedged shaped structure, common distinct slickenside, common hard, black iron manganese nodules; common faint brownish mottles; moderately to extremely calcareous; few, fine and medium pores.

160 – 200: dark grayish brown (2.5Y 4/2) moist, few fine mottles, clay loam to clay, structureless/massive, very hard when dry, friable when moist,

slightly stick and plastic when wet, no pores, no roots, extremely calcarous, and extreme compacted.

3.5.6. DESCRIPTION OF THE SOIL MAPPING UNITS

Soil units were defined based on stable characteristics of soils and their environment. In distinguishing criteria for mapping units balanced approach was used to maintain clear information, that can be identified as soil mapping units and be mapped with an acceptable degree of accuracy. There are different forms of soil mapping units. The major ones are:

- Simple mapping unit: in which identification and a boundary delineation consist mainly a single soil type or very similar to it. In soil nature it is very difficult to get uniform mapping unit at any large scale.
- Soil association mapping units: different soil types that occur together and differ in characteristics relating to local variations. Here the dominant soil is mainly described and mapped. Proportion of the dominant, associated and inclusion soils are dependent on the complexity of the specific soil mapping unit. In most of the cases inclusion soils constitute less than 15% of the soil mapping unit, while associated and dominant soils have more proportion.

For the survey area soil association mapping unit of FAO/UNESCO-ISRIC 1998 was adopted based on characteristics of the dominant soil units. Soils of the surveyed area were categorized into 14 groups (i.e., 13 soil mapping units and 1 miscellaneous type). Coding of soils mapping unit was based on specific criteria of each soil and land forms observed.

3.5.6.1. Mapping Unit Representation

Legends to the soil-mapping units were structured at three level of generalization in hierarchical order, namely: texture (level 1), soil unit (level 2) and slope class (level 3). A serial numbers, upper, and lower case letters designated the mapping unit symbols represents the three elements. The following general examples illustrated how mapping codes were constructed:

- First serial number shows the first level of generalization (texture, Table 7),
- Second (upper and lower case) letters show second level of generalization (soil type),
- Third upper case letter shows third level of generalization (slope class)

Example:

Table 7. Categorized soil textural classes for the soil mapping unit

Textural groups	Texture
1	Heavy clay
2	Clay
3	Clay loam
4	Silty clay
5	Loam
6	Silt clay loam
7	Sandy loam

Based on the land form the landscape of the project area is grouped into three (i.e., lower plain, piedmont and upper plain (see Table 8). See soil mapping unit on Figure 15.

Table 8. Categorized slopes classes for the soil mapping unit

Code	Slopes Classes	Land form
A	0-1%	Lower Plain
B	1-2%	Piedmont Plain
C	1-2%	Upper Plain

3.5.6.2. Soil Mapping Unit Description

14 soil mapping units are identified, as indicated above. Soil were mapped and described based on observed and analysed characteristics of dominant parameters. Summary descriptions of the soil mapping units are given in Table 9 and Table 10. Summary information of area coverage by each soil unit is indicated in Table 11. See Figure 16 for soil mapping discription categories.

Table 9. Description of soil legend

S/no	Soil Mapping Unit	Description
1	5CMvrA (358.50ha)	Very deep, grayish brown, clay loam to clay, imperfectly to poorly drained, non-calcareous, developed on lower plain (slope 0 – 1%)
2	3VRpeA (517.30ha)	Very deep, very dark gray, clay loam to clay, imperfect to poorly drained, calcareous developed on piedmont plain (slope 1 – 2%)
3	2VRpeB (327.70ha)	very deep, black, clay, imperfectly to poorly drained, slightly calcareous, developed on piedmont plain (slope 1 – 2%)
4	3VRpeCe (241.80ha)	Very deep, very dark gray, clay loam, imperfectly drained, slightly calcareous, eroded phase, developed on upper plain (slope 1 – 2%)
5	6VRpeCe (963.10ha)	very deep, very dark gray, silty clay, poorly drained, slightly calcareous, eroded phase, developed on upper plains (slope 1 – 2%)
6	3VRpeC (593.0ha)	Very deep, black, clay loam, imperfectly to poorly drained, calcareous, developed on upper plain (slope 1 – 2%)
7	1VRpeA (2237.0ha)	Very deep, black, heavy clay, poorly drained, slightly calcareous, moderately compacted, developed on upper plain (slope 1 – 2%)
8	3VRcrA (1374.0ha)	Very deep, very dark grayish brown, clay loam, poorly drained, slightly calcareous, developed on lower plain (slope 0 – 1%)
9	6LVcrA (1271.0ha)	Very deep, dark reddish brown, silty clay loam, well drained, slightly calcareous, developed on upper plain (slope 1 – 2%)
10	1VRcrB (2514.0ha)	Very deep, very dark brown, heavy clay, poorly to poorly drained, slightly calcareous, compacted, developed on piedmont plain (slope 1- 2 %)
11	2VRpeA (492.40ha)	Very deep, black, heavy clay, poorly to very poorly drained, strongly compacted, slightly calcareous, developed on lower plain (slope 0 – 1%)
12	2VRpeC (849.90ha)	very deep, very dark gray, clay, poorly to very poorly drained, extremely compacted, developed on upper plain (slope 1-2%)
13	6VRcrB (571.40ha)	very deep, very dark brown, Silty clay loam, imperfectly to poorly drained, extremely compacted, moderately calcareous, developed on upper plain (slope 1-2%)
14. Miscell. land		
Hi	708 ha	Hill
Sw	369. 0ha	Sw ampy

Table 10. Indicative physical and chemical properties of the Ada'a mapping units

Sr No	Map. Unit	Area		Eff. Soil depth (cm)	Text. class of top soil	BD g/cm ³	IR cm/hr	HC m/day	AWC (mm/m)	pH	CEC meq/100g of soil top 25cm	BS (%)	OC % Top 25 cm	EC ds/m top 100 cm	TNT% top 25cm	P ₂ O ₅ top 25cm	CaCO ₃ %	Drain. Class	Slope (%)	ESP top 100 cm	Flooding	Stones	Indicative example Profiles
1	5CMvrA	358.5	2.68	200	L	1.7	0.93	0.094	170.78	6.35	25.35	76.9	0.97	0.05	0.05	7.40	Tra	Imp to poor	0-1	2.34	N	N	AP-04
2	3VRpeA	517.30	3.86	200	CL	1.8	0.93	0.094	204.91	6.69	34.4	105.0	0.95	0.08	0.07	10.50	5.8	Imp to Poor	1-2	2.69	N	N	AP-03
3	2VRpeB	327.70	2.45	200	C	1.4	0.93	0.094	172.45	6.8	36.4	107.0	1.33	0.05	0.06	44.0	8.4	Imp.to poor	1 -2	1.3	N	N	AP- 01
4	3VRpeCe	241.80	1.81	200	CL	1.8	0.93	0.094	204.91	6.83	47.35	90.4	0.04	0.08	0.07	10.5	5.0	Imp.	1-2	0.51	N	N	AP- 07
5	6VRpeCe	963.10	7.19	200	SiC	1.87	1.16	0.12	241.27	7.0	56.4	79.4	0.84	0.07	0.04	39.0	6.25	Imp	1-2	0.75	N	N	AP- 06
6	3VRpeC	593.00	4.43	200	CL	1.6	1.44	0.16	204.91	6.4	36.4	127.0	1.23	0.11	0.06	23.2	Tra	Imp to poor	1-2	0.71	N	N	AP- 08
7	1VRpeA	2237.00	16.71	200	C	1.66	0.28	0.14	296.41	7.9	70.3	101.0	0.70	0.10	0.10	25.4	4.2	Poor	1-2	0.67	N	N	AP- 40
8	3VRcrA	1374.00	10.26	200	CL	1.6	1.44	0.17	296.41	7.6	61.2	80.4	0.61	0.09	0.01	31.6	6.3	Poor	0-1	0.78	N	N	AP- 15
9	6LVcrA	1271.00	9.49	200	SiL	1.66	5.29	0.13	273.34	6.8	56.0	87.1	0.90	0.09	0.08	13.7	9.00	Well	1-2	0.43	N	N	AP- 27
10	1VRcrB	2514.00	18.78	200	HC	1.8	1.2	0.12	352.26	6.8	46.4	126.07	0.92	0.1	0.05	21.10	7.98	Poorly to v. poorly	1-2	1.48	N	N	AP - 22
11	2VRpeA	492.40	3.68	200	HC	1.8	0.22	0.24	352.26	6.6	64.1	109.5	0.93	0.07	0.10	26.3	Tra	Poor to v.poor	0-1	0.57	N	N	AP - 48
12	2VRpeC	849.90	6.35	200	C	1.64	0.22	0.24	352.26	7.95	63.0	102.0	1.03	0.14	0.05	49.5	3.9	Poor to v.poor	1-2	0.35	N	N	AP – 32
13	6VRcrB	571.40	4.27	200	SiCL	1.9	0.93	0.094	241.27	7.20	57.4	104.4	0.07	0.17	0.07	39.0	8.41	Imp to poor	1 -2	0.37	N	N	AP-19
14. miscellaneous land																							
- Hills (369ha - swamp(708 ha)		1,077.0	8.05																				

Table 11. Major soils of the study area and their distribution

Major soil types	Identified soil unit	code	Area (ha)	Area (%)
Cambisols (CM)	Vertic cambisols	CMvr	358.5	2.68
Luvisols (LV)	Chromic luvisols	LVcr	1271.0	9.50
Vertisols (VC)	Chromic vertisols	VRcr	4459.40	79.78
	Pellic vertisols	VRpe	<u>6222.20</u>	
			10,681.60	
Hills, swampy area		H, S	1077.0	8.04
Total			13,388.10	100

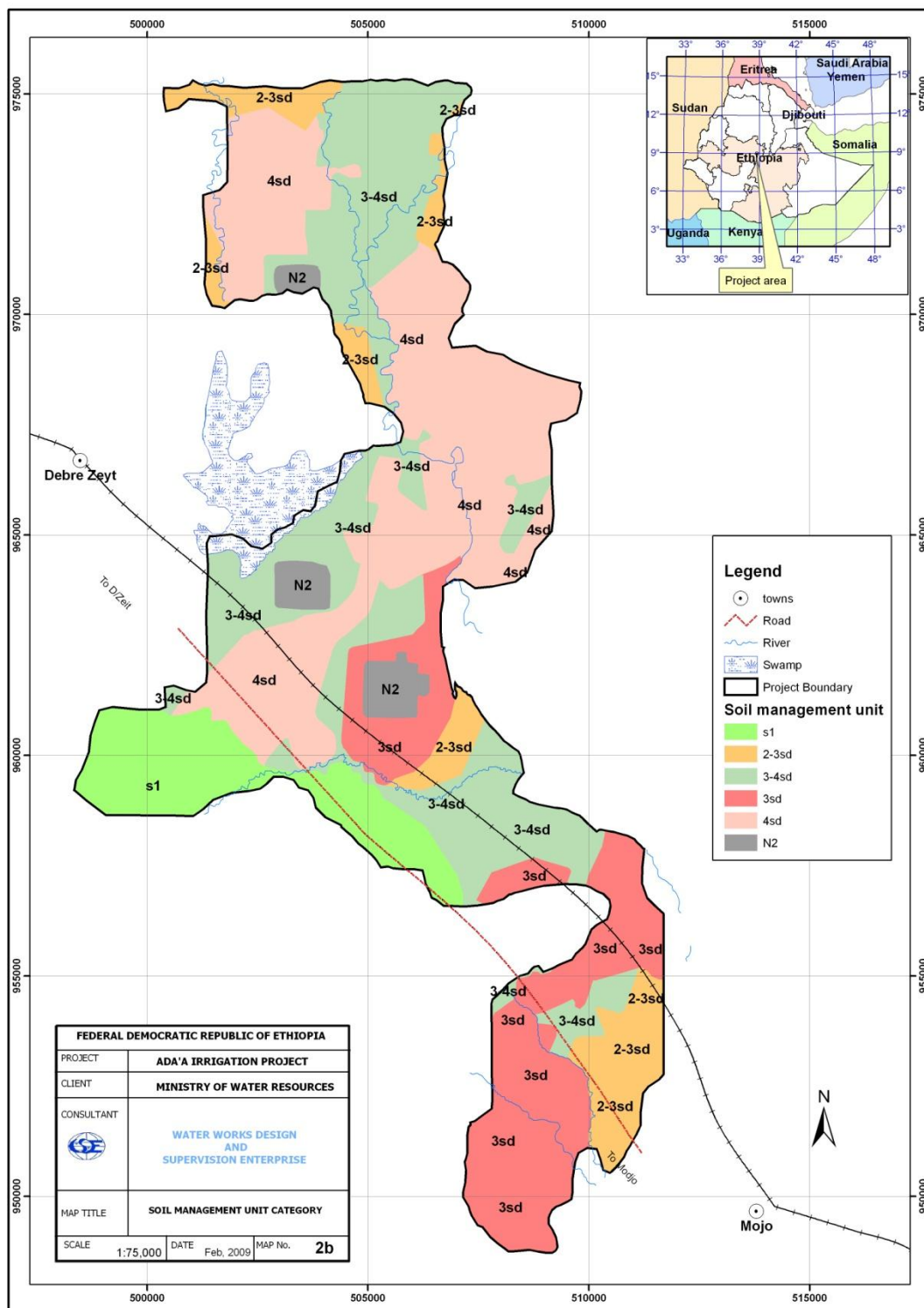


Figure 15. Adaa soil mapping unit

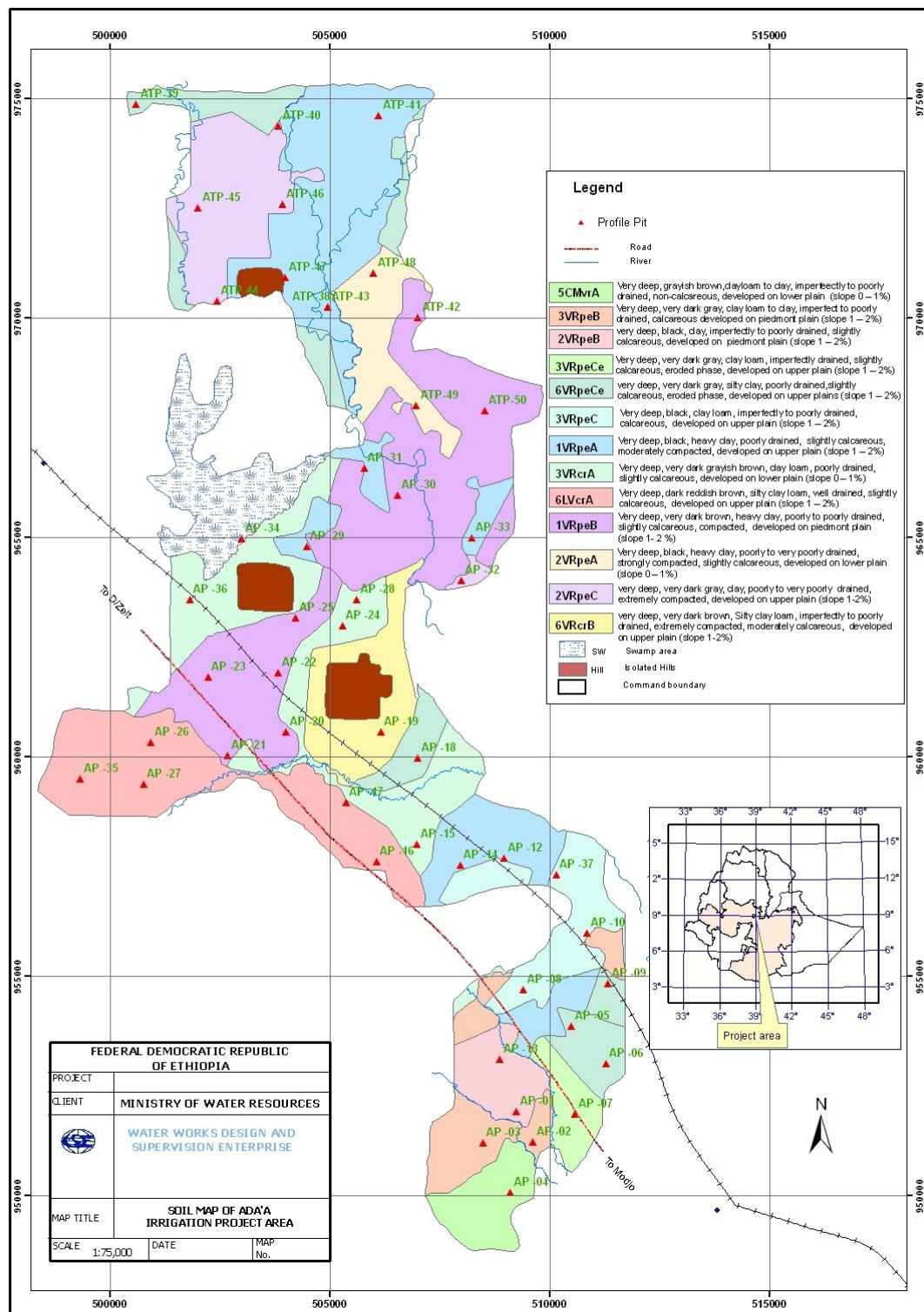


Figure 16. Ada'a Soil Map

3.6. TEF SUITABILITY

The classification scheme for raster calculation used to generate tef suitability map (shown in Figure 17) is presented in Table 12. Values presented here were based on literature review and experts consultation in Ethiopian Ministry of Water Resources to establish class limits for a modeling scenario where a chosen set of soils is deemed optimal for tef cultivation.

Table 12. Raster calculation values used to generate tef suitability map.

Elevation	Rain	Soil	Result	Result
2	3	5	30	Optimal
1	3	5	15	optimal rainfall and soil, elevation possible
2	1	5	10	optimal elevation and soil, rainfall possible
2	3	1	6	optimal elevation and rainfall, soil possible
1	1	5	5	optimal soil, possible elevation and rainfall
2	1	1	2	optimal elevation, rainfall and soil possible
			0	excluded (for any of the three factors)

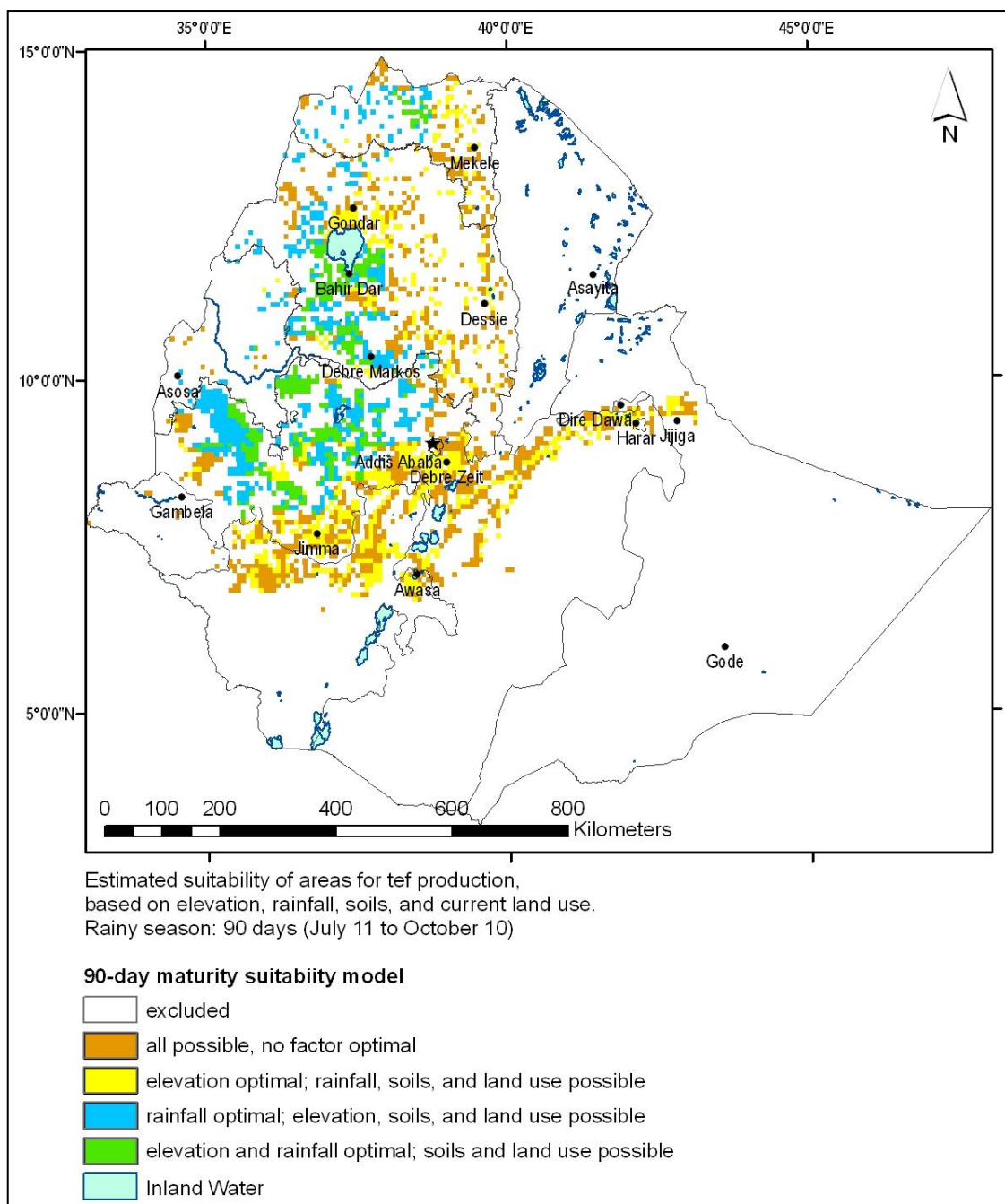


Figure 17. Estimated suitability map for tef production.

3.7. CHAPTER SUMMARY

In this chapter it was shown how data on climate, topography, land use/land cover and country scale soil information were collected and organized in a Geographic Information System. Ranges of optimal, sub-optimal and critical environmental and climatic conditions for new tef crops establishment were defined and applied through spatial analysis. Resulting tef suitability maps can be used by farmers interested in growing tef as an aid to decide on optimal locations for crop growing or on whether to grow tef or other crops on their lands. Politicians and decision makers can use these results to guide public policy and actions directed to increase tef sustainable production.

Soil local scale mapping provided more detailed information on soil characteristics that are important for tef development. This information will be incorporated into the GIS to improve tef suitability maps. Definition of optimal and critical ranges of soil characteristics related to tef development is necessary.

4. TEF LOCAL SCALE MAPPING

Although land use/land cover data is available from above mentioned ETHIOGIS in a country scale, more accurate tef mapping is considered necessary for crop management and production planning. For this reason, adaptation of methodologies for accurate tef mapping using high spatial resolution multi-spectral data is discussed in this section.

Remote sensing applications for agricultural areas monitoring have demonstrated the importance of temporal coverage for consistent and accurate crop identification and analysis of vegetative growth since the 70's (National Research Council, 2007). Tef grows rapidly (varies from 60 to 120 days) mainly between July and November (Ketema, 1989), which makes it an ideal candidate for crop identification through change detection techniques.

Tef is grown by smallholder farmers with properties smaller than 2.5 ha, which accounts for 96 percent of total area cultivated. Only 40 percent of the smallholders cultivate more than 0.90 ha (Taffesse *et al.*, 2011). These characteristics of cultivated areas determine the need for high spatial resolution satellite data, for an accurate crop identification and mapping.

A survey of commercially available satellite systems providing high spatial resolution multi-spectral data was accomplished, considering tef growing season. Most common high spatial resolution commercial satellites and their characteristics

are shown in Table 13. Decision on image selection was mainly defined by availability of data acquired before the growing season and during crop maturity, allowing identification through change detection techniques. Selected satellite data providers for this research are highlighted in light gray on Table 13.

Table 13. Most common high spatial resolution commercial satellites

	QuickBird	IKONOS	GeoEye-1	WorldView-2	Rapideye-1
Spatial Resolution	0.6m (P ¹) 2.4 (M ²)	0.82m (P ¹) 3.2 (M ²)	0.5m (P ¹) 1.65m (M ²)	0.46 to 0.5m (P ¹) 1.84 to 2.08m (M ²)	5m (M ² only)
Swath Width	16.5 km	11 km	15 km	16.4 km	20 km
Multi-Spectral ³	4 bands (R,G,B,NI)	4 bands (R,G,B,NI)	4 bands (R,G,B,NI)	8 bands (Coastal, R, Y,G, B, RE, NI1, NI2)	5 bands (RGB, RE, NI)
Average Revisit Time	3-4 days	2-3 days	2-3 days	2- 3 days	Daily to 5.5 days
Mapping Accuracy	20-meter	10-meter	2-meter	6.5 meter	50m
Pricing U\$/km ² (archive)	14-17	10-45	12.5 - 50	14-17	1.28 (500km2)
Pricing U\$/km ² (on demand)	20-23	20-45	25-50	20-23	

1 - letter P denotes images acquired in panchromatic mode

2 - letter M denotes images acquired in multispectral mode

3 - letters R, G, B, NI and RE denotes wavelengths of the electromagnetic spectrum in which image is acquired, corresponding to Red, Green, Blue, Near-infrared and Red-edge regions respectively.

4.1. STUDY AREA

Activities related to tef mapping at a local scale are concentrated on East Shewa, one of the Zones of the Ethiopian Region of Oromia. The area was selected giving its concentration of tef fields and easy access. Location of image collection within Oromia, East Shewa and its placement within Ethiopia are shown in Figure 18.

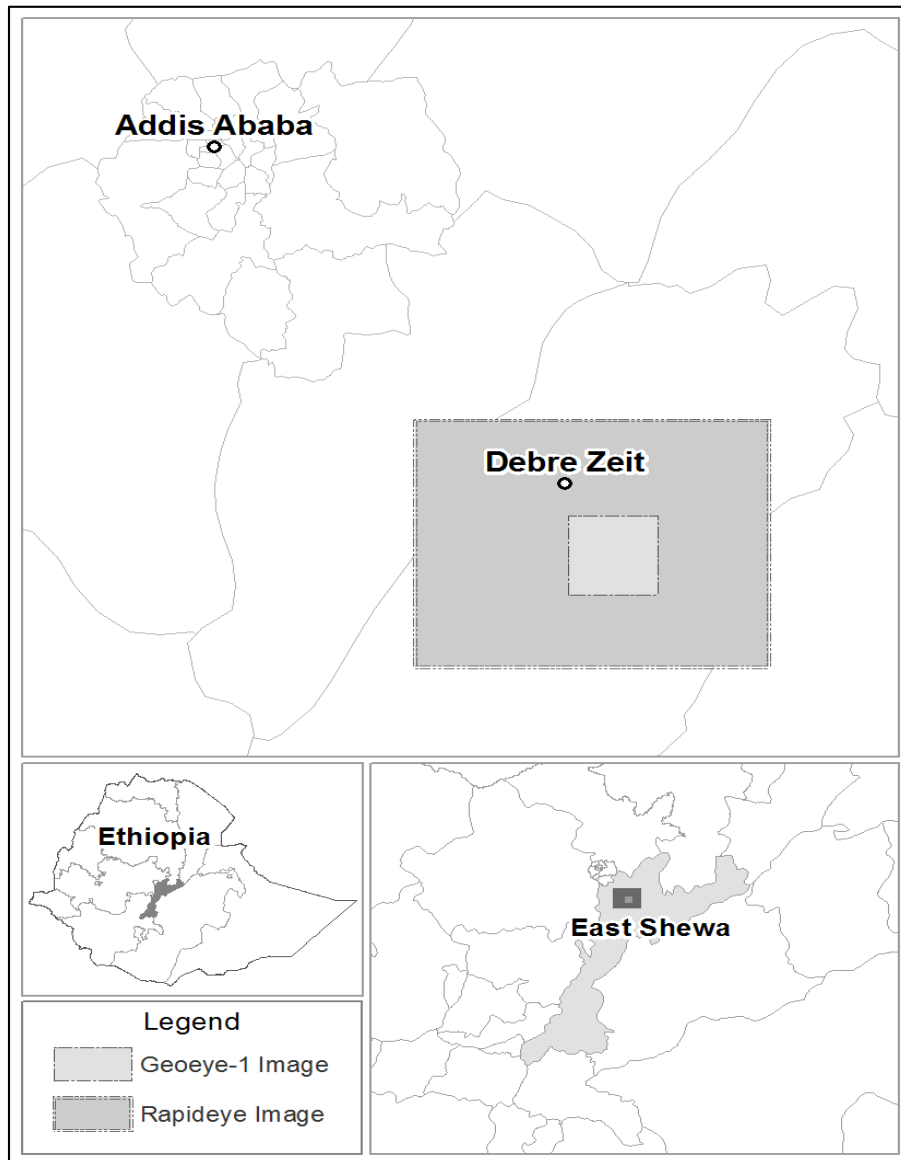


Figure 18. Study area and image acquisition location maps.

4.2. SATELLITE DATA

The selection of Image availability for the period before tef sowing was based on Geoeye-1 data. GeoEye Imaging System sensor onboard Geoeeye-1 satellite specifications and image characteristics are shown in Table 14. Image acquisition date was 28 July 2011, 07:52 GMT (Greenwich Mean Time).

Table 14. Parameter specification of the GIS instrument onboard Geoeye-1 satellite.

Imager type	Pushbroom imager. Line scan imaging system with TDI (Time Delay Integration) capability	
Imaging mode	Panchromatic (Pan)	Multispectral (MS)
Spectral range	450-900 nm	450-510 nm (blue) 520-580 nm (green) 655-690 nm (red) 780-920 nm (near infrared)
Spatial resolution at nadir	0.41 m GSD ¹	1.64 m GSD ¹
Swath width	15.2 km (multiple adjoining paths can be imaged in a target area in a single orbit pass due to S/C agility)	
Detectors	Pan: Si CCD array (8 μ m pixel size) with a row of > 35,000 detectors MS: Si CCD 4 arrays (32 μ m pixel size) with a row of > 9,300 detectors	
Data quantization	11 bit	
Geolocation accuracy of imagery	≤ 3 m (using a GPS receiver, a gyroscope and a star tracker) without any GCP (Ground Control Points)	
Optics	TMA telescope (5-element modified Cassegrain optical design) Aperture diameter of 1.1 m, focal length = 13.3 m, f/12	
FOV (Field of View)	> 1.28°	
Instrument size	3 m tall (the volume is 5.3 m ³)	
Total instrument mass	452 kg	

1-GSD (Ground Sample Distance)

Source: Earth Observation Portal (2012).

The Rational Polynomial Camera (RPC) model relates the object space (latitude, longitude, height) coordinates to image space (line, sample) coordinates (Grodecki and Dial, 2001). Geoeye-1 image was provided with a file containing RPC information, used to orthorectify the image along with ground control points and the USGS GTOPO30 DEM. Resulting image is presented in Figure 19 in Geographic coordinates, datum WGS-84.

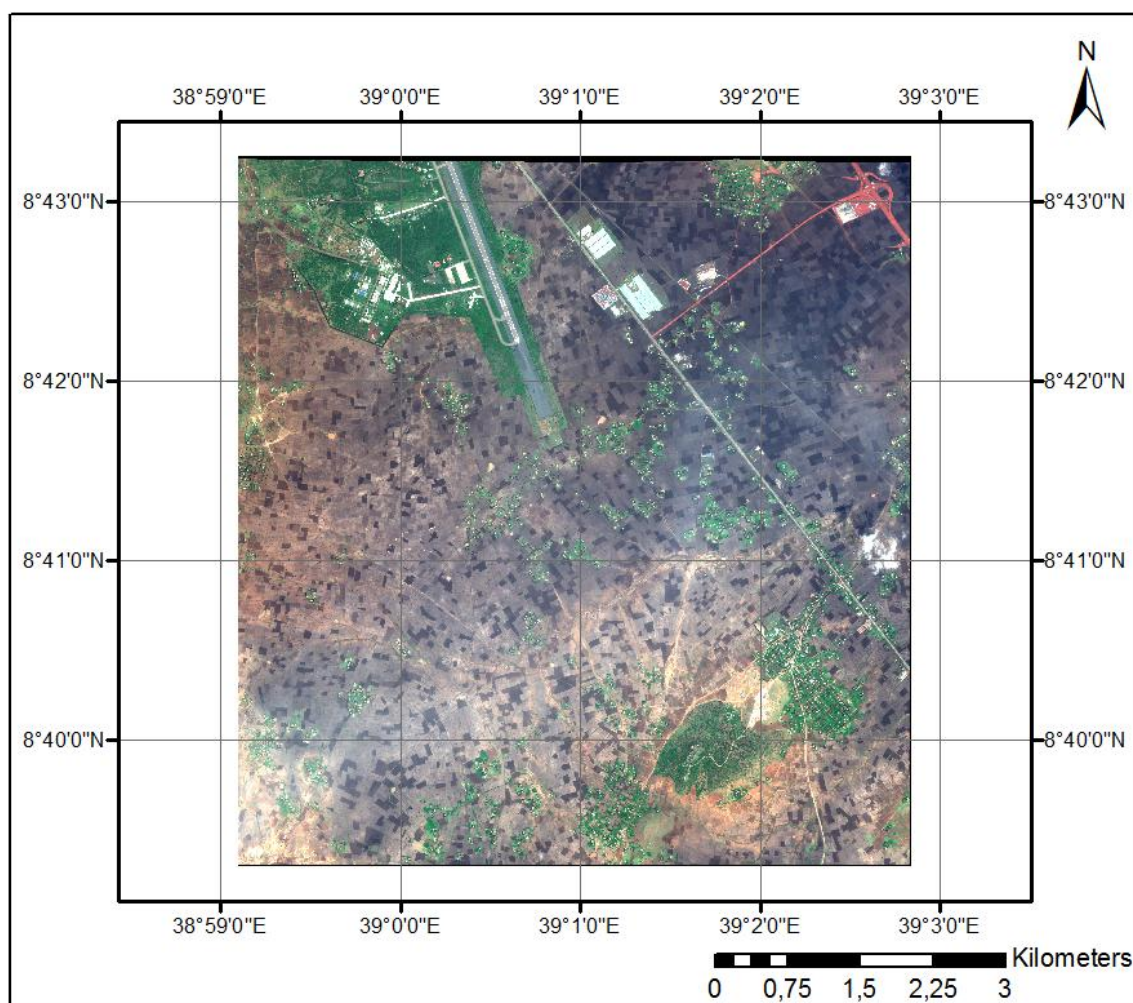


Figure 19. Geoeye-1 image bands 3, 2 and 1 on R, G and B channels, respectively.

Tef field sampling data was collected over October 2011 growing season. During crop maturity period only Rapideye image was available. The image was acquired on 27 October 2011, 08:59:15.55 GMT. REIS (RapidEye Earth Imaging System) characteristics are presented on Table 15.

Table 15. Parameter specification of the REIS instrument onboard Rapideye satellite.

Imager type	Pushbroom imager. CCD linear array with 12 k pixels (5 arrays in parallel, 1 for each spectral band), use of triple line CCDs with 3 x 12 k pixels in a ceramics baseplate, pixel size = 6.5 μm		
Imaging mode	Multispectral (MS)		
Spectral range	Band name	Spectral coverage (nm)	Center wavelength (μm)
	Blue	440-510	475.0
	Green	520-590	555.0
	Red	630-685	657.5
	Red edge	690-730	710.0
	NIR (Near Infrared)	760-850	805.0
IFOV ¹	6.5 m (spatial resolution), orthorectified pixel size = 5 m		
Swath width	77 km		
Imager CCD detector	Linear array, 12 k pixel		
Data quantization	12 bit		
Optics, aperture, f/No, focal length	TMA (Three Mirror Anastigmatic) design, 145 mm diameter, f/4.3, Effective focal length = 633 mm		
FOV ²	$\pm 6.75^\circ$ about nadir, corresponding to a swath of > 70 km at an orbital altitude of 620 km		
MTF (Modulation Transfer Function)	≥ 0.25 in along-track, ≥ 0.11 in cross-track		
Instrument size	Imager: 656 mm x 361 mm x 824 mm Payload Electronics Unit (PEU): 280 mm x 242 mm x 260 mm		
Total instrument mass	43 kg (imager+ electronics box)		

1-IFOV (Instant Field of View)

2-FOV (Field of View)

Source: Earth Observation Portal (2012).

Rapideye Ortho image product is radiometric, sensor and geometrically corrected and aligned to a cartographic map projection. The images are provided as 25 by 25 kilometer tiles referenced to a fixed, standard image tile grid system. Four sections of image tiles were delivered to compose an image of 500km². No mosaic was performed before image processing, to avoid alteration on pixels values. Figure 20 presents an image mosaic result generated for visual analysis and display.

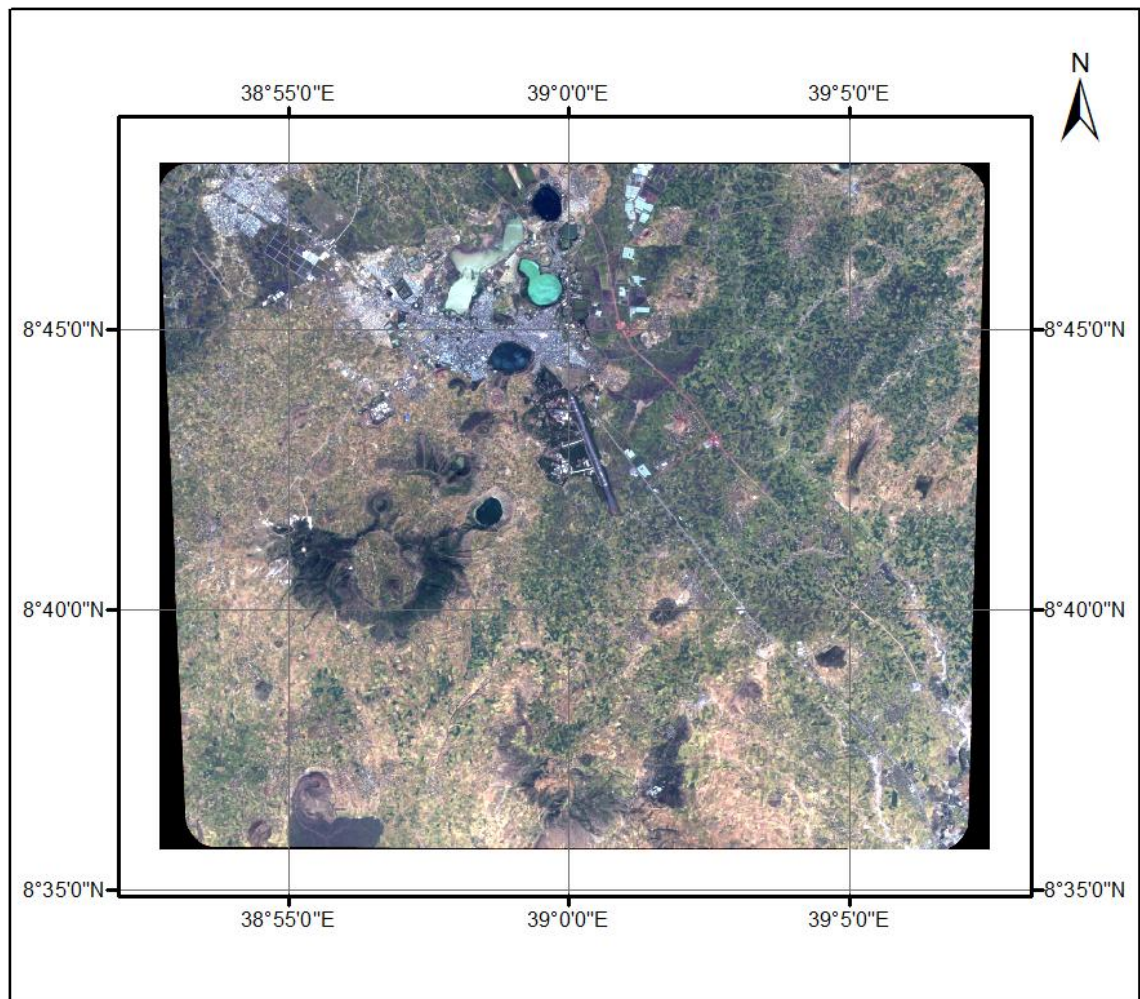


Figure 20. Rapideye image bands 3, 2 and 1 on R, G and B channels, respectively.

4.3. GPS DATA

Field samples were collected delineating tef fields in the study area. A hand-held GPS was used. GPS data collected in October 2011 are shown in Figure 21. Some tef crops had their limits defined through cinematic GPS survey as shown by the yellow rectangles over-layed in the image. These ground samples were used for image classification.

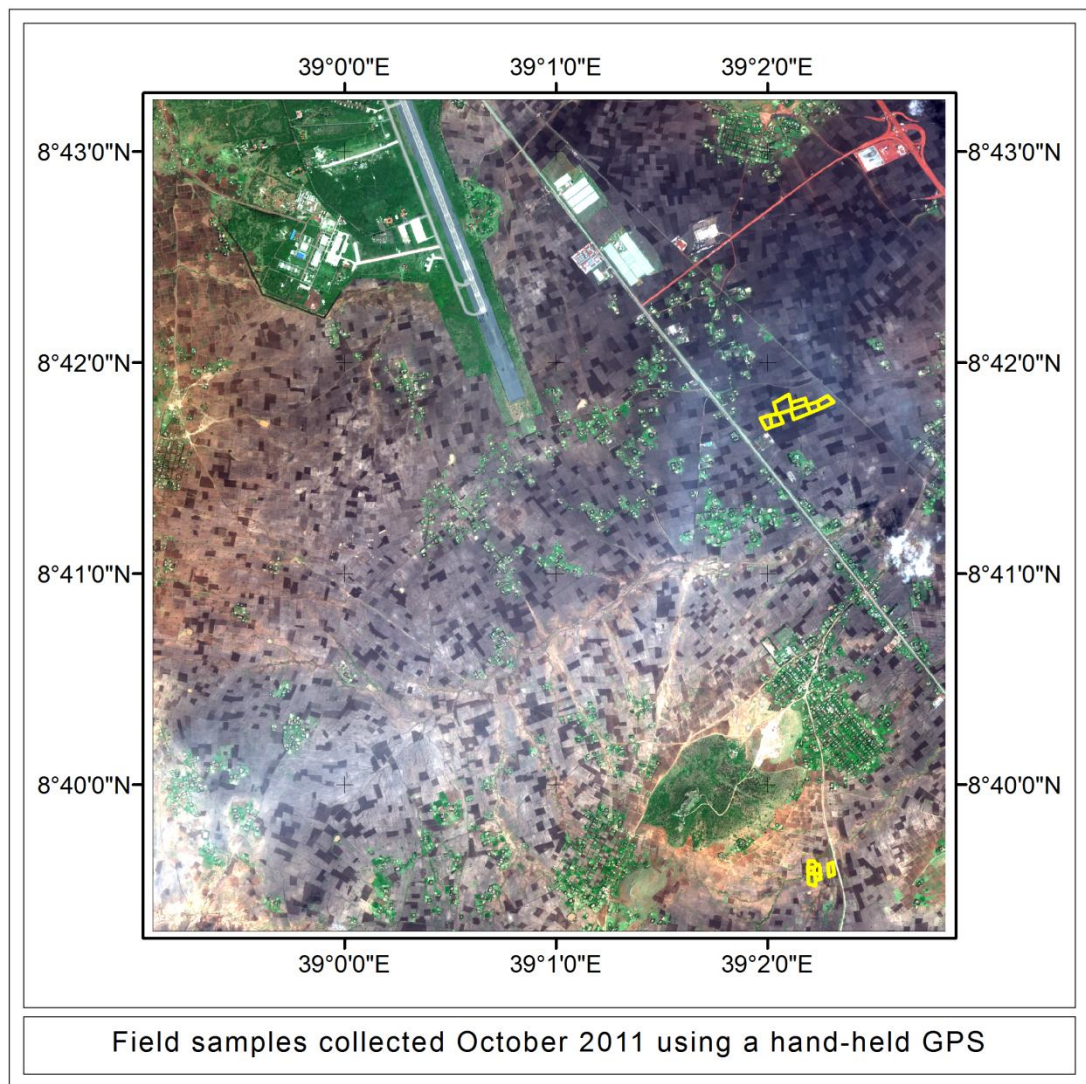


Figure 21. Field samples collected in October 2011 using a hand-held GPS.

4.4. IMAGE CLASSIFICATION

Geoeye-1 and Rapideye images were classified using example based feature extraction workflow available on Envi 5.0 software. This software tool includes image segmentation and supervised classification routines.

Supervised classification can be performed using one of the three classification algorithms available and all of them were applied to image segmentation objects (Envi 5.0 User's Guide, 2011):

- KNN: This method classifies segments based on their proximity to neighboring training regions. It is a more rigorous method compared to PCA that more accurately distinguishes between similar classes.
- PCA: This method assigns segments to classes using a principal components analysis.
- SVM: This is the most rigorous of the three classification methods. It is based on Support Vector Machine algorithm.

Samples of segmented image objects were collected using Region of Interest tool for spectral classes occurring in each image. Spectral classes collected samples were analyzed using Envi n-D Visualizer, which allows for n-dimension space sample data visualization and outliers removal. Regions of interest were used for segmentation-based image classification.

Rapideye data was a non-mosaic format, so each of the four images were treated separately to avoid differences in spectral response occurring in different parts of the image caused by sensor angle viewing and also avoiding image pixel resampling necessary during mosaicking procedures. Mosaicking was performed after image classification.

Spectral, texture and spatial attributes of image objects resulting from image segmentation were included in classification for an increased discrimination between spectral classes. All attributes included in image classification are described in Table 16.

Table 16. Spectral, texture and spatial attributes of image objects.

Spectral Attributes: Spectral attributes are computed on each band of the input image. The attribute value for a particular pixel cluster is computed from input data band w here the segmentation label image has the same value (i.e., all pixels in the same pixel cluster contribute to the attribute calculation).	
Attribute	Description
Spectral Mean	Mean value of the pixels comprising the region in band x
Spectral Max	Maximum value of the pixels comprising the region in band x
Spectral Min	Minimum value of the pixels comprising the region in band x
Spectral STD	Standard deviation value of the pixels comprising the region in band x
Texture Attributes: are computed on each band of the input image. Texture attribute computation is a two-step process where the first pass applies a square kernel of pre-defined size to the input image band. The attributes are calculated for all pixels in the kernel window and the result is referenced to the center kernel pixel. Next, the attribute results are averaged across each pixel in the pixel cluster to create the attribute value for that band's segmentation label.	
Attribute	Description
Texture Range	Average data range of the pixels comprising the region inside the kernel (whose size you specify with the Texture Kernel Size parameter in segmentation)
Texture Mean	Average value of the pixels comprising the region inside the kernel
Texture Variance	Average variance of the pixels comprising the region inside the kernel
Texture Entropy	Average entropy value of the pixels comprising the region inside the kernel
Spatial Attributes: are computed from the polygon defining the boundary of the pixel cluster, so band information is not required.	
Attribute	Description
Area	Total area of the polygon, minus the area of the holes. Values are in map units
Length	The combined length of all boundaries of the polygon, including the boundaries of the holes. This is different than the Major Length attribute. Values are in map units
Compactness	A shape measure that indicates the compactness of the polygon. A circle is the most compact shape with a value of $1 / \pi$. The compactness value of a square is $1 / 2(\sqrt{\pi})$. $\text{Compactness} = \sqrt{4 * \text{Area} / \pi} / \text{outer contour length}$
Convexity	Polygons are either convex or concave. This attribute measures the convexity of the polygon. The convexity value for a convex polygon with no holes is 1.0, while the value for a concave polygon is less than 1.0. $\text{Convexity} = \text{length of convex hull} / \text{Length}$
Solidity	A shape measure that compares the area of the polygon to the area of a convex hull surrounding the polygon. The solidity value for a convex polygon with no holes is 1.0, and the value for a concave polygon is less than 1.0. $\text{Solidity} = \text{Area} / \text{area of convex hull}$
Roundness	A shape measure that compares the area of the polygon to the square of the maximum diameter of the polygon. The "maximum diameter" is the length of the major axis of an oriented bounding box enclosing the polygon. The roundness value for a circle is 1, and the value for a square is $4 / \pi$. $\text{Roundness} = 4 * (\text{Area}) / (\pi * \text{Major Length}^2)$
Form Factor	A shape measure that compares the area of the polygon to the square of the total perimeter. The form factor value of a circle is 1, and the value of a square is $\pi / 4$. $\text{Form Factor} = 4 * \pi * (\text{Area}) / (\text{total perimeter})^2$
Elongation	A shape measure that indicates the ratio of the major axis of the polygon to the minor axis of the polygon. The major and minor axes are derived from an oriented bounding box containing the polygon. The elongation value for a square is 1.0, and the value for a rectangle is greater than 1.0. $\text{Elongation} = \text{Major Length} / \text{Minor Length}$

Table 16. Spectral, texture and spatial attributes of image objects (continuation)

Spatial Attributes: are computed from the polygon defining the boundary of the pixel cluster, so band information is not required.	
Attribute	Description
Rectangular Fit	A shape measure that indicates how well the shape is described by a rectangle. This attribute compares the area of the polygon to the area of the oriented bounding box enclosing the polygon. The rectangular fit value for a rectangle is 1.0, and the value for a non-rectangular shape is less than 1.0. Rectangular Fit = Area / (Major Length * Minor Length)
Main Direction	The angle subtended by the major axis of the polygon and the x-axis in degrees. The main direction value ranges from 0 to 180 degrees. 90 degrees is North/South, and 0 to 180 degrees is East/West.
Major Length	The length of the major axis of an oriented bounding box enclosing the polygon. Values are map units of the pixel size. If the image is not georeferenced, then pixel units are reported.
Minor Length	The length of the minor axis of an oriented bounding box enclosing the polygon. Values are map units of the pixel size. If the image is not georeferenced, then pixel units are reported.
Number of Holes	The number of holes in the polygon. Integer value.
Hole Area/Solid Area	The ratio of the total area of the polygon to the area of the outer contour of the polygon. The hole solid ratio value for a polygon with no holes is 1.0. Hole Area/Solid Area = Area / outer contour area

Spectral classes used in image classification were combined into 4 main land cover/land use classes: 1) exposed soil, 2) crops, 3) trees and shrubs and 4) urban areas (includes buildings, roads, and urban areas itself).

Results from classification of the four Rapideye images were mosaicked. Change detection based tef identification was performed. Geoeye-1 classified image was used as the initial state, representing the period in which soil is bare prior to tef sowing. The final state Rapideye classified image mosaic represents the period of crop maturity. Everything classified as exposed soils in the initial state image and classified as crops in the final state image were considered as tef, since no other crop is grown at the same time window as tef.

Object-based classification of Geoeye-1 image is presented in Figure 22. When comparing this initial state change detection map and original image (shown in Figure 198) it can be noticed a good performance of segmentation based feature extraction algorithms used. Exposed soils dominate the landscape this time of year, before tef planting. Urban areas, crops and trees and shrubs classes are well defined as well.

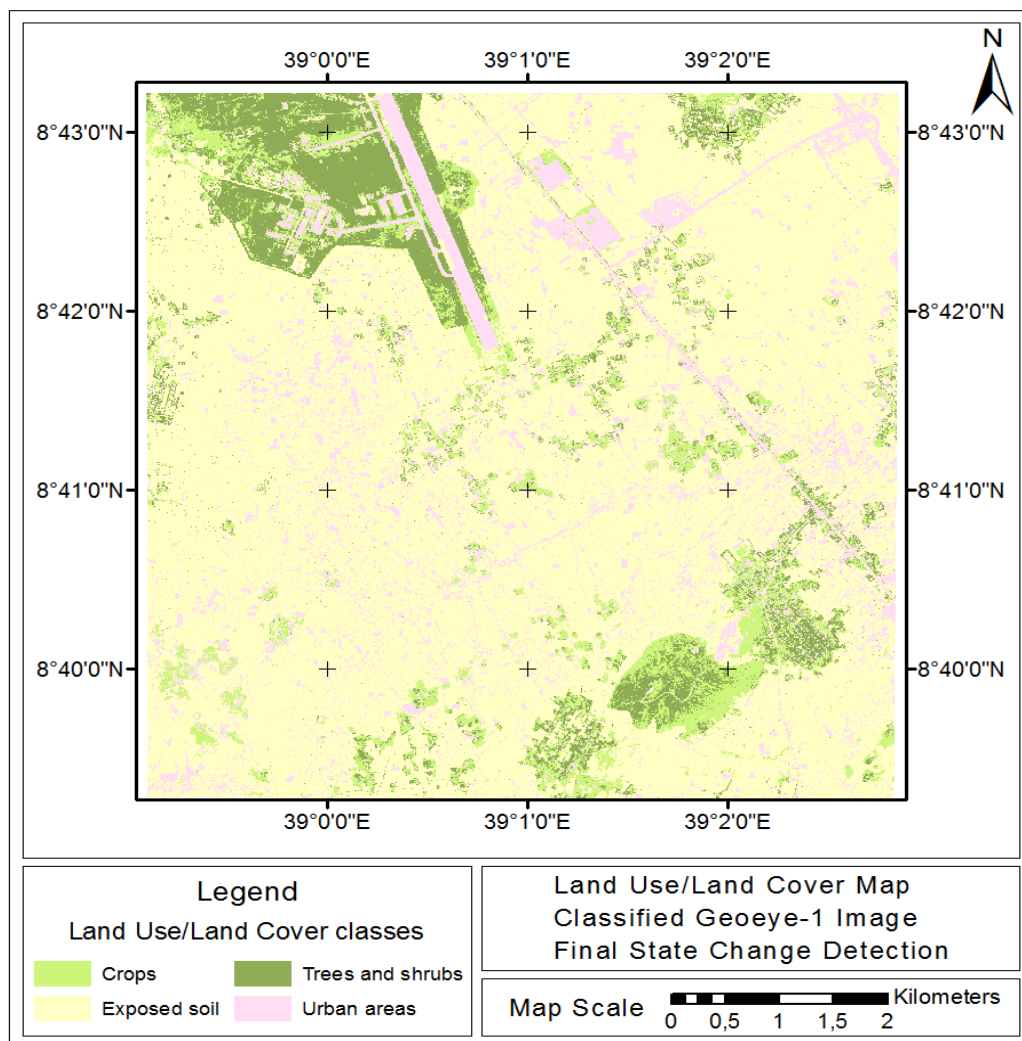


Figure 22. Geoeye-1 resulting object-based image classification.

Rapideye image classification results visual analysis revealed a good classification for the main classes of interest, exposed soils and crops (Figure 23). On the other hand, more classification mistakes could be noticed for urban areas and trees and shrubs.

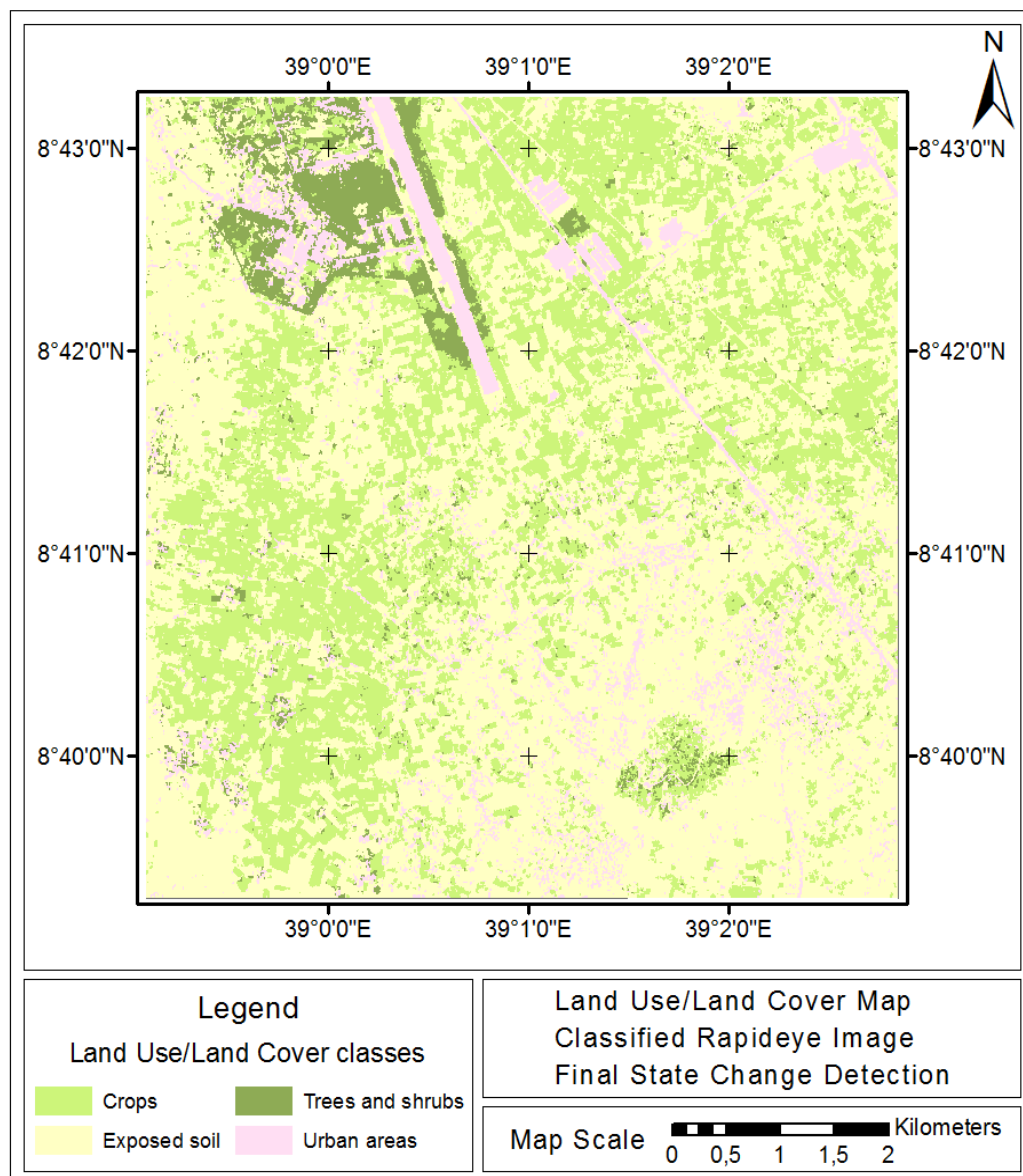


Figure 23. Rapideye resulting object-based image classification.

Even without statistics evaluation one can infer that poorer results obtained for Rapideye classification are related to spatial resolution. Coarser resolution images presents higher levels of pixel impurity, especially on objects boundaries or when small objects occur inside bigger ones, such as trees in a field. In Geoeye-1 image trees are clearly defined, whereas some smaller trees almost disappear in Rapideye image, having its spectral response mixed to those of surrounding fields.

Edge detection algorithm and full lambda schedule merging sets were adopted for image segmentation. Scale level equals to 25, merge settings equals to 10 and the default texture kernel size (equals to 3) was adopted after careful visual analysis of segmentation results. Performance of SVM algorithm was superior to other algorithms and this is the one adopted in this study. These segmentation parameters were used for both images.

Due to insufficient field sampling for classification verification, it was not possible to estimate final map accuracy. This task will be accomplished in a simpler manner in the future, using sample points over the original image itself, when statistics for image classification will be presented.

4.4.1. Change Detection

When comparing the final change detection maps to the original images, it can be argued that this is the appropriate technique for tef mapping at local scales. Taking advantage of the pronounced differences in multi-temporal images caused by characteristics of a rapidly growing crop such as tef is probably the best approach available for this kind of target detection.

As can be seen in Figure 24, no exposed soils remained in the final change detection image, indicating good classification results of feature extraction

techniques. Even for the poorly Rapideye classified class “trees and shrubs” demonstrated good agreement between image classifications. As it could be expected from a good change detection result, steady targets such as trees should appear as “no change” class.

On the other hand, a great amount of urban areas appear in the final change detection map. This error might be due to proximity of exposed soils and roads or urbanized areas and differences in image pixel sizes. Since Rapideye is a 5m spatial resolution image, many of the pixels that should receive roads or exposed soil spectral responses are mixed or mistakenly captured while image is acquired. Use of same sensor or same spatial resolution images would avoid some of these errors.

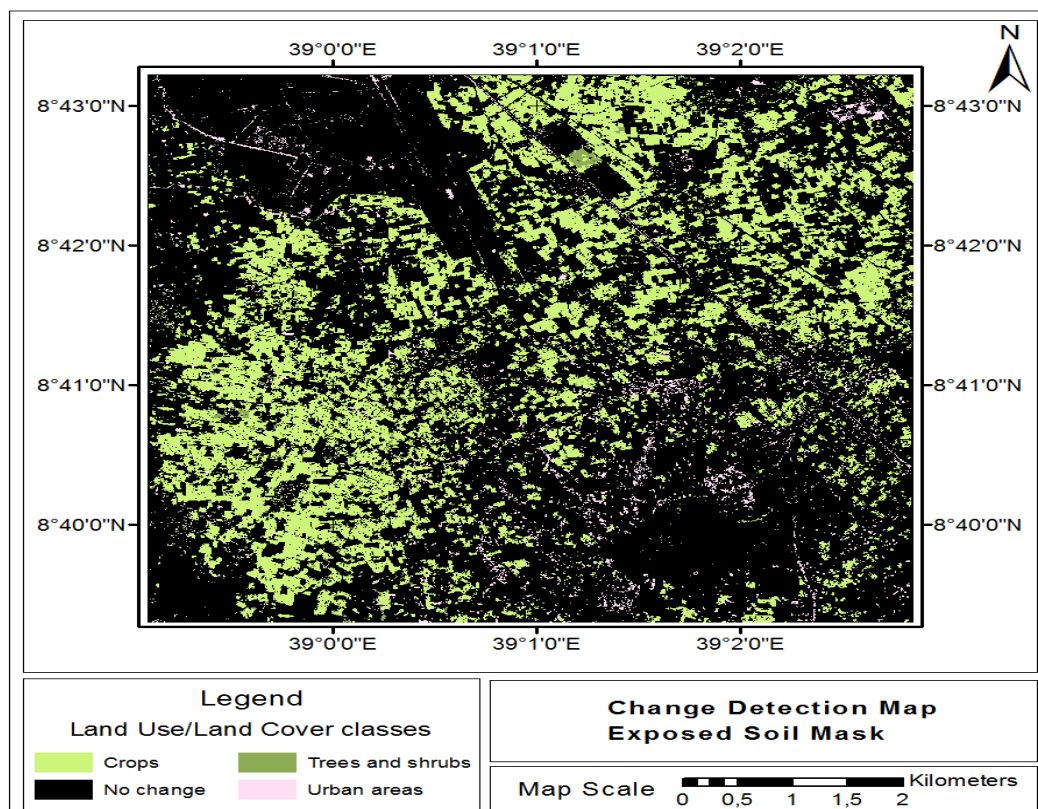


Figure 24. Change detection final map, exposed soil mask.

Results of change detection are presented in Table 17 in pixels, Table 18 in precentual values and Table 19 in square meters. The tables list the Initial State classes in the columns, represented by classification of Geoeye-1 image acquired before tef planting, and the Final State classes, represented by Rapideye image classification in the rows. The Class Total row indicates the total number of pixels in each Initial State Class, and the Class Total column indicates the total number of pixels in each Final State Class. The Row Total column is a class-by-class summation of all Final State pixels that fell into the selected Initial State classes. Class Changes row indicates the total number of Initial State pixels that changed classes. The Image Difference row is the difference in the total number of equivalently classed pixels in the two images, computed by subtracting the Initial State Class Totals from the Final State Class Totals. An Image Difference that is positive indicates that the class size increased.

Table 17. Change detection results in pixels

Initial State Geoeye-1	Final State Rapideye					
	Urban	Exposed soil	Crops	Trees and shrubs	Row Total	Class Total
Urban	59.016	51.894	21.877	15.862	148.649	149.159
Exposed	123.897	816.116	102.616	55.244	1.097.873	1.103.579
Crops	63.377	519.600	25.470	30.836	639.283	640.161
Trees	4.306	14.584	11.499	63.378	93.767	94.045
Class Total	250.596	1.402.194	161.462	165.320	0	0
Class Changes	191.580	586.078	135.992	101.942	0	0
Image Difference	-101.437	-298.615	478.699	-71.275	0	0

The most part of pixels initially classified as Urban Areas in the Initial State image were classified as Exposed Soil in the final State image (49.44%). Part of the Urban areas initially identified were later classified as crops (25.29%). Only 23.55%

of the urban areas remained unchanged. These results can be attributed to misclassification of urban areas, especially in the final state image.

Table 18. Change detection percent (%) results.

Initial State Geoeye-1	Final State Rapideye					
	Urban	Exposed soil	Crops	Trees and shrubs	Row Total	Class Total
Urban	23,55	3,70	13,55	9,60	99,66	100,00
Exposed	49,44	58,20	63,55	33,42	99,48	100,00
Crops	25,29	37,06	15,78	18,65	99,86	100,00
Trees	1,72	1,04	7,12	38,34	99,70	100,00
Class Total	100,00	100,00	100,00	100,00	0,00	0,00
Class Changes	76,45	41,80	84,23	61,66	0,00	0,00
Image Difference	-40,48	-21,30	296,48	-43,11	0,00	0,00

Areas initially classified as Exposed Soil were mostly classified as crops in the final state image (37.06%). These areas can be considered as tef crops due to the previously mentioned difference of tef planting dates in this region of Ethiopia.

As for crop areas, 63.55% were identified as exposed soil in the final state image whereas 1578% of the areas remained crops. Trees and shrub vegetation areas remained mostly unchanged (38.34%) and a large percentage were later classified as exposed soil (33.42%). Some significant change for this class into crop areas can also be observed (18.65%).

Table 19. Change Detection square meters results

Initial State Geoeye-1	Final State Rapideye					
	Urban	Exposed soil	Crops	Trees and shrubs	Row Total	Class Total
Urban	1.475.400,00	1.297.350,00	546.925,00	396.550,00	3.716.225,00	3.728.975,00
Exposed	3.097.425,00	20.402.900,00	2.565.400,00	1.381.100,00	27.446.825,00	27.589.475,00
Crops	1.584.425,00	12.990.000,00	636.750,00	770.900,00	15.982.075,00	16.004.025,00
Trees	107.650,00	364.600,00	287.475,00	1.584.450,00	2.344.175,00	2.351.125,00
Class Total	6.264.900,00	35.054.850,00	4.036.550,00	4.133.000,00	0,00	0,00
Class Changes	4.789.500,00	14.651.950,00	3.399.800,00	2.548.550,00	0,00	0,00
Image Difference	-2.535.925,00	-7.465.375,00	11.967.475,00	-1.781.875,00	0,00	0,00

It can be noticed that crops class presents the highest positive change from initial to final state, as expected. This class suffered a 296.74% change and a 11.967.475 square meters increase area.

Negative changes of around 40 percent are also observed for urban and trees and shrubs classes, probably due to differences in pixel size between images, as well as misclassification. Although changes for exposed soils account for only -21.30 percent, absolute pixel values demonstrate this is the class that lost more pixels (-298.615) and crops gained the most (478.699). This can be considered a reasonable result since crop planting occurs after first image was acquired.

4.4.2. Accuracy Evaluation

The amount of data regarding tef field sampling using GPS was considered insufficient for accuracy verification of the tef crops map generated by image classification and change detection techniques. Difficulties related to ground data collection required adoption of an alternative tef field sampling technique for accuracy verification.

Networks of random points were established over the study area, including 100 points at least 200m from each other. These points were used as an independent ground truth data for accuracy evaluation. Visual analysis by an interpreter was adopted for tef field's identification within the sample points. Figure 25 shows location of the sample points over Geoeye-1 image.

The Overall Accuracy for Geoeye-1 image classification resulted in 88.00% and calculated Kappa Coefficient was equal to 0,6964. Confusion matrix for Geoeye-1 image classification accuracy verification is shown in Table 20. Classes with higher classification accuracy were exposed soils (92.31%) and trees (81.82%). Urban areas were classified with 66.67% accuracy and crops classification accuracy equals 62.50%. Urban areas were mostly misclassified as exposed soil (33.33%) and crops were mostly misclassified as trees (25%) and exposed soil (12.5%). Other classes' misclassification was less than 10%. These values are considered acceptable for a reasonable image classification.

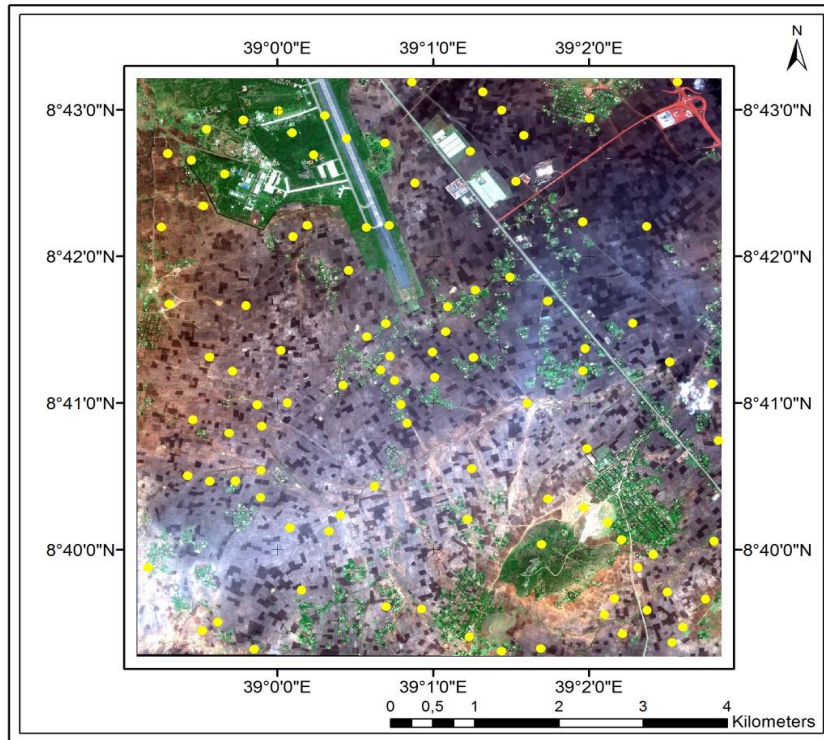


Figure 25. Samples points for accuracy verification of Geoeye-1 image classification.

Table 20. Confusion matrix of accuracy verification of Geoeye-1 classification result

Classes	Ground Truth									
	Number of pixels					Percent (%)				
	Urban	Exposed	Crops	Trees	Total	Urban	Exposed	Crops	Trees	Total
Urban	2	5	0	0	7	66,67	6,41	0	0	7,00
Exposed	1	72	1	1	75	33,33	92,31	12,50	9,09	75,00
Crops	0	1	5	1	7	0	1,28	62,50	9,09	7,00
Trees	0	0	2	9	11	0	0	25,00	81,82	11,00
Total	3	78	8	11	100	100	100	100	100	100

An independent set of sample points were collected for Rapideye image classification accuracy verification, similarly as the procedure adopted for Geoeye-1 classification evaluation. Points used for accuracy verification are shown in Figure 26.

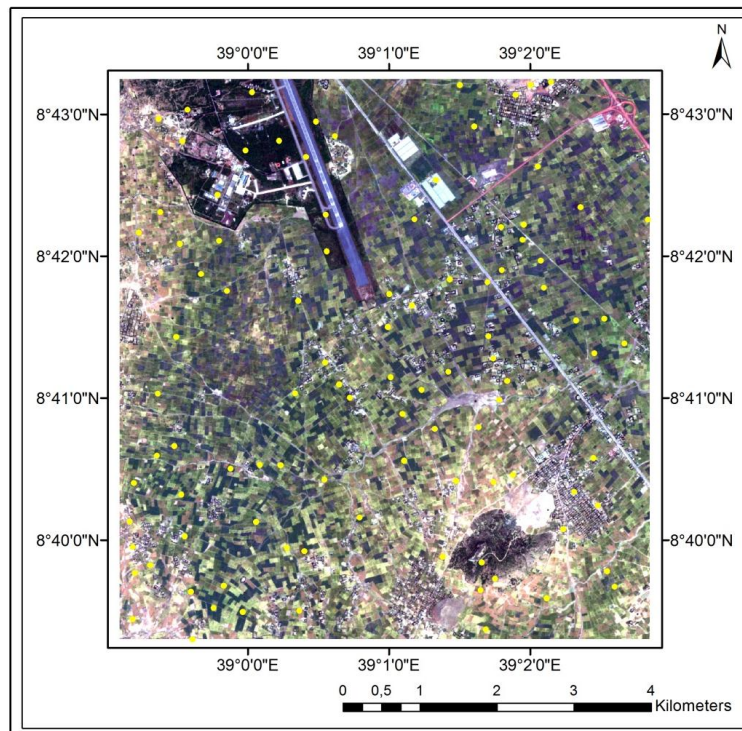


Figure 26. Samples points for accuracy verification of Rapideye image classification

The Overall Accuracy for Rapideye image classification resulted in 74.00%, and Kappa Coefficient equals to 0.5668 was calculated. These results are inferior to those obtained for the Geoeye-1 image classification. Considering that Rapideye image spatial resolution is coarser than 1meter of Geoeye-1 image, higher values of misclassification were expected. Another consideration to be made is the season for image acquisition. Geoeye-1 was acquired before crops planting and most of the image is covered with bare soil. Rapideye was acquired during tef crops growing

season, and different levels of crop development are observed. This factor certainly increases misclassification, especially for crops not fully grown, where bare soil is mixed with plant spectral response.

Confusion matrix for Geoeye-1 image classification accuracy verification is shown in Table 21. Exposed soils and trees were mostly correctly classified, presenting more than 80% correct classification (86.67% and 83.33% respectively). Trees were confused with exposed soils in an order of 16.67%. The urban areas presented highest values of misclassification, since 77.78% of the samples were misclassified as exposed soil, giving the similarities of spectral response and the occurrence of exposed soil within urban areas. Crops and trees were also misclassified as exposed soil in 30% and 16.67% respectively.

Table 21. Confusion matrix of accuracy verification of Rapideye classification result

Classes	Ground Truth									
	Number of pixels					Percent (%)				
	Urban	Exposed	Crops	Trees	Total	Urban	Exposed	Crops	Trees	Total
Urban	2	1	0	0	2	22,22	2,22	0,00	0,00	3,00
Exposed	7	39	12	1	7	77,78	86,67	30,00	16,67	59,00
Crops	0	4	28	0	0	0,00	8,89	70,00	0,00	32,00
Trees	0	1	0	5	0	0,00	2,22	0,00	83,33	6,00
Total	9	45	40	6	9	100,00	100,00	100,00	100,00	100,00

4.5. CHAPTER SUMMARY

A methodology of object-based image classification and change detection was demonstrated. Geoeye-1 image collected before tef crop planting and Rapideye image collected right before tef harvest composed the multitemporal database used to identify tef crops.

Object-based image classification has shown its potential for image classification and tef crop identification. Problems identified in image classification procedure were related to insufficient field data to separate classes, especially to discriminate grasses from tef crops. This problem was overcome with application of change detection post-classification technique. Most exposed areas classified in Geoeye-1 image were classified as crops in Rapideye image. The fact that most exposed soils were later classified as crops is related to the tef planting season, which helped discriminate crops.

Visual analysis of resulting map and verification accuracy demonstrates the potential of this technique in discriminating tef crops from other land use/land cover types. Ground truth data on tef crop is necessary for further accuracy evaluation.

5. CONCLUSIONS AND FUTURE DIRECTION

5.1. CONCLUSIONS

Information gathering was the focus on initial phase of this research. A database includes data of climate, soil, topography, land use/land cover and tef crop location was created to support a geographic information system (GIS). The GIS is used as a basis for spatial analysis and established as a helpful tool in further studies involving tef crops monitoring, productivity and condition estimation and establishment.

This database was used to create tef suitability maps. Information collected made possible achievement of initial goals, allowing production of a map of suitable areas for tef cultivation. Adjustments could easily be made on the final map in case more detailed information is obtained or whether different class limits are found for suitable cultivation areas.

Soil mapping at a local scale provided important information that can be used, for sampled area, to produce more detailed suitability maps not only for tef but for other crops as well. This information will be an important part of the Tef GIS and will be included in future analysis of tef production management and development.

Local scale tef mapping preliminary results indicate that the right path is pursued in the goal of identifying and mapping accurate tef. High spatial resolution has proven to be an important requirement for crop discrimination, especially as

reflected by that Geoeye-1 performed better than Rapideye. This result is directly related to the first image spatial resolution.

Change detection technique has also been proven to be the best approach for tef mapping, as well feature extraction, image segmentation and object-based classification. These techniques applied to the selected images have given promising results for local scale tef mapping.

Object-based image classification has shown its potential for image classification and tef crop identification. Problems identified in image classification procedure were related to insufficient field data to separate classes, especially to separate grasses from tef crops. This problem was overcome with application of change detection post-classification technique. Most exposed areas classified in Geoeye-1 image were classified as crops in Rapideye image. The fact that most exposed soils were later classified as crops is related to the tef planting season, which helped discriminate crops. Visual analysis of resulting map and verification accuracy demonstrates the potential of this technique in discriminating tef crops from other land use/land cover types.

As stated by Thenkabail *et al.* (2009), some of the main goals realized in the development of poorer nations over the last century were the attainment of food security, satisfaction of individual livelihoods, and the reduction of poverty. Agricultural sustainability has the highest priority in all countries, whether developed or developing. Remote Sensing and GIS technology are gaining importance as useful precision farming tools in sustainable agricultural management and development. This research is intended to demonstrate the applicability of these tools in suitability zoning, information extraction and mapping for agricultural development of tef crops in Ethiopia.

The solution for providing food security to all people of the world without affecting the agroecological balance lies in the adoption of new research tools, particularly from aerospace Remote Sensing, and combining them with conventional as well as frontier technologies like Geographic Information Systems (GIS). The broad objective of sustainable agriculture is to balance the inherent land resource with crop requirements, paying special attention to optimization of resource use towards achievement of sustained productivity over a long period (Lal and Pierce, 1991). Sustainable agricultural development / sustainable increase in crop production could be achieved by adopting a variety of agricultural technologies (Bhan *et al.*, 1996).

Along with tef crops development and increased production, an important secondary goal will be addressed. Encouraging tef establishment in suitable areas and providing tools for profitable and sustainable production, protection of tef as a culturally important and threatened species will be achieved.

5.2. APPLICATIONS OF THIS RESEARCH

Results of this research demonstrate how geospatial information on environmental and climatic conditions can be used to guide the establishment of new tef crops in Ethiopia. Results from this research can be used by farmers to decide on best crop planting in their fields and best places to grow tef. Decision makers and politicians can also use these results in a decision-making process to develop public policy guidelines to improve food security and sustainable production of tef.

This study using remote sensing showed that tef crop identification and mapping are feasible when multi-temporal imagery is adopted, considering that tef is a fast growing crop usually cultivated at the end of the season.

5.3. LIMITATIONS OF THIS WORK

Regarding tef suitability analysis, limitations of this work are related to definition of optimal environmental and climatic ranges for tef crop development. Refinement of limits for these ranges can improve suitability maps, especially with the inclusion of detailed soil information into the GIS database.

Remote sensing results were considered promising for tef crop identification and mapping but no accuracy assessment was performed giving insufficiency of field data for classification results verification. Field data is also necessary for tef crop condition and yield estimation.

Another gap identified in this study regarding remote sensing is acquisition of hyperspectral data, both at field- and satellite-level. Spectroradiometer measurements of leaf and canopy reflectance would provide valuable data for spectral behavior of tef crops and studies on vegetation indices for tef characteristics estimation. Acquisition of Hyperion data during crop season would also provide information on these aspects at regional level. One difficulty related to satellite image acquisition for tef crops is the need of planning for it and possibly rapid adjustments would have to be made regarding data collection. Tef is sometimes planted when other crops fail so there is no well-defined date for its maturity.

5.4. FUTURE WORKS

As mentioned before, suitability analysis seems to have achieved the objective of this study. Improvements would be related to new discoveries on limitations for tef growing abiotic factors, such as different and expanded elevation ranges or soil adaptation. In the case of cultivars development or genetic improvements, new maps could be easily generated altering threshold for suitable

areas mapping. The most important change in the suitability analysis would be inclusion of biotic and socio-economic information not available at the present time. Occurrence of pathogens, parasite and beneficial organisms could radically change the suitability map as well as information on cultural, political and marketing factors that affect crop performance or commercialization of production.

Another front for advances within the scope of this research study is related to tef mapping. Different satellites and sensors could be investigated for regional scale mapping, such as the hyperspectral image provider Hyperion sensor. Detailed spectral information such as those acquired by Hyperion could improve mapping at smaller scales, allowing information extraction for the entire Ethiopia. This is another step to be taken in case of image availability over tef growing areas. The only datasets currently available are located in southern Ethiopia, in areas where tef is not massively grown. Contact with Earth Observing branch of US Geological Survey has been made to order image acquisition on demand over tef growing areas.

Still in the remote sensing front, future achievements are certainly related to improvement of image classification through use of sample points for checking image accuracy. New maps will be created after sample collection using information on the main errors found in image classification. This will, in consequence, generate better change detection mapping as well as tef growing area maps.

Further steps to be taken in development of remote sensing techniques for sustainable tef production in Ethiopia are estimation of tef production using multi-spectral sensors as well as hyperspectral ones, correlating these data with more detailed spectroradiometer acquired data and crop biophysical variables. The final goal would be development of an operational system for tef production estimation. The system would include remote sensing data, spatial data collection added by GPS

equipment and GIS spatial analysis as a support for decision making process, crisis mitigation and drought assessment.

REFERENCES

- Abdel-Rahman, E. M.; Ahmed, F. B.; Ismail, R. (2013). Random forest regression and spectral band selection for estimating sugarcane leaf nitrogen concentration using EO-1 Hyperion hyperspectral data. *International Journal of Remote Sensing*, vol. 34, No. 2, pp.712-728.
- Adam K. Tilling, Garry J. O'Leary, Jelle G. Ferwerda, Simon D. Jones, Glenn J. Fitzgerald, Daniel Rodriguez, Robert Belford. (2007). Remote sensing of nitrogen and water stress in wheat, *Field Crops Research*, vol.104, No.1–3, October–December, pp.77-85.
- Afify, H. A. (2011). Evaluation of change detection techniques for monitoring land-cover changes: A case study in new Burg El-Arab area. *Alexandria Engineering Journal*, vol.50, No.2, pp. 187-195.
- Aguirre-Gutiérrez, J.; Seijmonsbergen, A. C.; Duivenvoorden, J. F. (2012). Optimizing land cover classification accuracy for change detection, a combined pixel-based and object-based approach in a mountainous area in Mexico, *Applied Geography*, vol. 34, pp.29-37.
- Anderson, M. C., Allen, R. G., Morse, A., & Kustas, W. P. (2012). Use of Landsat thermal imagery in monitoring evapotranspiration and managing water resources. *Remote Sensing of Environment*, No.122, pp.50-65.
- Asfaw, Z., & Tadesse, M. (2001). Prospects for sustainable use and development of wild food plants in Ethiopia. *Economic Botany*, vol. 55, No.1, pp. 47-62.
- Ashdown, I. (1994). *Radiosity: A Programmer's Perspective*. John Wiley & Sons, Inc., New York, NY, USA. 496 p.
- Asner, G.P., 1998, Biophysical and Biochemical Sources of Variability in Canopy Reflectance, *Remote Sensing of Environment*, 64:234-253.
- Assefa, K., Yu, J.-K., Zeid, M., Belay, G., Tefera, H. and Sorrells, M. E. (2011), Breeding tef [*Eragrostis tef* (Zucc.) trotter]: conventional and molecular approaches. *Plant Breeding*, 130: 1–9.
- Berry, J.K.; Delgado, J. A.; Khosla, R. Pierce, F.J. (2003) Precision conservation for environmental sustainability. *Journal of Soil and Water Conservation*, vol. 58, No.6, pp.332-339.
- Bhan, S.K.; Saha, S.K.; Pande, L.M.; Prasad, J. 1996. *Use of Remote Sensing and GIS Technology in Sustainable Agricultural Management and Development*. Indian Institute of Remote Sensing, NRSA DEHRADUN-248001, India.

- Bing-fang, W.; Ji-hua, M.; Feifei, Z.; Xin, D.; Miao, Z.; Xueyang, C. (2010). Applying remote sensing in precision farming-a case study in Yucheng. In: World Automation Congress (WAC), 2010 (pp. 1-6). IEEE.
- Broge, N. H., Leblanc, E. (2001) Comparing prediction power and stability of broadband and hyperspectral vegetation indices for estimation of green leaf area index and canopy chlorophyll density. *Remote Sensing of Environment* vol.76, no. 2 p.:156-172.
- Central Statistical Authority (CSA), 2008: *Statistical Abstract of Ethiopia 2008*. Ethiopian agricultural research organization, Addis Ababa, Ethiopia.
- Chauhan, H.J.; Mohan, B.K. (2012). Measures to improve crop classification using remotely sensed hyperion hyperspectral imagery. In: *Communications, Devices and Intelligent Systems (CODIS), 2012 International Conference on*, IEEE, pp. 596-599
- Chen, Z.; Li, S.; Ren, J.; Gong, P.; Zhang, M.; Wang, L. Xiao, S. and Jiang, D. (2008). Monitoring and management of agriculture with remote sensing. In: Liang, S (Ed). *Advances in Land Remote Sensing: System, Modeling, Inversion and Application*. Springer, pp.397-421.
- Costa, C. C. da; Guilhoto, J. J. M. (2011). Impactos da agricultura de precisão na economia brasileira. In: Inamasu, R. Y.; Naime, J. de M.; Resende, A. V. de; Bassoi, L. H.; Bernardi, A. de C. (Ed.). *Agricultura de precisão: um novo olhar*. São Carlos, SP: Embrapa Instrumentação, pp. 307-313.
- Crosta, A. P. (1993). *Processamento Digital de Imagens de Sensoriamento Remoto*. UNICAMP/Instituto de Geociências.
- Davison, J. and C. McKnight. (2004). *Tef Demonstration Plantings for 2003*. University of Nevada Reno Cooperative Extension. Reno, NV.
- Demissie, A. (2001). Tef Genetic Resources in Ethiopia. In: Tefera, H., Beley, G.; Sorrells, M. (Eds.). *Narrowing the Rift. Tef Research and Development. Proceedings of the International Workshop on Tef Genetics and Improvement*, Debre Zeit, Ethiopia, pp. 27-31.
- Doraiswamy, P. C., Moulin, S., Cook, P. W., & Stern, A. (2003). Crop yield assessment from remote sensing. *Photogrammetric Engineering and Remote Sensing*, vol. 69, pp. 665 - 674.
- Earth Observation Portal (2012). Available from <https://directory.eoportal.org/web/eoportal/satellite-missions/g/geoeeye-1>.
- Ebba, T. (1969) Tef (*Eragrostis tef*). The Cultivation, usage and some of its known diseases and insect pests. Part I. Expt. Stat. Bull. No. 60, HSIU, College of Agriculture, Dire Dawa, Ethiopia.
- Elvidge, C. D., & Chen, Z. (1995). Comparison of broad-band and narrow-band red and near-infrared vegetation indices. *Remote sensing of environment*, vol. 54, No. 1, pp. 38-48.
- Envi 5.0 (2011). *Envi 5.0 User's Guide*. Boulder, Colorado: Exelis Visual Information Solutions.

- Ess, D.R., Parsons, S.D., Strickland, R.M. Evaluation of commercially-available software for grain yield mapping. *American Society of Agricultural Engineers*, Paper No. 97-1033, St. Joseph, MI, USA. 1997.
- ETHIOGIS. Available from <http://www.ethiogis.net/>
- FAO - Food and Agriculture Organization of the United Nations. (2009) *The State of Food Insecurity in the World 2009*, FAO, Rome.
- FAO - Food and Agriculture Organization of the United Nations. (2010) *The state of food insecurity in the world, 2010*, FAO, Rome.
- FAO - Food and Agriculture Organization of the United Nations. World agriculture towards 2030/2050: the 2012 revision. Ed: Alexandratos, N., Bruinsma, J. ESA Working Paper No. 12 - 03, June, Rome. 2012.
- FAO, ISRIC. ISSS (1998) World reference base for soil resources." World soil resources reports vol. 84, No.88.
- FAO. (1990). Guidelines for soil description. Soil Resources, Management and Conservation Service, 3rd ed. FAO, Rome.
- FAO-Unesco, I. S. R. T. C. (1990). Soil map of the world. Revised legend. Reprinted with corrections. World Soil Resources Report, 60.
- Ferencz, C.S.; Bogнар, P.; Lichtenberger, J.; Hamar, D.; Tarcsai, G.; Timar, G.; Molnar, G.; Pásztor, S.Z.; Steinbach, P.; Székely, B.; Ferencz, O. E.; Ferencz-Árkos, I. (2004). Crop Yield Estimation by Satellite Remote Sensing. *International Journal of Remote Sensing*, vol. 25, No. 20, p.4113-4149.
- FEWS (Famine Early Warning System). Available from <http://earlywarning.usgs.gov/fews/africa/web/datatheme.php>
- Florenzano, T. G. *Imagens de satélites para estudos ambientais*. São Paulo: Oficina de Textos, 2002.
- Floros, J. D.; Newsome, R.; Fisher, W.; Barbosa-C'anvas, G. V.; Chen, H.; Dunne, C. P.; German, J.B.; Hall, R. L.; Heldman, D. R.; Karwe, M. V.; Knabel, S. J.; Labuza, T. P.; Lund, D. B.; Newell-McGloughlin, M. (2010). Feeding the world today and tomorrow: the importance of food science and technology. An IFT Scientific Review. *Comprehensive Reviews in Food Science and Food Safety*, vol. 9, pp.572–599.
- Foresight. (2001). *The Future of Food and Farming: Challenges and Choices for Global Sustainability*, London, Government Office for Science. Available from <http://www.bis.gov.uk/assets/foresight/docs/food-and-farming/11-546-future-of-food-and-farming-report.pdf>
- Fung, T.; LeDrew, E. (1987). Application of principal components analysis change detection. *Photogrammetric Engineering and Remote Sensing*, vol.53, pp. 1649- 1658.
- Gebbers R., Adamchuk V. I. (2010). Precision agriculture and food security. *Science*, vol. 327, No. 5967, pp.828–31.

- Gebreselassie, S., Sharp, K. (2007). Commercialisation of Smallholder Agriculture in Major Tef-growing Areas of Ethiopia'. In: Proceedings of the Fifth International Conference on the Ethiopian Economy. Ethiopian Economic Association, vol. 3, pp. 345.
- Gitelson, A. A. (2013) Remote estimation of crop fractional vegetation cover: the use of noise equivalent as an indicator of performance of vegetation indices. *International Journal of Remote Sensing*, ahead-of-print, published online: 29 Apr 2013. Available from <http://dx.doi.org/10.1080/01431161.2013.793868>
- Goel, P. K., Prasher, S. O., Landry, J. A., Patel, R. M., Bonnell, R. B., Viau, A. A., et al. (2003). Potential of airborne hyperspectral remote sensing to detect nitrogen deficiency and weed infestation in corn. *Computers and Electronics in Agriculture*, vol. 38, pp. 99 - 124.
- Gommes, R., Petrassi, F. (1994). Rainfall variability and drought in Sub-Saharan Africa since 1960. *Agro-meteorology series working paper 9*, Food and Agriculture Organization, Rome, Italy.
- Goswami *et al.*, 2012 A Review: The application of Remote Sensing, GIS and GPS in Precision Agriculture
- Grodecki, J and G. Dial (2001). IKONOS geometric accuracy. *Proceedings of Joint Workshop of ISPRS Working Groups I/2, I/5 and IV/7 on High Resolution Mapping from Space 2001*, University of Hanover, Hanover, Germany, Sept 19-21, pp. 19-21.
- Groten, S.M.E. (1993). NDVI-crop monitoring and early yield assessment of Brukina Faso, *International Journal of Remote Sensing*, vol.14, No. 8, pp.1495–1515.
- Haboudane, D., Miller, J. R., Pattey, E., Zarco-Tejada, P. J., & Strachan, I. B. (2004). Hyperspectral vegetation indices and novel algorithms for predicting green LAI of crop canopies: modeling and validation in the context of precision agriculture. *Remote Sensing of Environment*, vol. 90, pp. 337 - 352.
- Haboudane, D.; Miller, J. R.; Tremblay, N.; Zarco-Tejada, P. J. ; Dextraze, L. (2002). Integrated narrow-band vegetation indices for prediction of crop chlorophyll content for application to precision agriculture. *Remote Sensing of Environment*, vol. 81, No. 2, pp. 416-426.
- Haibo, Y.; Tian, L. (2003). A genetic-algorithm-based selective principal component analysis (GA-SPCA) method for high-dimensional data feature extraction. *Geoscience and Remote Sensing*, IEEE Transactions on, vol.41, No. 6, pp. 1469-1478.
- Hall, O.; Hay, G. J. (2003). A multiscale object-specific approach to digital change detection, *International Journal of Applied Earth Observation and Geoinformation*, vol 4, No.4, pp.311-327.
- Hanna, S. H. S.; Rethwisch, M. D. (2003). Characteristics of AVIRIS bands measurements in agricultural crops at Blythe area, California: III. Studies on Tef Grass. *Proceedings SPIE 4879, Remote Sensing for Agriculture, Ecosystems, and Hydrology IV*, 25.

- Hanna, S. H. S.; Rethwisch, M. D. (2004). Characteristics of AVIRIS bands measurements in agricultural: crops at Blythe Area, California: IV: studies on cotton varieties spectral data. *Proceedings SPIE 5232, Remote Sensing for Agriculture, Ecosystems, and Hydrology V*, 52. pp. 52-82.
- Hansen, P. M.; Schjoerring, J. K. (2003). Reflectance measurement of canopy biomass and nitrogen status in wheat crops using normalized difference vegetation indices and partial least squares regression. *Remote Sensing of Environment*, vol. 86, No. 4, pp.542-553.
- Harris, A. I. (2005). Spectroscopy with multichannel correlation radiometers. *Review of scientific instruments*, vol. 76, No. 5, pp.054503-054503.
- Hussain, M.; Chen, D.; Cheng, A.; Wei, H.; Stanley, D. (2013). Change detection from remotely sensed images: From pixel-based to object-based approaches, *ISPRS Journal of Photogrammetry and Remote Sensing*, vol 80, pp.91-106.
- Inamasu, R. Y.; Naime, J. de M.; Resende, A. V. de; Bassoi, L. H.; Bernardi, A. C. de C. (Ed.).(2011) *Agricultura de precisão: um novo olhar*. São Carlos, SP: Embrapa Instrumentação. 334 p.
- Institute of Biodiversity Conservation.(2005). *National Biodiversity Strategy and Action Plan (NBSAP) Project*. Addis Ababa: Institute of Biodiversity Conservation.
- Jackson, R. D. Remote sensing of biotic and abiotic plant stress. (1986). *Annual Review of Phytopathology*, vol. 24, No. 1, pp.265-287.
- Jain, N., Ray, S. S., Singh, J. P., & Panigrahy, S. (2007). Use of hyperspectral data to assess the effects of different nitrogen applications on a potato crop. *Precision Agriculture*, vol. 8, pp. 225 - 239.
- Jensen, J. R. (1986). *Introductory digital image processing: a remote sensing perspective*. New Jersey: Prentice-Hall. p 379.
- Jensen, J. R.; Jackson, M. W. (2001) *Introductory digital remote sensing image processing*. vol. 3. module 1: The remote sensing process. Available from www.cla.sc.edu/geog/rslab/
- Ji-hua, M.; Bing-fang, W. (2008). Study on the crop condition monitoring methods with remote sensing. *International Archives of the Photogrammetry, Remote Sensing and Spatial Information Sciences*, vol. 37, No. B8, p.945-950.
- Ketema, S. (1989). Production trends, germplasm resources, breeding, and varietals improvement of small millets, with special emphasis on tef in Ethiopia. In: Seetharam, A.; Riley, K.W.; Harianryana, G. (Eds.). *Small Illets in Global Agriculture*. DC, Oxford & 1BC0, India.
- Ketema, S., 1993. Tef (*Eragrostis tef*): breeding, genetic resources, agronomy, utilisation and role in Ethiopian agriculture. Institute of Agricultural Research, Addis Abeba, Ethiopia.
- Kumar, A., Manjunath, K. R., Bala, R., Sud, R. K., Singh, R. D., & Panigrahy, S. (2013). Field hyperspectral data analysis for discriminating spectral behavior

- of tea plantations under various management practices, *International Journal of Applied Earth Observation and Geoinformation*, vol.23, p.352-359.
- Li, X.; Yeh, A. G. O. (1998). Principal component analysis of stacked multi-temporal images for the monitoring of rapid urban expansion in the Pearl River Delta. *International Journal of Remote Sensing*, vol. 19, No.8, pp.1501-1518.
- Liaghat, S.; Balasundram, S.K. (2010) A review: The role of remote sensing in precision agriculture. *American Journal of Agricultural Biological Sciences*, vol. 5, No.5, pp. 50-55.
- Lillesand, T. M.; Kiefer, R. W. (1994). *Remote sensing and image interpretation*, Wiley, New York. 721 pp.
- Lu, D., Mausel, P.; Brondizio, E.; Moran. E. (2004). Change detection techniques. *International Journal of Remote Sensing*, vol. 25, No. 12, pp.2365-2401.
- Ma; Q.; Chen, Q.; Shang, Q.; Zhang, C. (2006). The data acquisition for precision agriculture based on remote sensing. *IEEE International Conference on Geoscience and Remote Sensing Symposium*, Denver Colorado, pp 888-891.
- Mac Arthur, A. (2011). Introduction to Field Spectroscopy. NERC Field Spectroscopy Facility Course Handbook, School of GeoSciences, University of Edinburgh. Available from http://cost-es0903.femenvironment.eu/uploads/MacArthur_Introduction%20to%20Field%20Spectroscopy.pdf
- Mahlein, A.-K.; Rumpf, T.; Welke, P. Dehne, H.-W.; Plümer, L.; Steiner, U. Oerke, E.-C. (2013). Development of spectral indices for detecting and identifying plant diseases, *Remote Sensing of Environment*, vol.128, No. 21, pp.21-30.
- Mamo, T.; Erkossa, T.; Tulema, B. (2001). Soil fertility and plant nutrition research on tef in Ethiopia. In: Tefera, H., Beley, G.; Sorrells, M. (Eds.). *Narrowing the Rift. Tef Research and Development. Proceedings of the International Workshop on Tef Genetics and Improvement*, Debre Zeit, Ethiopia, pp. 16-19.
- Mamush, B. (2011). Personal communication.
- McCoy, R. M. (2005). *Field methods in remote sensing*. The Guilford Press.
- Melesse, T., Rockstrom, J., Savenije, H.H.G., Hoogmoed, W.B., Dawit, A. (2008). Determinants of tillage frequency among smallholder farmers in two semi-arid areas in Ethiopia. *Physics and Chemistry of the Earth*, vol. 33, pp. 183–191.
- Melo, D.H.C.T.B. (2002). Uso de dados Ikonos II na análise urbana: testes operacionais na zona leste de São Paulo / D. H. C. T. B. Melo. - São José dos Campos: INPE, 146p.
- Mengistu, D. K.; Mekonnen, L. S. (2012). Integrated Agronomic Crop Managements to Improve Tef Productivity Under Terminal Drought. In: Rahman, I.; Hasegawa, H. (eds.). *Water Stress*, InTech. pp. 235-254.
- Mengistu, D.K. (2009). The influence of soil water deficit imposed during various developmental phases on physiological processes of tef (*Eragrostis tef*). *Agriculture, Ecosystems and Environment*, vol. 132, No. 3-4, pp.283–289.

- Meze-Hausken, E. (2004). Contrasting climate variability and meteorological drought with perceived drought and climate change in northern Ethiopia. *Climate Research*, vol. 27, pp.19–31.
- Milton, E. J. (1987). Review Article Principles of field spectroscopy. *Remote Sensing*, vol. 8, No.12, pp. 1807-1827.
- Milton, E. J.; Schaepman, M. E.; Anderson, K. Kneubühler, M.; Fox, N. (2009). Progress in field spectroscopy. *Remote Sensing of Environment*, vol.113, pp.S92-S109.
- Ministry of Agriculture & Rural Development, MoARD. (2010). *Tef production*. Addis Ababa. Federal Democratic Republic of Ethiopia. (unpublished paper)
- Ministry of Water Resources (MOWR). (2009) Federal Democratic Republic Ministry of Water Resources, Ethiopia. Evaluation of Water Resources of the Ada'a and Becho Plains Ground Water Basin for Irrigation Development Project. Draft Final. Pre-feasibility and Feasibility Report (Phase II & III). vol.II: Soil, Land Evaluation and Agronomy of Ada'a Plain.
- Mondal, P.; Basu, M. Adoption of precision agriculture technologies in India and in some developing countries: Scope, present status and strategies. *Progress in Natural Science*, vol. 19, No. 6, pp. 659-666.
- Moriondo, M., Maselli, F., & Bindi, M. (2007). A simple model of regional wheat yield based on NDVI data. *European Journal of Agronomy*, vol. 26, No.3, pp. 266-274.
- Mulla, D. J. (1997). Geostatistics, remote sensing and precision farming. In A. Stein, & J. Bouma (Eds.), *Precision Agriculture: Spatial and Temporal Variability of Environmental Quality*. Ciba Foundation Symposium, vol. 210, pp. 100 - 119. Chichester, UK: Wiley.
- Mulla, D.J. (2013). Twenty five years of remote sensing in precision agriculture: Key advances and remaining knowledge gaps, *Biosystems Engineering*, vol. 114, No. 4, pp. 358-371.
- NASA – Earth Observatory Website. (2013) Available from http://earthobservatory.nasa.gov/Features/RemoteSensing/remote_08.php
- National Research Council (U.S.). (2007). Committee on the Earth System Science for Decisions about Human Welfare: Contributions of Remote Sensing. *Contributions of Land Remote Sensing for Decisions about Food Security and Human Health: Workshop Report*. Washington, DC: National Academies Press.
- Neményi, M.; Mesterházi, P.Á.; Pecze, Zs.; Stépán, Zs. (2003) The role of GIS and GPS in precision farming, *Computers and Electronics in Agriculture*, vol. 40, No.1–3, pp-45-55.
- Nidamanuri, R.R.; Zbell, B. (2011). Use of field reflectance data for crop mapping using airborne hyperspectral image. *ISPRS Journal of Photogrammetry and Remote Sensing*, vol.66, No. 5, pp.683-691.

- Novo, E. M. L. de M. (1989). Sensoriamento Remoto: Princípios e Aplicações. Editora Edgar Blücher Ltda. São José dos Campos, 308p.
- Pena-Yewtukhiw, E.M.; Grove, J.H.; Beck, E.G. (2000). Nonparametric geostatistics / probabilistic sourcing of nitrate to a contaminated well. *Proceedings of Fifth International Conference on Precision Agriculture* (CD), July 16–19, 2000. Bloomington, MN, USA.
- Ramankutty, N., Foley, J. A., & Olejniczak, N. J. (2008). Land-use change and global food production. In *Land Use and Soil Resources*. Springer Netherlands, pp. 23-40.
- Robertson, M. J.; Carberry, P. S.; Brennan, L. E. (2009). The economic benefits of precision agriculture: Case studies from Australian grain farms. *Australian Journal of Agricultural Research*, vol. 60, pp. 799–807.
- Robertson, M. J.; Llewellyn, R. S.; Mandel, R.; Lawes, R. A.; Bramley R. G. V.; Swift, L.; Metz, N.; O'Callaghan, C. (2012). Adoption of variable rate technology in the Australian grains industry: status, issues and prospects. *Precision Agriculture*, vol.13, No. (2), pp.181-199.
- Robertson, M., Isbister, B., Maling, I., Oliver, Y., Wong, M., Adams, M., Tozer, P. (2007). Opportunities and constraints for managing within-field spatial variability in Western Australian grain production. *Field Crops Research*, vol. 104, No. 1, pp. 60-67.
- Rojas, O.; Vrieling, A.; Rembold, F. (2011). Assessing drought probability for agricultural areas in Africa with coarse resolution remote sensing imagery, *Remote Sensing of Environment*, vol. 115, No. 2, pp. 343-352.
- Roseberg, R. J.; Norberg, S.; Smith, J.; Charlton, B.; Rykbost, K.; Shock, C. (2006). *Yield and Quality of Tef Forage as a Function of Varying Rates of Applied Irrigation and Nitrogen*. Research in the Klamath Basin 2005 Annual Report. Oregon State University Agricultural Experiment Station Special Report 1069, pp. 119-136.
- Rosegrant, M. W.; Cline, S.A. (2003). Global food security: challenges and policies *Science*, vol. 302, pp. 1917–1919
- Runquist, S.; Zhang, N.; Taylor, R. (2001). Development a field-level geographic information system. *Computers and Electronics in Agriculture*, vol. 31, pp. 201–209.
- Sasson, A. (2012). Food security for Africa: an urgent global challenge. *Agriculture and Food Security* 1, 2. <http://dx.doi.org/10.1186%2F2048-7010-1-2>.
- Schowengerdt, R. A. (1983). *Techniques for Image Processing and Classification in Remote Sensing*. University of Arizona. 249p.
- Seelan, S. K.; Laguette, S.; Casady, G. M.; Seielstad, G. A. 2003. Remote sensing applications for precision agriculture: a learning community approach. *Remote Sensing of Environment*, vol. 88, No.1–2, pp. 157-169.

- Senay, G. B.; Verdin, J. (2003). Characterization of yield reduction in Ethiopia using a GIS-based crop water balance model. *Canadian Journal of Remote Sensing*, vol. 29, No. 6, pp. 687-692.
- Silva, C. B.; Moraes, M. A. F. D.; Molin, J. P. (2011). Adoption and use of precision agriculture technologies in the sugarcane industry of São Paulo State, Brazil. *Precision Agriculture*, vol.12, No.1., pp.67-81.
- Smith, R.B. (2001a) Introduction to hyperspectral imaging. Available from www.microimages.com
- Smith, R.B. (2001b) Introduction to remote sensing of the environment. Available from www.microimages.com
- Sonka, S.T., Bauer, M.E., Cherry, E.T., Colburn, J.W., Heimlich, R.E., Joseph, D.A., Leboeuf, J.B., Lichtenberg, E., Mortensen, D.A., Searcy, S.W., Ustin, S.L., Ventura, S.J. (1997). *Precision Agriculture in the 21st Century. Geospatial and Information Technologies in Crop Management*. Committee on Assessing Crop Yield: Site-Specific Farming, Information Systems, and Research Opportunities, Board of Agriculture, National Research Council. National Academy Press, Washington, DC.
- Spaenij-Dekking, L.; Kooy-Winkelaar, Y.; Koning, F. (2005). The ethiopian cereal Tef in celiac disease. *New England Journal of Medicine*, vol. 353, No. 16.
- Stafford, J. V. (2000). Implementing precision agriculture in the 21st century. *Journal of Agricultural Engineering Research*, vol. 76, No. 3 pp. 267-275.
- Stefen, C. A. & Moraes, E. C. (1993). *Introdução à Radiometria*. In: *Simpósio Brasileiro de Sensoriamento Remoto*, 6., Curitiba, 10 - 14 May.
- Taffesse, A. S., Dorosh, P.; Asrat, S. (2011). *Crop Production in Ethiopia: Regional Patterns and Trends*. Development Strategy and Governance Division, International Food Policy Research Institute, Ethiopia Strategy Support Program II, Addis Ababa, Ethiopia.
- Taylor, P. (1977). *Quantitative Methods in Geography: An Introduction to Spatial Analysis* (Boston, Massachusetts: Houghton Mifflin Company).
- Tey, Y. S.; Brindal, M. (2012). Factors influencing the adoption of precision agricultural technologies: a review for policy implications, *Precision Agriculture*, vol. 13, No. 6 pp.1-18.
- Thenkabail, P. S., Enclona, E. A., Ashton, M. S., Legg, C., & De Dieu, M. J. (2004b). Hyperion, IKONOS, ALI, and ETM+ sensors in the study of African rainforests. *Remote Sensing of Environment*, vol. 90, No. 1, pp. 23-43.
- Thenkabail, P. S., Smith, R. B., De Pauw, E. (2002). Evaluation of narrowband and broadband vegetation indices for determining optimal hyperspectral wavebands for agricultural crop characterization. *Photogrammetric Engineering & Remote Sensing*, vol 68, No. 6, pp. 607-621.
- Thenkabail, P. S.; Enclona, E. A.; Ashton, M. S.; Van Der Meer, B. (2004a). Accuracy assessments of hyperspectral waveband performance for vegetation analysis applications. *Remote Sensing of Environment*, vol. 91, No. 3, pp. 354-376.

- Thenkabail, P.; Lyon, G. J.; Turrall, H.; Biradar, C.M. (2009). *Remote Sensing of Global Croplands for Food Security*. CRC Press, Taylor and Francis, Boca Raton, London, New York.
- Thenkabail, P.S.; Smith, R.B.; Pauw, E.D. (2000). Hyperspectral Vegetation Indices and Their Relationships with Agricultural Crop Characteristics, *Remote Sensing of Environment*, vol.71, no.2, p.158-182.
- Thomasson, J. A. 2003. Remote sensing in agriculture. In: Encyclopedia of Agricultural, Food, and Biological Engineering. New York: Marcel Dekker.
- Tian, Y. C.; Yao, X.; Yang, J.; Cao, W. X.; Hannaway, D. B.; Zhu, Y. (2011). Assessing newly developed and published vegetation indices for estimating rice leaf nitrogen concentration with ground-and space-based hyperspectral reflectance. *Field Crops Research*, vol. 120, No. 2, pp. 299-310.
- Ting, K.C. 2008. Systems Approach to Precision Agriculture – Challenges and Opportunities. Available at: <http://www.docstoc.com/docs/21081830/Systems-Approach-to-Precision-Agriculture>.
- Tsegay, A.; Raes, D.; Geerts, S.; Vanuytrecht, E.; Abrha, B.; Deckers, J.; Bauer, H.; Gebrehiwot, K. (2012) Unravelling crop water productivity of tef [*Eragrostis Tef* (Zucc.) Trotter] through AquaCrop in Northern Ethiopia. *Experimental Agriculture*, vol. 48, No. 2, pp. 222–237.
- Twomlow, S.; Hove, L.; Mupangwa, W.; Masikati, P.; Mashingaidze, N. (2009). Precision conservation agriculture for vulnerable farmers in low potential zones. In: Humphreys, E.; Bayot, R. S. (Eds.). Increasing the productivity and sustainability of rainfed cropping systems of poor smallholder farmers. *Proceedings of the CGIAR Challenge Program on Water and Food International Workshop on Rainfed Cropping Systems*, Tamale, Ghana, 22-25 September 2008.
- Von Grebmer, K.; Ruel, M. T.; Menon, P.; Nestorova, B.; Olofinbiyi, T.; Fritschel, H.; Yohannes, Y.; Von Oppeln, C.; Towey, O.; Golden, K.; Thompson, J. (2010). *Global Hunger Index 2010: The Challenge of Hunger: Focus on the Crisis of Child Undernutrition*. Washington: International Food Policy Research Institute.
- Watson, L., and Dallwitz, M. J. (1992). *Grass Genera of the World*, CAB International, Wallingford, UK.
- Werner, A.; Doelling, S.; Jarfe, A.; Kuhn, J.; Pauly, S.; Roth, R. (2000). Deriving maps of yield-potentials through the use of crop growth models, site information and remote sensing. *Proceedings of Fifth International Conference on Precision Agriculture* (CD), July 16–19, 2000. Bloomington, MN, USA.
- Wolfe, W. L. (1998). Introduction to radiometry. SPIE Press, vol. 29.
- Wu, C., Niu, Z.; Tang, Q.; Huang, W. (2008). Estimating chlorophyll content from hyperspectral vegetation indices: Modeling and validation. *Agricultural and Forest Meteorology*, vol. 148, No. 8, pp.1230-1241.

- Yang, C., Everitt, J. H., Bradford, J. M., & Escobar, D. E. (2000). Mapping grain sorghum growth and yield variations using airborne multispectral digital imagery. *Transactions of the ASAE*, vol. 43, pp. 1927 - 1938.
- Yihun, Y. M.; Haile, A. M.; Schultz, B.; Erkossa, T. (2013). Crop water productivity of irrigated tef in a water stressed region, *Water Resources Management*, vol 27, No. 8, pp. 3115-3125.
- Yu, B.; Nin-Pratt, A.; Funes, J.; Asrat. S. (2010). Cereal production and technology adoption in Ethiopia. *8th International Conference of the Ethiopian Economic Association*, Addis Ababa, Ethiopia, June 25.
- Zarco-Tejada, P. J., Miller, J. R., Morales, A., Berjón, A., Agüera, J. (2004). Hyperspectral indices and model simulation for chlorophyll estimation in open-canopy tree crops. *Remote Sensing of Environment*, vol. 90, pp. 463 - 476.
- Zenebe, G. Y. (2012). Estimation of tef yield using remote sensing and GIS techniques in Tigray region, Northern Ethiopia. *Proceedings of the Third RUFORUM Biennial Meeting*, 24 - 28 September 2012, Entebbe, Uganda, pp. 399-404.
- Zhang, N., Wang, M., & Wang, N. (2002). Precision agriculture: a worldwide overview. *Computers and Electronics in Agriculture*, vol. 36, pp. 113 – 132
- Zhou, L.; Xu, B.; Ma, W.; Zhao, B., Li, L.; Huai, H. (2013) Evaluation of hyperspectral multi-band indices to estimate chlorophyll-a concentration using field spectral measurements and satellite data in dianshan lake, China. *Water*, vol. 5, No.2, pp.525-539.

BIOGRAPHY

Balehager Ayalew graduated from Eleanor Roosevelt High School, Greenbelt, Maryland, in 1996. He received his Bachelor of Science from the University of the District of Columbia (2000). He was employed as a Project Manager in Washington Metro for two years and received his Master of Science in Civil and Environmental Engineering from George Washington University (2001). He was employed as a Chief City Engineer for the City of College Park from 2003 till 2005 and received Professional Engineering Degree in Civil and Environmental Engineering from the George Washington University (2004). This was followed by employment at the District Department of Transportation (DDOT), Infrastructure Project Management Administration (IPMA) as a Deputy Program Manager from 2005 till 2008. During his stay at DDOT he received Master Certificate on Project Management administration at the George Washington University, School of Business and Public Management and ESI International on May 2005. Following DDOT, he was CEO for BMDA Engineering PLC in Ethiopia, East Africa till 2011 and joined LMG Energy LLC, Washington DC, East Africa VP.